Natland, J.H., Dick H.J.B., Miller, D.J., and Von Herzen, R.P. (Eds.)
Proceedings of the Ocean Drilling Program, Scientific Results Volume 176

Stratigraphy and Composition of Gabbros Drilled in Ocean Drilling Program Hole 735B, Southwest Indian Ridge: A Synthesis of Geochemical Data[1]

James H. Natland[2] and Henry J.B. Dick[3]

ABSTRACT

Olivine gabbros, allied troctolitic gabbros, and troctolites, together making up the *olivine gabbro suite*, comprise some 76% of the section cored in Hole 735B on the eastern transverse ridge of the Atlantis II Fracture Zone, Southwest Indian Ridge. These rocks hold the keys to the processes of crustal accretion and magmatic differentiation beneath the floor of the rift valley. We develop the sequential stratigraphy of the olivine gabbro suite by itself, stripping out all later, crosscutting, usually more deformed, and more strongly differentiated oxide gabbros and felsic veins that comprise the remaining 24% of the section. The fundamental unit of crustal construction in the olivine gabbro suite appears as alternations in grain size that we term olivine gabbro sequences. Uniformly textured masses of coarse-grained olivine gabbro range from meters to tens of meters thick and alternate with finer-grained and usually more olivine-rich rocks that have higher Mg# and Ni, such as troctolite and microtroctolite. There are 97 such sequences in the core. However, only 35 are more than 10 m thick and contribute substantially to the section. Several sequences are >40 m thick, and one is 120 m thick. We consider that each sequence represents either a single pulse of magma, in which olivine tended to concentrate toward the base during injection, or several pulses of magma, mostly marked by sutured,

[1]Natland, J.H., and Dick, H.J.B., 2002. Stratigraphy and composition of gabbros drilled in Ocean Drilling Program Hole 735B, Southwest Indian Ridge: a synthesis of geochemical data. *In* Natland, J.H., Dick, H.J.B., Miller, D.J., and Von Herzen, R.P. (Eds.), *Proc. ODP, Sci. Results,* 176, 1–69 [Online]. Available from World Wide Web: <http://www-odp.tamu.edu/publications/176_SR/VOLUME/SYNTH/SYNTH.PDF>. [Cited YYYY-MM-DD]
[2]Rosenstiel School of Marine and Atmospheric Science, University of Miami, Miami FL 33149, USA. **jnatland@rsmas.miami.edu**
[3]Woods Hole Oceanographic Institution, Woods Hole MA 02543, USA.

Initial receipt: 26 March 2001
Acceptance: 6 June 2002
Web publication: 15 October 2002
Ms 176SR-002

interpenetrative igneous contacts and small changes in grain size, but all injected quickly and at one place in the section.

The sequences together make up three series of olivine gabbro and allied troctolite. The upper two occupy about the upper one-third of the cored section. They are more primitive than the lowest, being more calcic and magnesian in bulk composition and having more calcic plagioclase and forsteritic olivine. Each shows a general upward trend to more differentiated compositions, and the two are separated by the one portion of the core, some 50 m thick, of massive oxide gabbros, rich in the oxide minerals ilmenite and magnetite. The deepest and thickest series of olivine gabbro shows only subtle internal variation and no marked trend toward more differentiated compositions at any level, even though it is crosscut in hundreds of places by narrow seams of oxide gabbros. It crystallized from dozens of small injections of magma more differentiated than that which supplied the upper two series but not as differentiated as that which produced the oxide gabbros.

We interpret the upper two series of olivine gabbros as originally portions of cupolas or small magma chambers emplaced near the top of the gabbro section. These were repetitively injected by comparatively primitive magma and probably vented some lava to the seafloor. The third and deeper series consists of gabbro crystallized from more differentiated magma than ever erupted, but nevertheless which either leaked or was forcibly expelled laterally at or beneath the brittle–ductile transition in the crust from the tops or midsections of those or similar cupolas after their links to deeper sources in the lower crust or upper mantle closed off or were cleaved from their sources in the mantle. This explains the broad pattern of inverted or upside-down differentiation seen among olivine gabbros in Hole 735B and why evolved rather than primitive gabbro is so commonly recovered with peridotite in dredge hauls from transverse ridges worldwide.

The earliest stages of basaltic differentiation are not represented by any cumulates in Hole 735B, but those rocks may be restricted to narrow columns that froze from central feeders beneath each cupola, analogous to those recently imaged seismically along a portion of the Mid-Atlantic Ridge. Alternatively, the primitive, frozen relics of such conduits may have been asymmetrically displaced to the north beneath the rift valley while the gabbros of Hole 735B were being unroofed and uplifted along detachment faults to the summit of the transverse ridge to the south. Prior to this, beneath the axial rift, primitive magma ascending in the narrow conduits was free to incorporate ferrobasaltic melt dispersed in differentiated gabbro beneath and between active shallow cupolas through which the conduits had to pass. This explains the hybrid compositions of many abyssal tholeiites at slowly spreading ridges and the apparently inconsistent fact that unadulterated ferrobasalt does not itself erupt on such ridges.

The final stages of differentiation overlapped the first stages of high-temperature crystal-plastic deformation. Differentiation by deformation enhanced the efficiency of expulsion of buoyant intercumulus melt and its coalescence and ascent in an open network of cracks, gaps, fissures, and zones of concentrated shear. Seams of oxide gabbro and late-stage granitic veins lace the core at all levels but diminish in abundance with depth. The numerous small intrusions responsible for the massive oxide gabbro appear to have concentrated preferentially along a permeability pathway between the two upper plutons that caught and directed the flow of ascending late-stage, strongly differentiated melt.

INTRODUCTION

This chapter is a synthesis of geochemical information now available for the gabbroic rocks of Ocean Drilling Program (ODP) Hole 735B. The rocks were unroofed along a detachment fault near a ridge-transform intersection at this slowly spreading ridge (Fig. **F1**) some 9–13 m.y. ago (Dick et al., 1991b). They comprise the only long section of the lower ocean crust so far obtained in the ocean basins. Average recovery was 87% during both Legs 118 and 176 and ranged from 90% to 95% for most of the core.

F1. Location of Hole 735B on the Southwest Indian Ridge, p. 47.

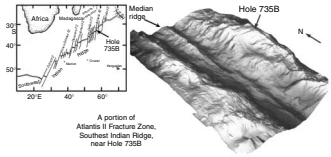

A short history of the planning and drilling of Hole 735B and a summary of drilling objectives are presented in Natland and Dick (**History Chap.,** this volume). The core and its setting are described in several places (Shipboard Scientific Party, 1989; 1999c; Dick et al., 1991a, 2000; Robinson et al., 2001; Natland and Dick, 2001). Briefly, Hole 735B was drilled atop the flat summit of Atlantis Bank, which is a portion of an uplifted transverse ridge on the eastern side of the Atlantis II Fracture Zone near the Southwest Indian Ridge. The summit was flattened by waves when the massif was lifted to sea level from beneath a rift valley floor, currently about 110 km to the north. Since then, seafloor spreading has carried Atlantis Bank to the south, and it has subsided to a depth of 719 m at the site of Hole 735B. The core was first occupied in 1987 during Leg 118 and drilled to a depth of 504 meters below seafloor (mbsf). It was reoccupied in 1997, and the drilling was carried to a depth of 1508 mbsf, almost all of it in gabbro.

Core stratigraphy in prior reports is based mainly on shipboard data, including whole-rock and trace element measurements obtained by X-ray fluorescence (XRF). Such data have traditionally provided the basis for defining the chemical stratigraphy of basalts obtained by ODP and its predecessor, the Deep Sea Drilling Project. During Legs 118 and 176, more than 330 chemical analyses of gabbros were obtained using the shipboard XRF unit. Postcruise analyses have expanded this total to 862, plus 3 analyses of the single diabase dike that intruded the core. Many petrologists would likely prefer using mineral analyses rather than bulk compositions to define gabbro stratigraphy. However, such a strategy at the outset would have deferred definition of any stratigraphy for Hole 735B until years after Leg 176, and mineral data sets are still not sufficiently integrated for us to attempt this just yet. For the present, then, we retain bulk compositions as the principal basis of defining the gabbro stratigraphy, realizing that it is likely to be revised when mineral data can be more fully integrated into a general scheme and other synoptic studies incorporated. Nevertheless, we use some mineral data to augment our discussion and to consider particular problems of petrogenesis.

Hole 735B gabbros record extended differentiation of abyssal tholeiite magma, including formation of oxide-rich ferrogabbros and felsic, or more generally granitic, veinlets that together comprise some 24% of the core. The formation of these rocks and their relationship to zones of deformation in the core was a major concern of the igneous petrologists of Leg 118 and also of some of those of Leg 176. In the following, however, we focus instead on the 76% of core that is more primitive olivine gabbro, troctolitic gabbro, and troctolite, which we term the *olivine gabbro suite*, which likely was emplaced beneath the rift valley floor before much deformation and extended differentiation took place. These

rocks, more than the oxide gabbros, are central to the problem of accretion of the lower ocean crust at a slowly spreading ridge.

Until now, views on this have largely been structured by the results of explosion seismology. Not even ophiolites have provided much insight on the deep structure of slowly spreading ocean crust. Hole 735B currently provides the only detailed lithologic perspective on gabbros at any type of ocean crust obtained thus far by drilling. Part of our task will therefore be to disentangle some of the overlapping threads of late-stage deformation and deformation and reconstruct the section as it originally was. We shall try to imagine what the rocks tell us about the process of accretion beneath the rift valley before or at least while only the earliest stages of deformation were taking place.

MODELS OF MAGMA CHAMBERS AT SLOWLY SPREADING RIDGES

Hole 735B was drilled in part to test developing models of magma chambers at slowly spreading ridges, derived over the past 25 yr by successive integration of geophysical observations, seafloor sampling of basalt, observations on ophiolites, and basalt stratigraphy deduced from drilling. Early on, distinctions between unrifted fast-spreading ridges and deeply rifted slow-spreading ridges provided a duality to general consideration of accretion of the ocean crust. Initially, the concept that large magma chambers span the widths of rift valleys and the thickness of the entire lower ocean crust (e.g., Fig. F2A) (Bryan and Moore, 1977) ran afoul of the failure of seismic refraction experiments to detect any melt bodies beneath the axial rifts of slow-spreading ridges. Thus Nisbet and Fowler (1978) proposed that the crust of the Mid-Atlantic Ridge accretes not by the crystallization of layers of cumulates about a large crystallizing magma chamber, likened to an "infinite onion" (Fig. F2A), but by injection and crystallization along narrow vertical fractures from the base to the top of the crust (an "infinite leek") (Fig. F2B). If "infinite onions" exist anywhere in the ocean crust, they would have to be beneath the East Pacific Rise (Rosendahl, 1976).

In the leek hypothesis, Nisbet and Fowler (1978) proposed that melt collects in pods below a rheological barrier beneath the width of the axial rift; each pod may be the root of one or more fractures that vent lava to the seafloor. The small bodies in effect should crystallize in the form of "nested plutons," each with a separate history of crystallization and differentiation. Nisbet and Fowler (1978) also proposed that ascending magma comes temporarily to rest in a shallow high-level reservoir, where much of the mixing between comparatively primitive magmas, evidenced by the compositions and zonation of phenocryst minerals, takes place.

Sinton and Detrick (1992) again seized on the lack of seismic evidence for molten material in the crust beneath the axes of slow-spreading ridges. With little to go on from interpretation of ophiolites for this type of crust, they borrowed heavily from Marsh's (1989) concept, derived from linked sill complexes in continental crust, to postulate that there are also linked sills in the midst of a nearly consolidated crystal mush in the lower ocean crust beneath rift valleys (Fig. F2C). The concept suggests that magmatic differentiation should march in step from one sill to the next one above, as long as they are interconnected or resupplied with melt. The most differentiated magma would likely con-

F2. Models of magma-chamber complexes, p. 48.

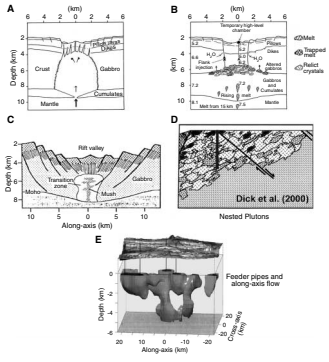

centrate toward the top of the linked plumbing system nearer the cold ocean floor, at least until different parts of the system become physically isolated. Marsh (1989) defined mush, however, as material that behaves like a liquid even though it is laden with crystals. As such, it must contain at least 50% melt, which would be seismically detectable if present in any volume beneath a ridge axis. Therefore, either mush zones beneath slow-spreading ridges are too narrow to detect by seismic refraction techniques or they are ephemeral. Thus in 1992, the linked-sill hypothesis was entirely conjectural and could only be tested by drilling. Citing some prior studies including Leg 118 drilling results, Sinton and Detrick (1992) did indicate that steep faults curving from the rift valley and its walls might root in hot cumulates adjacent to the mush zone.

Drilling in Hole 735B began in 1987, but the 504 m of core recovered during Leg 118 was not really sufficient to provide much insight into these problems. The drilling verified the importance of high-temperature crystal-plastic deformation in guiding transport of strongly differentiated liquids along zones of shear. The bulk of the core, however, consists of primitive (high temperature) olivine gabbros and even some troctolite, arranged in two bodies, each more differentiated upward. Were these the manifestations either of nested plutons or of linked sills? Renewed drilling in 1997 carried the hole to about three times its original penetration and resulted in a new postulate, based on shipboard data, that the olivine gabbros there represent as many as five nested plutons (Fig. **F2D**), each on the order of 200–400 m thick (Dick et al., 2000; Robinson et al., 2000) and each more differentiated upward. Even though the lower two-thirds of the core still contains hundreds of thin, crosscutting, and oftimes deformed oxide gabbros, the essential underlying stratigraphy of the olivine gabbros is intact.

Now we have some new seismic results to link to this picture. Magde et al. (2000) report a tomographic experiment on a rift valley of the Mid-Atlantic Ridge. They did not actually detect melt bodies or lenses comparable to those found along the East Pacific Rise but rock with somewhat attenuated seismic velocities that they interpret as defining the geometry of dispersed melt flow beneath this ridge axis (Fig. **F2E**). Essential features of their zone of hot rock are (1) concentration of low-velocity material beneath several small volcanoes on the seafloor, (2) *lateral* linkage of these low-velocity zones along the rift axis, and (3) the presence of two pipes of such material extending from the mantle to the laterally linked near-surface masses and directly beneath two of the volcanoes. Magde et al. (2000) propose that the other volcanoes are supplied melt by lateral diking in the shallow low-velocity zone along the rift axis from these two sources to distances of ~20 km in either direction. Such dikes should be present in the gabbroic portion of the ocean crust, even if they crystallized to coarse grain size.

Although this is certainly a more detailed picture of the shallow seismic structure of the lower crust at a slow-spreading ridge than we have ever had before, it does not explain how the *entire* mass of the lower crust is formed. Specifically, where does the large mass of material *surrounding* the vertical pipes and underlying the laterally linked shallow low-velocity material (light gray in Fig. **F2E**) originate? Also the scale of any one zone of hot rock detected seismically beneath an axial volcano is on the order of the entire thickness of rock cored in Hole 735B. The experiment does not resolve whether there are linked sills or nested plutons at any scale smaller than 1–2 km.

The several models we have so briefly summarized have each contributed to a developing conception of crustal accretion at slow-spreading ridges, and although some may have been largely discredited on the basis of one line of evidence or another, there are conceptual threads that link them all which may still turn out to be important. The crystallization of cumulates, the role of deformation, the progress and physical locus of extended igneous differentiation; the likely small dimension and ephemeral existence of bodies of magma; the concept that such bodies of magma are linked in a continuity of space and process from the mantle to the seafloor, perhaps also along the rift axis; the question of whether there are small sills or larger plutons that are relieved of their contents by means of ascent of buoyant melt along vertical cracks; all are still a part of the story. Finally, how the totality of the ocean crust accretes in this environment remains substantially unknown.

PRESENTATION OF RESULTS

We consider the detailed stratigraphy of Hole 735B in "Appendix A," p. 32, based on combining all available analyses of rocks from the hole into one table, "Appendix B," p. 46. This table is available in Excel format in the volume "**Supplementary Materials.**" Full citations to data sources are given there. All data including determinations of major oxides, trace elements, rare earth elements, and isotopes are included. In constructing the stratigraphy, however, we used mainly the major oxides and some trace elements. Most of these were determined by XRF techniques, but some of the trace element data sets were measured using inductively coupled plasma–mass spectrometry (ICP-MS). Procedures and calibrations to standards are given in the separate contributions to this volume and prior publications cited in "Appendix B," p. 46. We made no attempt to correct the full data set internally to a standard measured in common but for our plotting parameters found, in general, that trends existing in one data set for a given portion of core were well duplicated by those in others.

A core as complicated as that of Hole 735B and upon which so much data has been collected cannot be presented in a simple way. Also, the details of our stratigraphy and their justification may be of little interest to many readers. This is why we have placed the bulk of this material and the corresponding figures in "Appendix A," p. 32. There, justification of our revised stratigraphy and reasons for modifications to the original shipboard stratigraphy are provided. In the following, we consider only those conventions and other matters pertinent to the general stratigraphy, which we illustrate with representative figures. "Appendix A," p. 32, also provides a comparison to nearby Hole 1105A, drilled during ODP Leg 179 (Pettigrew, Casey, Miller, et al., 1999) and to gabbros obtained during a near-bottom postcruise survey of the entire summit of Atlantis Bank (Coogan et al., 2001). This is to place Hole 735B in the larger context of the body of work done thus far in the vicinity.

To begin, we take up a summary lithologic description of the core and follow this with the chemical stratigraphy.

THE LITHOLOGIC SECTION

The fundamental descriptive component of the rocks recovered during both Legs 118 and 176 is the *lithologic interval*. This formally is a facies or lithology in the core of consistent mineralogy and bounded by other rock with different mineralogy, different texture, or both. Time restraints on board ship forbade breakdown of the core into lithologic intervals of gabbro smaller than 5 cm thick, although felsic veins smaller than this were readily noticed and separately annotated. The boundaries between intervals are variously igneous or tectonic and gradational or sharp, although some were not recovered. A total of 953 lithologic intervals were identified and described over the entire hole (Dick et al., 1991a; Shipboard Scientific Party, 1999c). The average thickness of an interval is thus ~1.7 m, but because few are very thick, most are much smaller than the average.

Rock names were given to each lithologic interval based on the International Union of Geological Sciences (IUGS) classification (Streckeisen, 1974) with some modifications (Shipboard Scientific Party, 1999a). More than a dozen different rock names were applied to the majority of rocks in Hole 735B. Only two broad groupings of primitive gabbro and differentiated gabbro need concern us, however. The first group consists of rock that contains essential olivine but <0.5% oxide minerals (ilmenite and magnetite). It includes troctolite, troctolitic gabbro, and olivine gabbro. We term this the *olivine gabbro suite*. These rocks comprise nearly 80% of the recovery, and of these, olivine gabbro is by far the most abundant. There are 504 intervals of this material containing 175 intact interval boundaries of these rocks against themselves; an additional 12 were not recovered but inferred from contrasting lithologies. Assembling these end to end and leaving out all of the more differentiated gabbros, the accumulated thickness of the olivine gabbro suite is 1153 m; thus, the average thickness of rock between contacts of primitive gabbro is ~6.5 m. Technically, this is the average *expanded* thickness, which apportions total curated thickness by core to the core length, even if core recovery was less (or sometimes more) than 9.5 m apiece (Dick et al., 1991a, 2000). About 94% of the intact contacts are igneous, in the sense that they are irregularly sutured, gradational, graded, or obviously intrusive in character. Only 6% are tectonic, variously being sheared, mylonitic, or sharply planar with deformed rock on one side.

Most of the remaining 766 interval boundaries represent places where the olivine gabbro suite is crosscut by differentiated rocks of the second group, termed the *oxide gabbro suite*. Many of these rocks lack olivine, and they usually contain fairly large crystals of low-Ca pyroxene. Most of them also contain readily visible amounts of the magmatic oxides, ilmenite and magnetite. They include simple gabbro, gabbronorite, oxide-bearing gabbro, and oxide-rich gabbro. The oxide-bearing gabbros contain 0.5%–1% of the oxide minerals and are termed disseminated-oxide gabbros in the site report. They are usually physically associated with the oxide-rich gabbros, but the latter stand out visually because they abruptly have much more abundant ilmenite and magnetite, in many cases comprising 5%–10% and, at the extreme, >30% of the rock. Most seams of oxide gabbro have sharp, usually planar contacts with adjacent rock, whether it is olivine gabbro or another oxide gabbro. They thus appear to be generally intrusive in character, although some sharp contacts represent narrow deformation surfaces.

Very few have diffuse boundaries; thus, the melts from which the oxide minerals were not emplaced in a preexisting, spongy, porous matrix of more primitive minerals. Each lithologic interval was encountered sequentially and numbered downward beginning with "one" at the top of the hole. Over the course of the two legs, coherent groupings of these intervals, each having some predominant set of characteristics, allowed the combining of them into lithologic units, numbered again downward from I to XII (Fig. F3). The lithologic units include some dominated by intervals of olivine gabbro and troctolite and others by oxide-bearing + oxide-rich gabbro. Lithologic Units III and VI, made up of alternations of both, were termed "compound olivine gabbro." Lithologic Unit I at the top of the hole was based not on lithology but on an average high extent of crystal-plastic deformation.

F3. Lithologic units, p. 49.

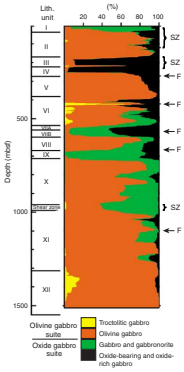

There is therefore little genetic connotation to either the intervals or the lithologic units, largely because they were intended to be simply descriptive but also in part because they were identified one at a time, from the top of the hole downward as coring proceeded, with no knowledge of what would lie underneath. This circumstance of the logistics of receiving core on deck extended to every observation made on the core. Therefore, however thorough the descriptions might be, attempts to assemble a unified picture were consistently colored by the piece-wise way in which the cores were described. Furthermore, outside of contacts that clearly demonstrate intrusive relationships on the scale of the diameter of the core, there was no way to establish sequence. Thus, although the cores have a stratigraphy, they have almost no definable succession.

The term *interval* is not one usually encountered in stratigraphic descriptions of plutonic rocks, especially those of layered intrusions, and the term *unit* is generally used in a different way (Irvine, 1982). An interval here has no more meaning than the rock name given to it and the fact that it occupies a precise portion of the core. The use of the word *unit* as described above is partly an accident of history, the borrowing of a term normally applied to sediments in time-stratigraphic sequence and of a particular lithology. In sediments, this is partly to avoid the use of the word *formation* when considering a core only 6 cm in diameter. However, use of the word for lithologic *units* means that another term must be found if and when we need something comparable to its meaning in layered intrusions.

Intervals of oxide-bearing and oxide-rich gabbro are usually quite narrow, and many are less than the minimum 5-cm thickness used to define an interval. Based on routine shipboard measurement of magnetic susceptibility, which is strongly sensitive to the presence of magmatic magnetite (and with it magmatic ilmenite) in the rocks during Leg 176, there are 476 seams of oxide gabbro in the lower 1004 m of the core (Natland, **Chap. 11,** this volume). Only 192 of these were thick enough to be defined as intervals. This is responsible for one of the principal problems of interpreting the chemical data, namely that some samples chosen for analysis inadvertently combine two or more very different gabbro facies. Hart et al. (1999) attempted to get around this by deliberately obtaining narrow strip samples from 1.13 to 4.15 m long in an effort to secure representative analyses combining multiple lithologies along putatively representative portions of the core obtained during Leg 118. Some problems with this approach are considered in **"Appendix A,"** p. 32.

Many seams detected by magnetic susceptibility also are thinner than the 4-cm spacing of the measurements, but assuming that this is

about the resolution of the technique, then the average thickness of oxide seams measured during Leg 176 is 13.4 cm with a large standard deviation. The thickest oxide-rich seam revealed in this way is only 1.7 m thick. The seams tend to be clustered, and from 700 to 900 mbsf, they make up the majority of the rock. Even so, each is still clearly discrete in this part of the core and is bounded by primitive gabbro above and below.

In the upper 504 m of the core described during Leg 176, only the lithologic observations of Dick et al. (1991a) record the presence of oxide-rich seams at this scale. Most are isolated, but a large concentration of oxide-rich seams is present between 223 and 274 mbsf. The sequence is sufficiently thick and distinctive enough to have been accorded the status of a lithologic unit (Unit IV) during Leg 118 (Fig. **F3**). It contains 32 intervals, mostly disseminated-oxide, oxide-olivine gabbro, and oxide gabbro, within which there are 4 intervals of olivine gabbro totaling 1.35 m, the largest of which is 0.72 m thick (Dick et al., 1991a). These are evidently screens in the larger body of oxide gabbro. The remaining 28 intervals of oxide gabbro average 1.76 m thick—far thicker than the average thickness of seams measured by magnetic susceptibility during Leg 176—and most are in contact with each other. Most of the contacts are igneous in character but a few are undeformed, and there are three cycles, each ~10 m thick, in which the rocks change downward from undeformed through gneissic then porphyroclastic and finally to mylonitic degrees of deformation. In the lower 20 m of Unit IV, 6 of 10 contacts are foliated and are judged to be tectonic in origin; the rest are foliated igneous contacts (Dick et al., 1991a). The basal contact is with a nearly homogeneous body of olivine gabbro >100 m thick. The contact is an intrusion breccia of the olivine gabbro riddled with anastomosing felsic veins that lend the bulk rock an average composition of diorite (Hertogen et al., **Chap. 6,** this volume).

This one large mass represents the acme in the core of aggregation of seams of oxide gabbro. There are dozens of narrow seams of similar material above it and fairly strong, albeit fluctuating, concentrations of oxide gabbro in the core beneath. In general, however, the proportion of oxide-bearing and oxide-rich seams diminishes with depth away from the massive oxide gabbro; below 1000 mbsf they are only 3.6% of the core (Dick et al., 2000). In any case, there is no immediate relationship between the seams or the massive lithologic Unit IV and the compositions of host olivine gabbros. They were not generated by differentiation in situ, rather they came in from somewhere else (i.e., deeper in the cored section, below even that, or from the side) and are thus, at least in the broad sense, intrusive rocks.

In the core described during Leg 176, many of the contacts between narrow seams of oxide gabbro and their more primitive hosts and with each other are tectonic, in the sense that they are sheared, mylonitic, or sharply planar with more deformed rock on one side. Orientations of shear fabric and planar surfaces are usually conformal to the larger-scale deformation fabrics in adjacent cored rock. Shipboard scientists noted a strong association of the oxide-bearing and oxide-rich gabbros with zones of strong crystal-plastic deformation in the core, although over an entire interval or series of adjacent intervals the most oxide-rich gabbros are not always the most strongly deformed.

This tendency of the oxide gabbros to be rather strongly deformed is not easy to quantify, especially since many olivine gabbros are as strongly deformed. However, olivine gabbros are much more abundant than oxide gabbros through the entire core, and most of them are ei-

ther undeformed or only very weakly deformed. The proportion of strongly deformed primitive gabbro is thus considerably less than in differentiated gabbro. Over the lower 1000 m of the core described during Leg 176, the smaller proportion of oxide gabbro is about 15 times as likely as olivine gabbro to exhibit gneissic, porphyroclastic, or mylonitic textures (Natland, **Chap. 11,** this volume). Deformation is often strongest at interval boundaries, whether or not the oxide minerals are most concentrated at those boundaries.

A general conclusion of the scientists of both Legs 118 and 176 is that crystal-plastic deformation occurred at very high temperatures, at the minimum under granulite-facies metamorphic conditions, but very likely also at magmatic temperatures, as the resulting fabrics themselves are crosscut by granitic veins. In this light and given that the oxide gabbros are all in the broad sense intrusive rocks, were the deformed but oftimes very sharp "tectonic" contacts between oxide gabbros and more primitive hosts originally igneous in origin? The question is partly semantic. The modifier "igneous" should mean that at least some melt was present on one side or the other of a contact, however the present gabbro cumulates on either side may have formed. The only thing it precludes is the case where solids formally are juxtaposed across sharp boundaries, presumably in the course of subsolidus crystal-plastic deformation and plastic flow. Thus, among the rocks of Hole 735B, crystal-plastic deformation continued to act while melt was present, modifying many contacts between primitive and differentiated gabbros after and however they formed.

One rock type rarely included in the sequence of lithologic intervals is granitic veinlets. During Leg 176, some 203 of these were sufficiently prominent in the lower 1000 m of the core to be tabulated as "felsic veins" in the site report. Because they consist mainly of quartz and sodic plagioclase, they stand out starkly against their gray or dark gray host gabbros. Few of these are >1 cm thick, and many are sharply bounded, with straight edges standing at highly oblique angles to the core. From estimates of their volumes, they comprise about 0.5% of the material recovered during Leg 176.

Based on modes and chemical analyses (Shipboard Scientific Party, 1999c; Hertogen et al., **Chap. 6,** this volume; Niu et al., **Chap. 8,** this volume), the purest of these veins are trondhjemite and tonalite; one is granodiorite. Usually, however, some amount of matrix gabbro is either caught up in the veins themselves or was not completely removed from the samples selected for chemical analysis. The compositions of the resulting hybrids thus are dioritic. Also, there are many places in the core where such material is rather finely dispersed, either in sworls or vein breccias (Natland, **Chap. 11,** this volume). These instances were not included in estimates of vein volume, and not all are noted on the core barrel sheets in the site report.

Felsic veins crosscut all lithologies, but they are more decidedly associated with oxide gabbros than olivine gabbros. Even felsic veins in many olivine gabbros are immediately associated with narrow seams of oxide gabbro, sometimes splitting them down the middle (Natland, **Chap. 11,** this volume). Along the core, felsic veins are present at a rate of approximately one per meter in oxide gabbro, as opposed to one per 5 m in olivine gabbro. Almost certainly this means that rather than being anatectectites, most felsic veins represent an end product of magmatic differentiation following crystallization of oxide minerals, as demonstrated experimentally for abyssal-tholeiite liquids (Dixon and Rutherford, 1979; Juster et al., 1989); thus, they are preferentially asso-

ciated with oxide gabbros, which are nearest to them in stage of differentiation. From these locations, some of them branch into olivine gabbros.

The likely sequential cumulates of such extended magmatic differentiation, namely troctolite, olivine gabbro, gabbro, gabbronorite, disseminated-oxide gabbro, and oxide-rich gabbro, are all present in the core, and most, indeed, are represented in any given 50-m portion of the core. However, the complexly crosscutting relationships prevent tracing of the process of differentiation through any simple sequence or stratigraphic succession of these rocks in any part of the core, in the manner, for example, of the stratigraphy of upwardly more differentiated layered intrusions. Among the rocks of Hole 735B, no simple pattern of cryptic mineralogical variation exists (e.g., Ozawa et al., 1991; Dick et al., **Chap. 10,** this volume). The most striking and perhaps most fundamental feature of the core is that all of the later differentiates are simply not in place in the following sense: they do not encase a "sandwich horizon" including granophyres as they do at the Skaergaard Intrusion (Wager and Deer, 1939; Wager and Brown, 1967); indeed, they are not concentrated anywhere but are present at all levels in the core, invariably in small, sharply bounded bodies. Consequently, they attained their stages of differentiation elsewhere and were interleaved by some combination of intrusion and deformation in a matrix of primitive gabbros (Natland and Dick, 2001). They are examples of what Bowen (1920) termed "discontinuous differentiation" in a paper where he first outlined the general consequences of differentiation in masses of deforming, partially molten, igneous rock. Discontinuous differentiation is but one manifestation of what Bowen termed "differentiation by deformation." Much later, Dick et al. (1991a) used the term "synkinematic differentiation" to describe the same thing. Although differentiation by deformation has not been considered important in the crystallization of layered igneous intrusions, in the gabbros of Hole 735B it was a major process (Natland and Dick, 2001).

Another contrast with layered intrusions is that <2% of the total section of the core from Hole 735B has modal or graded layering of the type that is produced either by mechanical sorting of minerals separating from moving magmas or from compositional changes in magma during deposition of the minerals. The longest sequence of such material is only 9 m, within which there are 34 normally graded layers of olivine gabbro, each with plagioclase proportions and grain sizes increasing downward and ranging from 6 to 22 cm in thickness. The cause of this layering has not been determined. To some extent, this goes along with the small size of intervals of primitive gabbro, many of which are only a few tens of centimeters to a few meters thick. If these represent the typical dimensions of bodies of magma individually added to the lower crust, then they were never large enough to generate or sustain convective currents of magma within which minerals of different density might have separated.

THE OLIVINE GABBRO SUITE SEPARATELY CONSIDERED

Although injection of oxide gabbros at so many places in the core has greatly fragmented the stratigraphy of the underlying olivine gabbro suite, the spreadsheet for igneous contacts appended as a supple-

ment to the site report (Shipboard Scientific Party, 1999c) and Appendix II of Dick et al. (1991a) allow each group of rocks to be treated separately. There are 504 intervals of the olivine gabbro suite, most of them separated by one, and a few by more than one, narrow seam of oxide gabbro. Stacked end to end and leaving out all seams of the more differentiated gabbros, the olivine gabbro suite totals 1153 m of the core in terms of expanded recovery, as defined earlier. This is 76.4% of the 1508 m drilled. Within the 504 intervals, again neglecting the seams, the principal variations in the olivine gabbro suite are in grain size and percentage of olivine. Often, the two go hand in hand. That is, finer-grained rocks tend to be more olivine rich than coarser-grained rocks. The higher olivine proportion shows up especially in the high MgO and Ni contents of analyses of troctolites and troctolitic gabbros and in corresponding modal data (Shipboard Scientific Party, 1989, 1999c), but not every interval has been chemically analyzed. In many parts of the core, several consecutive intervals of medium- to coarse-grained olivine gabbro, leaving out the oxide-gabbro seams, are bounded by fine-grained olivine gabbro, fine-grained troctolitic gabbro, or fine-grained troctolite, using the terminology of Leg 176. Dick et al. (1991a) term the first two of these olivine microgabbro and troctolitic microgabbro, respectively. Usually grain-size transitions occur across fairly well defined sutured or gradational contacts. In some cases, transitions are more abrupt, as when certain fine-grained troctolitic gabbros have sharp, planar, evidently intrusive boundaries with medium- or coarse-grained olivine gabbro.

Within the olivine gabbro suite, there are 175 recovered internal contacts where one rock adjoins another of different grain size, mode, or mineralogy (Table T1). Add to these all others where contacts were not recovered, and there are 273 separate bodies of olivine gabbro intervals with uniform texture, grain size, and mineralogy that we term *composite intervals*. Since almost all of the recovered contacts are sutured igneous contacts, each of these might be a separate small intrusion. The average thickness of a composite interval is 4.2 m.

T1. Olivine-gabbro sequences, p. 54.

Each alternation of coarse-grained olivine gabbro and finer-grained, more olivine-rich gabbro or troctolite beneath it, combining two or more composite intervals, can be treated as a potential individual injection or series of pulses of magma that contributed to the thickness of the crust of Hole 735B at any one place in the section. Also, coarse- and fine-grained composite intervals do not merely alternate, but they are often separated by members of medium-grained olivine gabbro. Thus general *cycles* of grain size decreasing downward are common, with the finest-grained and most olivine-rich gabbros lying just above the coarsest-grained and least olivine-rich portion of the next underlying cycle of olivine gabbro. Finally, whereas coarse- and medium-grained members are usually up to several meters thick, fine-grained gabbros are almost always thin. The fine grain size may result from quenching of hot magma in cooler surroundings. Whatever the case, the olivine-charged magmas that supplied the thin, fine-grained intervals likely were fairly dense. For these reasons, we place the most olivine-rich rocks at the base of each alternation or cycle in grain size rather than the top.

Some complications to this pattern near the base of the hole are produced by several thick, graded, even layered intervals. Near the base of the hole as well are several intervals with variable grain size, including some with thin, vertical, pipelike bodies of troctolitic gabbro. These we include in the thicknesses of otherwise uniformly textured coarse olivine gabbro. Nevertheless, most of the primitive gabbros of Hole 735B

consist of an orderly succession of coarser olivine gabbros alternating with finer-grained olivine gabbro, olivine microgabbro, or troctolitic microgabbro (Table T1).

In the core, there are 97 such alternations or cycles of the olivine gabbro suite, which we term *olivine gabbro sequences*. For reasons discussed earlier, we use *sequence* in place of *unit,* a word that commonly refers to cyclicity in phase-layered igneous rocks and is the smallest subdivision of a *zone* within a *series* (Irvine, 1982). However, we connect *sequence* here not to phase layering over long distances but to disjunctions in grain size and/or modal proportions of olivine just in this single core. As with *cyclic units* in layered gabbros and peridotites, olivine is most concentrated at the base of each (e.g., Jackson, 1967, 1969; Irvine, 1969, 1980; Bédard et al., 1988; Emeleus et al., 1996).

This is somewhat arbitrary, but it forms the basis for a hypothesis: if all cycles result from one to several quickly spaced injections or pulses of magma at one place in the core, there were 97 such injections. If the individual composite intervals in a sequence are unrelated, then the olivine gabbro suite is made up of a maximum of 273 separate smaller intrusions. These alternatives are testable using chemistry and mineralogy and are useful to pose at the beginning of an evaluation of chemical stratigraphy. Sequences also provide a convenient shorthand means of assigning the rocks a stratigraphic order, of depicting them graphically, and of comparing one portion of the core to another.

Leaving out intervening oxide gabbros, olivine-gabbro sequences at Hole 735B average 12.0 m in thickness but only 35 of them are >10 m thick. The 35 thickest sequences themselves average 25.5 m thickness and together make up 917 m of the core, or 79% of the length of all the olivine gabbro sequences cored during both Legs 118 and 176. One sequence between 274 and 396 mbsf contains a series of olivine gabbro intervals that are separated by 11 seams of oxide gabbro. Most of this is one massive body of uniform olivine gabbro almost 112 m in composite thickness. This is one composite interval. Below this >9 m of core, the sequence has eight internal contacts of one olivine gabbro against another, all being somewhat more olivine rich than higher up and generally differing in grain size. A narrow olivine microgabbro is at the base. The olivine gabbro intervals, when combined, are 121 m thick, thickest in the entire core. Because the entire sequence is geochemically coherent, becoming more differentiated toward the top (see "Appendix A," p. 32), we view it as one intrusive mass with the several internal contacts perhaps being caused by pulses of magma injection or differences in the sizes, proportions, or densities of crystals—mainly olivine—the flowing magma was carrying at any given time, with these more concentrated toward the base of the intrusion. A similar group of composite intervals in another sequence is nearly 57 m in aggregate thickness, and two others are 43 and 40 m thick.

We do not know how any of these sequences thicken or thin in any direction, although they must. Portions of these sequences also are likely to have been displaced by faulting away from this vertical section, although most of the faults noted in the core descriptions are planar features in zones of crystal-plastic deformation and many are present at junctions between oxide and olivine gabbros. Doubtless, the core has numerous small lacunae, and perhaps substantial portions of the original section of olivine gabbros are now missing.

The thin basal fine-grained rocks are only a small proportion of each sequence (Table T1). Of the 96 basal intervals, 91 are fine or medium grained, and the remaining 5 are graded and perhaps are not at the

bases of complete sequences, which may have been obscured by or even removed along small faults during deformation. Of the 91 that are not graded, most are <0.5 m thick. The aggregate thickness of all 91 olivine-rich basal intervals is only 65.5 m, or <6% of all the primitive gabbro cored. Some are sill-like with sharp contacts on both sides and may have split preexisting olivine gabbro. However, the basal fine-grained facies of most of these is separated from coarser-grained overlying olivine gabbro by sutured, partially penetrative, or gradational igneous contacts. The rock on both sides thus was at least partially molten when the contacts formed, indicating rapid sequential injection.

Of the 97 potential composite injections of magma, only about a third really mattered, in the sense that they substantially thickened the crust (Fig. F4). The thinnest sequences tend to be strongly grouped. The most olivine-rich intervals are present in clusters of thin sequences, perhaps indicating pulses of variably phenocryst-charged magma. Many of the thicker sequences are deep in the hole, and between 800 and 1100 mbsf there are no very thin sequences. The very thickest stands out not just because it is so thick but also because it is near the top of the hole, and two clusters of narrow coarse–fine sequences bracket it. One small screen of olivine gabbro, an interval 8 cm thick, lies within the oxide gabbro ~1 m above the main body of lithologic Unit V, and there are three other screens of olivine gabbro near the top of the oxide gabbro. The one truly substantial mass of oxide gabbro in the core therefore is a composite body of extensively differentiated material that intruded the section right at the top of the largest mass of olivine gabbro cored in the entire hole. However, Figure F4 shows this as a line, since all intervals of differentiated gabbro have been left out of the diagram. The most important faults and shear zones, annotated to their actual depths in Figure F4, tend to occur where thin sequences of olivine gabbro are clustered. Perhaps they truncate or cause repetitions of sequences of olivine gabbro in these portions of the core.

F4. Olivine gabbro thickness, p. 50.

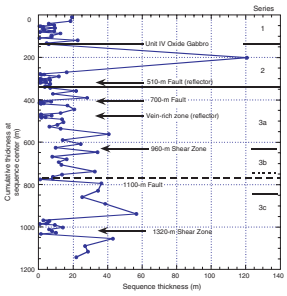

POSTCRUISE MODIFICATIONS TO THE SHIPBOARD CHEMICAL STRATIGRAPHY

Based on shipboard analyses, a fairly straightforward interpretation of the downcore trends in bulk-rock geochemistry seemed apparent at the end of Leg 176. It was that five major bodies of primitive gabbro, each more differentiated toward the top, each having olivine-rich, even troctolitic, gabbro at its base, and each some hundreds of meters thick, had contributed to the thickness of gabbros cored at the site (Shipboard Scientific Party, 1999c; Dick et al., 2000; Natland and Dick, 2001). These were subsequently intruded at hundreds of places by the more differentiated gabbros, most of them carrying visible oxide minerals, and this added several hundred more meters of rock to the section.

The five masses were called “plutons” (Shipboard Scientific Party, 1999c; Dick et al., 2000). Whether this term is technically appropriate may be questioned. However, each was viewed as having served separately for some time as a sustained locus of magma injection and differentiation before ceasing to function; thus, they might have been potential sources for chemically distinctive fine-grained dikes and extrusives that perhaps erupted at monogenetic cones of the type found on the rift valley floor along the Mid-Atlantic Ridge (Smith and Cann, 1992). Mineral compositions partially match those of common pheno-

crysts in abyssal tholeiites from the Indian Ocean (Natland and Dick, 2001). Each pluton also consists of rock crystallized from many separate injections of magma, as represented by igneous contacts between many lithologic intervals, so that there never was any single mass of molten material in the crust larger than several meters, or several tens of meters, thick. The original thicknesses of each injection, however, are difficult to say, since only a portion of them are present as cumulates from which almost all interstitial melt was expelled. The rocks now are adcumulates, with very low retained percentages of now-crystallized interstitial melt, most of which was removed by combinations of matrix compaction or filter pressing, partial dissolution and reprecipitation of silicate minerals, and deformation (Bloomer et al., 1991; Ozawa et al., 1991; Natland et al., 1991; Dick et al., 1991a; Natland and Dick, 2001). If the original intercumulus porosity was 40%–50% (Jackson, 1961), each injection then was about twice the thickness of the compacted crystalline residue that now remains.

The oxide gabbros, then, can be viewed as complementary to this process, since they seem to express, at least partly, where the expelled, and necessarily more differentiated, interstitial liquids went. The close association between oxide gabbros and zones of rock with gneissic, porphyroclastic, and mylonitic textures also implicated deformation with shear as a likely contributor to the forces that drove residual melt from the mass of consolidating and compacting cumulus minerals.

Natland and Dick (2001) used the procedure of Lange and Carmichael (1990) to calculate densities of synthetic liquids produced during equilibrium crystallization of parental abyssal tholeiites in the course of several studies. The synthetic liquids cover a full range in the extent of differentiation, and are all less dense than normative densities of Hole 735B gabbros, even when the latter are presumed to be hot and to contain several percent of interstitial melt. Normative densities are calculated from CIPW normative proportions using the procedure of Niu and Batiza (1991) and are only slightly higher than grain densities measured on actual specimens from Hole 735B (Shipboard Scientific Party, 1989, 1999c). Both are significantly higher than densities calculated for synthetic abyssal tholeiite liquids. When no other forces acted on them besides their own buoyancy, basaltic liquids in the crystallizing gabbros of Hole 735B thus tended to migrate generally upward in the mass of rock. They flowed along whatever avenues of escape they could find, following fluctuating patterns of porosity structure in the deforming rock on scales ranging from that between individual mineral grains to networks of fractures and channels, the largest of which correspond to the widths or thicknesses of oxide gabbro seams and many lithologic intervals. The process of compaction and expulsion of intercumulus melt continued even during the emplacement and crystallization of these rocks since they, as well as the olivine gabbros, are adcumulates. As the course of this flow was generally upward, it was also toward cooler rock; thus additional differentiation occurred, leading to formation of the late and usually undeformed veins of tonalite and trondhjemite.

This picture, however complicated it is in detail, was fairly satisfying and is still, for all the new analyses, mainly correct, at least as regards processes. What has changed, however, is the status of the five plutons. The three based on geochemical trends during Leg 176 and which comprise almost all the core retrieved during that leg have largely disappeared with the more complete perspective the new chemical analyses

provide. Nor do extensive mineral analyses provide a different picture. We now believe that the core should be described in the following way.

In a pair of downhole trends (Fig. F5), two principal bodies of olivine gabbro and allied more primitive types are apparent in the upper 540 m of core. The most differentiated rocks, with lowest Mg# and greatest TiO_2 contents, are at the tops of each. These are laced with seams of oxide gabbro—still lower in Mg# and very high in TiO_2. The new data reveal these trends more completely and precisely than before.

Splitting the two principal bodies almost exactly is lithologic Unit IV, the oxide gabbro complex already described, which has very high TiO_2 contents and is >50 m thick. Overall, however, the superposition of oxide gabbros onto more primitive olivine gabbros and troctolites provides a strong bimodality of composition to the upper 500 m of the core (Dick et al., 1991a). This is evident not just in geochemistry but in mineralogy as well (e.g., Ozawa et al., 1991). This is not to say that intermediate compositions are lacking, only that the preponderance of the core obtained during Leg 118, whether viewed from the perspectives of lithology, bulk composition, or mineralogy, falls into two main groupings.

With the Leg 176 drilling, however, the bimodality disappears below 540 mbsf. Instead, in both Mg# and TiO_2 contents the new samples align between the two principal ranges in Mg# and TiO_2 contents present in the upper third of the core (Fig. F5), and they are intermediate in other aspects of geochemistry as well. There are fewer oxide gabbros, particularly below 1100 mbsf, and there are fewer troctolites at all levels. A tendency toward more primitive compositions only emerges toward the bottom of the hole.

This gap filling was evident from the Leg 176 shipboard analyses, nevertheless, breaks in the trend, for example of Mg# among olivine gabbros at ~950 and 1350 mbsf, still suggested a continuation of the sequence of plutons. Now, however, with all the new data, there are no breaks in the trend of TiO_2 contents with depth to correspond with much feebler apparent discontinuities in Mg# at these depths. Although there is a cluster of somewhat more differentiated gabbros between 540 and 750 mbsf representing gabbronorites of lithologic Unit VII (denoted by dark gray symbols in Fig. F5), these actually intrude olivine gabbros and rare troctolites (light gray and black symbols, respectively). The latter, considered separately, are not especially more differentiated than olivine gabbros extending downward to 1200 mbsf. The apparently more differentiated upper portion of the pluton postulated between 540 and 950 mbsf that was construed from shipboard data therefore was an artifact of the tendency to sample the most representative rocks in a given core for XRF analysis. The minor olivine gabbros in a 9.5-m core were not sampled simply because there was not time to analyze everything. Also misconstrued was the top of the pluton postulated below 1350 mbsf. By improving coverage, the new analyses demonstrate greater chemical variability over short lengths of the core, and this has erased false boundaries between bodies of rock originally thought to represent major divisions of the core. This is supported by lack of discontinuities in the compositions of major silicate minerals (Dick et al., **Chap. 10,** this volume) and by measurements of magnetic susceptibility (Natland, **Chap. 11,** this volume). The latter clearly delineate the contrast between gabbros with and without magmatic oxide minerals up and down the core (Natland, **Chap. 11,** this volume) and

F5. Compositions of gabbros, p. 51.

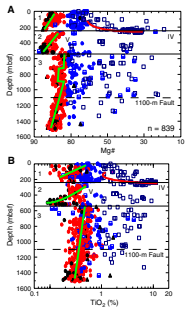

show that both types, not just the more differentiated oxide-bearing gabbros, are present at the tops of the formerly postulated plutons.

What alternatives are there now? Dick et al. (**Chap. 10,** this volume) believe that there are simply two domains of olivine gabbro in the core, one above and one below 540 mbsf, the two differing only in their degree or stage of differentiation. By different means, both Natland (**Chap. 11,** this volume) and Miller and Cervantes (**Chap. 7,** this volume) postulate some internal stratigraphy to the lower of these but do not see breaks in composition at the same places. Dick et al. (**Chap. 10,** this volume) raise the prospect that substantial reequilibration of some olivine gabbros toward more differentiated compositions has occurred because of wholesale migration of the melts that produced oxide-rich seams throughout fine porosity structure in much of the core. This in itself may have erased original petrochemical discontinuities among olivine gabbros. Dick et al. (**Chap. 10,** this volume) even propose this as the reason why the two upper chemical cycles in olivine gabbros above 540 mbsf—the two remaining of the original plutons—should now be treated as one.

For the present, we consider that there are three main *series* (Irvine, 1982) of olivine gabbro and allied troctolite down the core (Fig. **F5**). The upper two may still reasonably be interpreted as plutons in the sense described above, but the third may not, although we go so far as to recognize *zones* within it based on small shifts in composition down the core. The precise boundaries of series and zones and their relationships to sequences are given in **"Appendix A,"** p. 32. There may have been some significant shifts in the compositions, especially of ferromagnesian silicates, toward more differentiated compositions at various places in the core during reequilibration with percolating iron-rich melts, but to establish this, we need to consider mineral compositions in more detail than is possible at this time. These rocks cored during Leg 176, nevertheless, clearly are far more subtly variable than was originally determined on board ship.

MINERALOGY AND RELATIONSHIP TO THE COMPOSITION OF PARENTAL LIQUIDS

Figure **F6** compares compositions of olivine and plagioclase at all depths in the core (data compilation of Dick et al., **Chap. 10,** this volume). All mineral analyses from individual samples are plotted. The general trends in Mg# presented thus far are mimicked by variability in olivine compositions. The bimodal contrasts between the olivine-gabbro and oxide-gabbro suites are clearly evident in the upper 520 m of the core. The shift toward more differentiated olivine gabbro compositions below 520 mbsf can be seen in trends for both olivine and plagioclase. Wiggles in trends for bulk compositions in Zones 3a–3c show up here in trends of mineral compositions, as well.

Liquid Mg#s (= Mg_L) calculated from olivines using the formulation of Roeder and Emslie (1970) are indicated at the top of Figure **F5A.** The most primitive liquids involved in production of gabbros in Hole 735B were actually fairly strongly differentiated, with Mg_L no higher than ~61. Values of melt Mg_L down to 50, which would correspond to nearly the least Mg_L in glasses from abyssal tholeiites from either the Central or Southwest Indian Ridges in the Indian Ocean (Natland and Dick, 2001), represent only a small fraction of the core, all of it in the lower

F6. Olivine and plagioclase, p. 52.

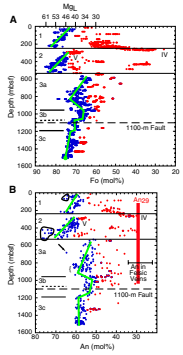

sequences of Series 1 and Series 2. Olivine gabbros of Series 3 crystallized from more differentiated (Mg_L = 46–35) ferrobasaltic liquids of types commonly found along the fast-spreading East Pacific Rise, but not to 98% of basalts erupted along slowly spreading ridges in the Indian Ocean.

The still more differentiated gabbros, including all of the oxide gabbros, crystallized from even more differentiated magma (e.g., Natland et al., 1991; Natland and Dick, 2001). Along the Southwest Indian Ridge, their evolution is locked up entirely in abyssal gabbros such as those from Hole 735B. Since oxide minerals and, in many cases, low-Ca pyroxenes were on the liquidus, comparison with experimental data on abyssal tholeiites (Walker et al., 1979; Juster et al., 1989) indicates that the relevant liquids were at least ferroandesitic in composition, although this depends on the precise character of the later development of the liquid line of descent. Analogy to experimental data suggests that magma temperatures were from ~1180° to 1150°C during the earliest stages of crystallization of the upper two plutons. From there they ranged down to perhaps 1100°C for the remaining olivine gabbros. Ilmenite and magnetite then reigned on the liquidus to below 1050°C if the environment was fairly dry. Trondhjemite at or near the "basalt solidus" crystallized at ~1000°C (Dixon and Rutherford, 1979).

CONSTRUCTION OF THE LOWER OCEAN CRUST

There is something fascinating about science. One gets such wholesale returns of conjecture out of such trifling investment of fact.—Mark Twain

Whereas gabbros of Series 1 and 2 may plausibly have been linked to eruptions on the floor of a rift valley, producing eruptives similar in composition and mineralogy to the usual types of abyssal tholeiite found on slowly spreading ridges, most of the gabbro locked in the lower ocean crust of Atlantis Bank experienced a more extended and profound differentiation. This in its later stages, as we have seen, was accompanied and perhaps even propelled by extensive crystal-plastic deformation (differentiation by deformation) (Bowen, 1920) to dramatic effect in the core. However, the more significant result of drilling in Hole 735B is that the entire lower two-thirds of the core and ~40% of the upper one-third crystallized in situ from magmas as least as differentiated as ferrobasalt, mainly before deformation. Comparing inferred compositions of liquids that crystallized to produce the olivine gabbro suite of Hole 735B and dredged gabbros (e.g., Bloomer et al., 1989) with glasses from basalts dredged in the vicinity (Dick et al., 1991a; Natland et al., 1991; Mahoney et al., 1992) and elsewhere (e.g., Natland, 1980; Sinton and Detrick, 1992), the economy of ferrobasalt at slowly spreading ridges thus seems to be that it forms extensively but it stays in the lower crust and only erupts extremely rarely.

Perhaps this should not be such a surprise. Rhodes et al. (1979) showed that many abyssal tholeiites from the Mid-Atlantic Ridge are hybrids, combining aliquots of both primitive and strongly differentiated basalt. One consequence of this, for example, is that Ni contents are higher in basalts of intermediate composition than in those that experience only crystallization differentiation and follow a simple closed-system line of descent. Mixing between primitive and differentiated components is evident in the compositions of phenocrysts as well, es-

pecially their zoning patterns (Rhodes and Dungan, 1979). Similar relationships exist in abyssal tholeiites from the Indian Ocean (Natland, 1991). The chemical data from the Mid-Atlantic Ridge indicate that the evolved mixing component must commonly be as differentiated as ferrobasalt (Natland, 1980). Therefore, rather than saying that ferrobasalt does not erupt at slowly spreading ridges, more accurately, some ferrobasalt does reach the seafloor, only it is in combination with more primitive material. Ferrobasalt is, to a degree, occult in the composition of many abyssal tholeiites at slowly spreading ridges.

The abundance of normally zoned phenocrysts at first suggested that many eruptions are immediately preceded by addition of primitive, phenocryst-laden magmas to shallow magma reservoirs containing extensively differentiated liquid. The precise location of mixing was presumed to be the interior of some kind of a magma chamber, within which cumulates had already lined the walls, floor, and roof (e.g., Bryan and Moore, 1977) (Fig. F2A). Indeed, entrainment of cumulates is a potential source for some of the large refractory megacrysts and phenocrysts found in many of the basalts. However, no one asked why such concentrated pods of ferrobasalt never seem simply to be displaced to the seafloor during an inflation–eruption cycle at a slowly spreading ridge as, for example, analogous lavas are along rift zones of Hawaiian volcanoes (e.g., Wright and Fiske, 1971) and the fast-spreading East Pacific Rise (Natland, 1980).

Hole 735B suggests a different sequence for the mixing. It is that it occurs prior to arrival in a magma chamber, while primitive magmas en route to high-level cupolas in pipelike conduit systems (Fig. F2E) pass through more differentiated gabbros still containing some amount of interstitial melt. Small magma chambers, or cupolas, clearly do form, produce normal successions of fairly primitive cumulates, and supply melt to the seafloor. But in Hole 735B, they formed at the top of the gabbroic section. We thus suggest that the upper two olivine gabbro series of Hole 735B represent a section through a portion of a shallow, laterally connected, body of hot, low-velocity rock analogous to that detected seismically along the Mid-Atlantic Ridge by Magde et al. (2000) and therefore that those comprise relatively primitive intrusions, whereas Series 3 represents the material below this and in between conduits (gray in Fig. F2E) and that this material is more differentiated.

Where does so much ferrobasaltic melt originate, and why does it crystallize below more primitive gabbro cupolas? We believe that the ferrobasaltic magma ultimately came from the interiors of small plutons like those cored at the top of the section but that such liquids were expelled, forced or squeezed out of those bodies once their links to mantle sources were broken and their internal overpressure dissipated (Fig. F7). Without this impulse, eruption to the seafloor became almost impossible, yet forces imparted by overburden, crustal dilation, and perhaps lateral penetration of low-angle detachment faults were still acting to drive residual magma from those cupolas into porous and partially molten surroundings. Even the minutest quantities of residual melt were driven out in the course of transformation of crystal mushes to adcumulates.

Flow of ferrobasalt magma was both along and across the ridge axis and probably was mainly directed beneath a permeability barrier at the brittle–ductile transition. Along the axial zone of hot, low-velocity rock, this barrier was quite shallow. Off axis to either side of the rift valley floor and over time with continued spreading, however, the brittle–ductile transition probably descended into the gabbroic section as heat was

F7. Shallow plutons, underplated olivine gabbro, and primitive cumulates, p. 53.

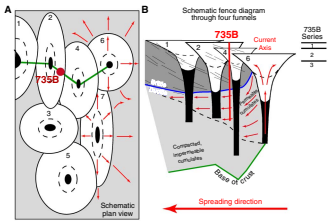

drawn off and crystallization proceeded. However, tectonic forces related to uplift of the plutonic section from beneath the rift valley floor and its eventual exposure (Natland and Dick, **History Chap.,** this volume) may actually have served to warp the transition upward and even to lower the pressure of accumulated rocks above it by removing them along high-angle detachment faults (Natland and Dick, **History Chap.,** this volume). In this way, buoyant magma could continue to aggregate beneath the brittle–ductile transition, even as its locus shifted deeper into the gabbros. Thus, we envision a process of thickening of the lower crust by injection of differentiated magma beneath inactive shallow cupolas as they are carried away from the center of the rift valley by spreading, while the total crustal thickness lessens with the removal of extrusives and dikes. This likely would sever vertical conduits from their sources in the mantle and probably dismember them in the process.

Students of layered intrusions commonly visualize them to be contained by impermeable country rock—the ultimate natural crucible. At a ridge axis, however, new pulses of magma released from the mantle encounter a range of hot, partially molten, and variable permeable material, namely cumulates that are not yet completely solid, and crystal mushes (Sinton and Detrick, 1992). At a slowly spreading ridge, we picture this process as being intermittent rather than continuous, at least over a span of tens of kilometers along axis. Ascending magma therefore must penetrate a sheath of partly molten cumulates before it can erupt. It will be buoyant even in a crystalline matrix containing as much as 20% pore melt (Natland and Dick, 2001), thus will tend to pass through whatever is already there, including the fraction of melt retained by the hot cumulates, and coalesce at the top of the stack at the brittle–ductile transition. The gauntlet from the mantle to this barrier is consequently where mixing with ferrobasaltic liquid occurs. Ascending magma is not plunged into a ferrobasalt bath; instead, ferrobasalt is added to it bit by bit along a tortuous passage.

Since uplift and exposure of plutonic sections at transverse ridges is an asymmetrical process, with extrusives and dikes being faulted away from the ridge axis in the opposite direction (Natland and Dick, **History Chap.,** this volume), so this process also is likely to be axially asymmetrical. Rupture of cupolas and expulsion of their residual ferrobasaltic magma into surrounding partly molten cumulates will be easier to the one side where crustal overburden is being relieved than to the other. The seismic thickness of the crust carried into rift mountains on either side of a rift valley might wind up being similar, but on one side the gabbroic portion of the crust will be thinner and, on the average, fairly primitive in composition; it will also contain almost all of the dikes and pillow lavas. On the other side, the dikes and pillows are largely missing, but the gabbro is thicker and carries a preponderance of more strongly differentiated compositions.

Figure **F7** represents the cupolas, or eventual plutons, as the cross-sections of funnels. This is a shape inferred for some layered intrusions (e.g., Muskox; Irvine, 1980; Great Dyke, Worst, 1958; Wilson, 1996), but we have no evidence that the two cored at Hole 735B were any particular shape at all. Funnels, however, are useful to make a point about the possible distribution of primitive cumulates, those derived from near primary magmas, in the lower ocean crust—what Coogan et al. (2001) term the *missing cumulates* of Atlantis Bank. Earlier, we mentioned that such cumulates might not be present in a layer between the bottom of Hole 735B and mantle peridotite, wherever that is, but in-

stead could lie out of the section. Bloomer et al. (1989) and Dick et al. (2000), for example, suggest that primitive cumulates are concentrated nearer the centers of spreading segments along slowly spreading ridges; thus, they may not even be present at transverse ridges near transform faults. Figure F7, however, is drawn to suggest that primitive cumulates do not have to be very far away. They could be in narrow columns marking the feeders to every shallow, flatter cupola and thus are surrounded, undercut, and probably crosscut and distorted by subsequently emplaced differentiated gabbro. Perhaps as well, most conduits are separated asymmetrically during spreading to the other side of the rift valley. In such a case, we would rarely, if ever, encounter remnants of these conduits on transverse ridges. This may be why differentiated gabbros similar to those of Hole 735B rather than primitive gabbros are so commonly recovered in the same dredge hauls as peridotite from transverse ridges in the Indian Ocean and elsewhere (Francheteau et al., 1976; Dick, 1989; Bloomer et al., 1989).

Magde et al. (2000) identified two columns in their seismic experiment that they described as active vertical magma conduits (Fig. F2E). The two columns are places where injections of magma from the mantle "travel upward until they intersect the brittle–ductile transition, where they are then diverted along-axis to supply shallow intrusive bodies and seafloor eruptions along much of the ridge segment (Magde et al., 2000, p. 55)."

Although this interpretation has appeal, the geophysical data by themselves do not demonstrate either that the two columns are long lived or that they are responsible for the entire interconnected shallow zone of low velocity. The columns may instead be the only two currently detectable, the roots of older ones having solidified completely by formation of adcumulates and then cooled after perhaps thousands of years of inactivity. The shallow along-axis low-velocity region then is simply a series of coalesced cupolas, their sources now completely choked off, which are not yet completely frozen. Along-axis flow is likely restricted to some few kilometers between these; it need not extend for ≥20 km from the ones that are currently active. Whatever the case, the seismic images lend credence to the notion that early high-temperature cumulates may be restricted to columns beneath individual volcanoes, and they demonstrate that there is a large volume of lower crust with higher seismic velocities through which these columns extend.

In terms of previous models for magma chambers at slowly spreading ridges, we suggest that the "temporary high-level chamber" of the infinite leek in Figure F2B (Nisbet and Fowler, 1978) and the shallow, axially linked, low-velocity rocks of Magde et al. (2000) in Figure F2E are one and the same and correspond to our two uppermost plutons. They are present at the top of the gabbroic layer because primitive basaltic melt is buoyant in the hot, nearly consolidated cumulates that they typically encounter upon arrival from the mantle (Nisbet and Fowler, 1978; Natland and Dick, 2001). Rocks cored below the upper two plutons in Hole 735B, however, actually represent the bulk of the lower ocean crust in either model. In the leek model, these are viewed as accreted from myriad vertical fissures, many of them derived from distributed melt pods in the lower crust that do not necessarily link to the shallow, temporary chambers. In part, we view the equivalent process in Hole 735B as that which produced the hundreds of seams of crosscutting oxide gabbros and their associated felsic/granitic veins, except

that the flow paths for these were distorted from the vertical by tangential shear.

The feeder pipes in the model of Magde et al. (2000) are the only ones currently detectable seismically at that place on the Mid-Atlantic Ridge, and they have no counterparts in scale in the leek model. However, in our conception, they consolidate by expulsion of melt, crystallization, and compaction and are cut off at their bases as spreading proceeds. This is very much in the way Nisbet and Fowler (1978) proposed that their vertical fractures expel their melt and seal off. There may be fossil off-axis feeder pipes on one side or other of the rift-valley floor, which simply were not detected seismically in the experiment reported by Magde et al. (2000). The along-axis flow they propose may therefore be quite limited if the three volcanoes without detectable feeder pipes in Figure F2E actually have fossilized, consolidated, or pinched-off ones beneath them.

COMPARISON TO FAST-SPREADING CRUST AND THE OMAN OPHIOLITE

At ocean islands, crust is thickened directly beneath high volcanoes by intrusion of primitive hot-spot magmas at the crust–mantle transition, a process termed underplating (e.g., McNutt and Bonneville, 1999). The process that we have described is similar, except that it occurred just off axis at a slowly spreading ridge and it probably was not symmetrically distributed about the ridge axis. Nevertheless, a wedge of plutonic material, gabbro, is also driven between shallow igneous masses and the mantle.

Deep intrusion near the crust–mantle transition has recently been proposed to occur at fast-spreading ridges. However, it is different from the case of Hole 735B. Crawford et al. (1999) suggest that the lowermost crust just at the mantle transition along the East Pacific Rise is a zone of rheological contrast that favors lateral injection of primitive magma supplied from the mantle. These produce high-temperature and perhaps sill-like cumulates of the type found at Hess Deep in the eastern Pacific (Hékinian et al., 1993) and Oman (Boudier et al., 1996; Kelemen et al., 1997; Kelemen and Aharanov, 1999). Magma appears to follow the path of least resistance at the mantle transition, perhaps because it is charged with olivine phenocrysts and is thus fairly dense (Natland and Dick, 1999).

Along the slowly spreading Southwest Indian Ridge, however, imagine that crustal construction is centered on small and often isolated cupolas arrayed along the ridge axis. Imagine also that these are emplaced infrequently and in disconnected fashion, as befits a slowly spreading ridge (Flower and Robinson, 1979). Now consider the next substantial packet of magma to arrive from the mantle. Where will it find the path of least resistance? We argue that in this situation it should be near the top of the crystallizing cupolas, not the mantle transition.

Neutral buoyancy has little to do with this. The strength of the sidewalls to conduits has everything to do with it. Water under pressure flowing through a sprinkler system does not care whether the tubing is made of dense copper or light plastic. It only cares where the holes are or where it can make a hole if there is enough pressure. In a magma plumbing system, if the surrounding rock contains no melt, even if it is still hot, it is impermeable, whether it is made of peridotite or gabbro.

Magma will rise through it until overpressure overcomes the vertical load, and then it can flow sideways, lifting the rocks overhead. With enough overpressure, magma can leak sideways at many points all along the length of a long column (drip irrigation) as long as there is an impermeable cap at the end of the path. Obviously, wherever there already is significant melt porosity, that is an easy place to make a hole or to expand one already there.

Formation of adcumulates, which was undoubtedly important in the rocks of Hole 735B (Natland et al., 1991; Natland and Dick, 2001), is thus a critical process that determines the size and distribution of permeability pathways at spreading ridges. At the East Pacific Rise, melt porosity in cumulates right at the ridge axis is very low, only a few percent, and this is an important factor in melt transport through the lower crust and in the formation of shallow melt lenses (Natland and Dick, 1996). In the lower crust at a slowly spreading ridge, where the magma recharge rate is much smaller than along the East Pacific Rise, residual melt right beneath the ridge axis under the rift valley floor is expelled even more nearly to completion between each inflation–injection cycle. The rock, especially that deep in the crust, and though still quite hot—well above the basalt solidus—becomes virtually impermeable beyond distances of more than a few meters. It can fracture, but magmas ascending in the fractures sense only barriers on either side. The mantle transition therefore is transparent. It cannot be a preferred place for lateral magma injection. The only place where ascending magma may ultimately find some horizontal leeway is where any bit of melt is puddled, and the most likely place for this is near the tops of slowly crystallizing magma cupolas, where the crustal load is also less and where there is also a permeability cap. This in general explains why central conduits through nearly crystalline gabbroic material form at slowly spreading ridges (Magde et al., 2000) (Fig. **F2E**).

A fine point must come during formation of adcumulates when they effectively become solid and impermeable, yet they can still contribute some strongly differentiated liquid to an ascending magma column. Perhaps mixing between primitive magma and ferrobasalt is not strictly between melts but consists of ascending magma reacting with and partially assimilating engulfed blocks containing bits of melt in the diameter of a conduit network. The effect of this on foundered blocks at the Skaergaard intrusion, for example, was that they lost total iron as FeO*, TiO_2, and P_2O_5 to liquids in surrounding cumulates (Sonnenthal and McBirney, 1998).

The East Pacific Rise, in one final contrast, is a place where a considerably higher rate of magma recharge ensures that there will still be melt pockets deep in the lower crust. Residual melt is expunged from cumulates, but not so efficiently and completely as at a slowly spreading ridge. Here, the wall is weak. Thus, a rising packet of magma will first encounter potential porosity in the column at the base of the crust and is able to spread laterally in sill-like masses. Crustal accretion above this may be mainly by straightforward diking or by drip irrigation from intrusions that are dikelike in character. The upper melt lens forms at a permeability barrier, the cap at the end of the system.

LATE-STAGE DIFFERENTIATION

Throughout Series 3 in Hole 735B, gabbro compositions are quite uniform. They are not appreciably more differentiated upward, unlike

gabbros of Series 1 and 2. Temperatures of crystallization were restricted, whereas steeper thermal gradients prevailed when the rocks of Series 1 and 2 crystallized. Probably this is because the two plutons were emplaced at shallow depths at the ridge axis, where the full extrusive layer had not yet accumulated, and hydrothermal circulation could readily draw off considerable heat from the shallow magma bodies, forcing differentiation. Later, off axis, a thickened insulating upper crustal blanket capped the gabbros and continued intrusion of small magma bodies at many levels (drip irrigation) stabilized the temperature gradient, driving isotherms upward even as the section moved away from its primary source of heat. This was intrinsically a convective redistribution of heat by moving magma. Thus, the deeper olivine gabbros of Series 3 are at once more differentiated and more uniform in composition. Most of them also have a very coarse grain size (Shipboard Scientific Party, 1999c).

After initial injection and crystallization of axial plutons and off-axis intrusion, the third and final stage of the development of the lower crust in Hole 735B was relocation of late, imprisoned differentiates along numerous zones of weakness and shear that developed during initial stages of high-temperature crystal-plastic deformation. These tried to escape but could not. In a body of upraised isotherms and nearly uniform temperature from top to bottom, extremely differentiated oxide gabbros and trondhjemites could crystallize virtually anywhere in the section, and they did.

However, even the most iron-rich of these melts were buoyant in their crystalline matrix (Natland and Dick, 2001); thus, they tended to rise and concentrate higher in the section. Buoyancy was not the only force that acted on the melts, but it is the only one that was always present. The flow likely was modified by encounter with permeability barriers and possibly by dilatancy that opened in the course of deformation. The thick oxide gabbro of lithologic Unit IV represents a coalescence of strongly differentiated magmas. Some hundreds of meters of equivalent vertical section of differentiated cumulates are necessary to explain the thickness of Unit IV (Natland and Dick, 2001), although these need not immediately underlie these rocks. Unit IV is sandwiched precisely between two plutons, and it supplied trondhjemetic veinlets to cement the breccias at the top of the one underneath. We suggest that the repeated intrusion of these very late stage differentiates at this special location occurred because of the presence of a permeability pathway between two impermeable rock masses. The one beneath is the largest sequence of olivine gabbro in the entire section. Above it was the base of the upper pluton. The two together served to direct the flow of extreme differentiates into this narrow zone as expelled melt ascended from underlying compacting cumulates.

The oxide gabbros of lithologic Unit IV formed well within the gabbroic portion of the crust and seemingly at a location dictated by the existence of a narrow permeability pathway between more massive rocks. Therefore, it was never a melt lens of the kind detected seismically at the top of gabbros along the axis of the East Pacific Rise, and it never contained enough melt in it at any one time to be detectable seismically on its own, had that been possible 11 m.y. ago. It was merely the closest that this particularly slowly spreading ridge could produce in the way of a melt lens, given its low rate of magma supply. The oxide gabbros and other zones with strong preferred orientations of minerals provide potential analogs to sources of deep seismic reflections elsewhere in the ocean crust (Itturino et al., 1991; **Chap. 5,** this volume).

AFTERMATH

From this point, the rocks cooled slowly to below their solidus. U-Pb ages on zircons from granitic veins average 11.93 ± 0.14 Ma (John et al., submitted [N1]). This is ~0.2 m.y. older than the age of magnetization of the rocks as estimated from the placement of Hole 735B in crust that formed slightly earlier than Anomaly C5r.2n, which spanned 11.48–11.53 Ma (Dick et al., 1991b). This was the time it took after the last igneous minerals crystallized for the rocks to drop below their Curie temperatures. Other minerals, namely amphibole, biotite, and titanite obtained from shear zones in oxide gabbros and felsic veins, give younger ages that indicate conductive cooling at a rate of 65°C/m.y., following an initial rapid cooling of 800°C in the first 0.5 m.y. at depths between 2 and 3.4 km beneath the rift valley floor. About 30% of the original heat was present after the uplift of this portion of Atlantis Bank from beneath the rift valley floor (John et al., submitted). The gabbros of Hole 735B therefore took a long time to cool. Why?

Thickening of the lower crust by asymmetrical intrusion as described here is one way of sustaining geothermal gradients for some distance off axis. We believe that it extended to the rift valley walls because master faults that reached downward from those walls penetrated partially molten rock that included a great thickness of underplated gabbro. The distance from the present ridge axis to the rift valley wall to the south is only 4.3 km. Spreading toward this wall occurs at 1.0 cm/yr (Dick et al., 1991b); thus, the rocks of Hole 735B evidently spent ~0.4 m.y. beneath the rift. In this time, all crystallization, all high-temperature deformation and metamorphism, and all locking in of magnetic structure took place. The rocks have somewhat scattered but nevertheless consistent magnetic orientations throughout and are sufficiently magnetized to account for the intensity of the magnetic anomaly measured over the site (Dick et al., 2000). Possible long-lived, long-offset faults marked by brittle–ductile shear zones at 490, 560, and 690–700 mbsf noted by John et al. (submitted) do not disturb the magnetic orientation of the rocks and, in fact, do not mark important differences in core composition or lithology. They were evidently active mainly before magnetic properties were locked in, and thus did not disturb them. The entire section in Hole 735B consequently cooled through the Curie temperature virtually as a unit. This was because crystallization and crystallization differentiation earlier had ceased in all the rocks at about the same time and at nearly the same temperature. This was a consequence of the thermal regime imposed by thickening of the lower crust, the condition that allowed very late stage melts to crystallize as oxide gabbros with associated granitic veinlets throughout the core.

The gabbro drilled in Hole 735B continued to behave as a coherent structural block from the time the magnetic structure was set up until the present, leaving it with a single, consistent magnetic inclination throughout (Kikawa and Pariso, 1991; Pariso et al., 1991; Kikawa and Ozawa, 1992; Pariso and Johnson, 1993; Shipboard Scientific Party, 1999c; Dick et al., 2000). This spans the time from initial exposure of the boundary of the block at the rift valley wall, uplift to sea level, erosion and partial sedimentation of the summit, loss of the last 30% of heat the block contained to its present levels (John et al., submitted), and subsidence to the present depth of 719 m. The vertical displacement of the top of the hole from an original location in a rift valley ~3 km below the seafloor to its maximum elevation was ~9 km. The total

displacement along whatever master fault this required must have been significantly greater than this. This did not significantly perturb the thermal structure. Exposure of the block did not accelerate the cooling rate (John et al., submitted) or disrupt it structurally other than tilting it by ~19°.

The coring success in Hole 735B has been ascribed to serendipity, in reference to the way in which the site was seemingly targeted by chance during Leg 118. The site selection was more thought out than this (Natland and Dick, **History Chap.,** this volume). However, an epitaph for Hole 735B might be that if there was serendipity involved in the site selection, it consisted in dropping the hard-rock base on such a coherent block, one that cored magnificently, and that this good fortune finally allowed us, 17 yr after the drilling was first proposed, to reconstruct much of the early history of accretion of the lower ocean crust at this slowly spreading ridge.

ACKNOWLEDGMENTS

Our synthesis would have been impossible without the stimulating environment aboard *JOIDES Resolution* provided by the frequent arrival of spectacular core and the care with which observations were made on it. The ship's officers and crew, and particularly the rig crew, ensured the former, and the scientific parties of Legs 118 and 176 provided the latter. We are also indebted to the Shipboard Scientific Parties for a great deal of the intellectual substance of our synthesis. We are especially indebted to the co-chief scientists of Leg 118, Richard Von Herzen and Paul Robinson, for their many considerations over the years. Peter Meyer, H.R. Naslund, and an anonymous reviewer commented extensively on the manuscript, to its great benefit.

REFERENCES

Banerji, D., Casey, J.F., and Miller, D.J., 2000. Compositional ranges, cryptic chemical variations, and lateral correlation of gabbroic rocks between Holes 1105A and 735B, Southwest Indian Ridge. *Eos,* 81:F1131.

Bédard, J., Sparks, R.S.J., Renner, R., Cheadle, M.J., and Hallworth, M.A., 1988. Peridotite sills and metasomatic gabbros in the Eastern Layered Series of the Rhum complex. *J. Geol. Soc.,* 145:207–224.

Bloomer, S.H., Meyer, P.S., Dick, H.J.B., Ozawa, K., and Natland, J.H., 1991. Textural and mineralogic variations in gabbroic rocks from Hole 735B. *In* Von Herzen, R.P., Robinson, P.T., et al., *Proc. ODP, Sci. Results,* 118: College Station, TX (Ocean Drilling Program), 21–39.

Bloomer, S.H., Natland, J.H., and Fisher, R.L., 1989. Mineral relationships in gabbroic rocks from fracture zones of Indian Ocean ridges: evidence for extensive fractionation, parental diversity, and boundary-layer recrystallization. *In* Saunders, A.D., and Norry, M.J. (Eds.), *Magmatism in the Oceanic Basins*. Spec. Publ.—Geol. Soc. London, 42:107–124.

Boudier, F., Nicolas, A., and Ildefonse, B., 1996. Magma chambers in the Oman Ophiolite: fed from the top and the bottom. *Earth Planet. Sci. Lett.,* 144:239–250.

Bougault, H., Joron, J.L., and Treuil, M., 1979. Alteration, fractional crystallization, partial melting, mantle properties from trace elements in basalts recovered in the North Atlantic. *In* Talwani, M., Harrison, C.G., and Hayes, D.E. (Eds.), *Deep Drilling Results in the Atlantic Ocean: Ocean Crust.* Am. Geophys. Union, Maurice Ewing Ser., 2:352–368.

Bryan, W.B., and Moore, J.G., 1977. Compositional variations of young basalts in the Mid-Atlantic Ridge rift valley near lat 36°49′N. *Geol. Soc. Am. Bull.,* 88:556–570.

Casey, J.F., Miller, D.J., Banerji, D., and the Leg 179 Scientific Party, 1999. Correlation of gabbroic units over a distance of 1.2 km between ODP Holes 1105A and 735B. *Eos*, 80:F956.

Coogan, L.A., MacLeod, C.J., Dick, H.J.B., Edwards, S.J., Kvassnes, A., Natland, J.H., Robinson, P.T., Thompson, G., and O'Hara, M.J., 2001. Whole-rock geochemistry of gabbros from the Southwest Indian Ridge: constraints on geochemical fractionations between the upper and lower oceanic crust and magma chamber processes at (very) slow-spreading ridges. *Chem. Geol.,* 178:1–22.

Crawford, W.C., Webb, S.C., and Hildebrand, J.A., 1999. Constraints on melt in the lower crust and Moho at the East Pacific Rise, 9°48′N, using seafloor compliance measurements. *J. Geophys. Res.,* 104:2923–2939.

Dick, H.J.B., 1989. Abyssal peridotites, very slow spreading ridges and ocean ridge magmatism. *In* Saunders, A.D., and Norry, M.J. (Eds.), *Magmatism in the Ocean Basins*. Spec. Publ.—Geol. Soc. London, 42:71–105.

Dick, H.J.B., Meyer, P.S., Bloomer, S., Kirby, S., Stakes, D., and Mawer, C., 1991a. Lithostratigraphic evolution of an in-situ section of oceanic Layer 3. *In* Von Herzen, R.P., Robinson, P.T., et al., *Proc. ODP, Sci. Results,* 118: College Station, TX (Ocean Drilling Program), 439–538.

Dick, H.J.B., Natland, J.H., Alt, J.C., Bach, W., Bideau, D., Gee, J.S., Haggas, S., Hertogen, J.G.H., Hirth, G., Holm, P.M., Ildefonse, B., Iturrino, G.J., John, B.E., Kelley, D.S., Kikawa, E., Kingdon, A., LeRoux, P.J., Maeda, J., Meyer, P.S., Miller, D.J., Naslund, H.R., Niu, Y., Robinson, P.T., Snow, J., Stephen, R.A., Trimby, P.W., Worm, H.-U., and Yoshinobu, A., 2000. A long in situ section of the lower ocean crust: results of ODP Leg 176 drilling at the Southwest Indian Ridge. *Earth Planet. Sci. Lett.,* 179:31–51.

Dick, H.J.B., Schouten, H., Meyer, P.S., Gallo, D.G., Bergh, H., Tyce, R., Patriat, P., Johnson, K.T.M., Snow, J., and Fisher, A., 1991b. Tectonic evolution of the Atlantis II Fracture Zone. *In* Von Herzen, R.P., Robinson, P.T., et al., *Proc. ODP, Sci. Results,* 118: College Station, TX (Ocean Drilling Program), 359–398.

Dixon, S., and Rutherford, M.J., 1979. Plagiogranites as late-stage immiscible liquids in ophiolite and mid-ocean ridge suites: an experimental study. *Earth Planet. Sci. Lett.,* 45:45–60.

Dungan, M.A., and Rhodes, J.M., 1978. Residual glasses and melt inclusions in basalts from DSDP Legs 45 and 46: evidence for magma mixing. *Contrib. Mineral. Petrol.,* 67:417–431.

Emeleus, C.H., Cheadle, M.J., Hunter, R.H., Upton, B.G.J., and Wadsworth, W.J., 1996. The Rum layered suite. *In* Cawthorn, R.G. (Ed.), *Layered Intrusions:* Amsterdam (Elsevier), 403–439.

Flower, M.J.F., and Robinson, P.T., 1979. Evolution of the 'FAMOUS' ocean ridge segment: evidence from submersible and deep-sea drilling investigations. *In* Talwani, M., Harrison, C.G., and Hayes, D.E. (Eds.), *Deep Drilling Results in the Atlantic Ocean: Ocean Crust.* Am. Geophys. Union, Maurice Ewing Ser., 2:314–330.

Francheteau, J., Choukroune, P., Hékinian, R., LePichon, X., and Needham, H.D., 1976. Oceanic fracture zones do not provide deep sections in the crust. *Can. J. Earth Sci.,* 13:1223–1235.

Hart, S.R., Blusztajn, J., Dick, H.J.B., Meyer, P.S., and Muehlenbachs, K., 1999. The fingerprint of seawater circulation in a 500-meter section of ocean crust gabbros. *Geochim. Cosmochim. Acta,* 63:4059–4080.

Hékinian, R., Bideau, D., Francheteau, J., Lonsdale, P., and Blum, N., 1993. Petrology of the East Pacific Rise crust and upper mantle exposed in the Hess Deep (eastern equatorial Pacific), *J. Geophys. Res.,* 98:8069–8094.

Holm, P.M., 2002. Sr, Nd, and Pb isotopic composition of in situ lower crust at the Southwest Indian Ridge: results from ODP Leg 176. *Chem. Geol.,* 184:195–216.

Irvine, T.N., 1969. Crystallization sequences in the Muskox intrusion and other layered intrusions. I. Olivine-pyroxene-plagioclase relations. *In* Visser, D.J.L., and Von Bruenewaldt, G. (Eds.), *Symposium on the Bushveld Igneous Complex and Other Layered Intrusions*. Spec. Publ.—Geol. Soc. S. Africa, 1:441–476.

————, 1980. Magmatic infiltration metasomatism, double-diffusive fractional crystallization, and adcumulus growth in the Muskox Intrusion and other layered intrusions. *In* Hargraves, R.B. (Ed.), *Physics of Magmatic Processes:* Princeton, NJ (Princeton Univ. Press), 325–384.

————, 1982. Terminology for layered intrusions. *J. Petrol.,* 23:127–162.

Iturrino, G.J., Christensen, N.I., Kirby, S., and Salisbury, M.H., 1991. Seismic velocities and elastic properties of oceanic gabbroic rocks from Hole 735B. *In* Von Herzen, R.P., Robinson, P.T., et al., *Proc. ODP, Sci. Results,* 118: College Station, TX (Ocean Drilling Program), 227–244.

Jackson, E.D., 1961. Primary textures and mineral associations in the ultramafic zone of the Stillwater complex, Montana. *Geol. Surv. Prof. Pap. U.S.,* 358.

————, 1967. Ultramafic cumulates of the Muskox, Great Dyke, and Bushveld intrusions. *In* Wyllie, P.J. (Ed.), *Ultramafic and Related Rocks:* New York (Wiley), 20–38.

————, 1969. The cyclic unit in layered intrusions—a comparison of repetitive stratigraphy in the ultramafic parts of the Stillwater, Muskox, Great Dyke, and Bushveld Complexes. *In* Visser, D.J.L., and Von Gruenewaldt, G. (Eds.), *Symposium on the Bushveld Igneous Complex and Other Layered Intrusions*. Spec. Publ.—Geol. Soc. S. Africa, 1:391–424.

Johnson, H.P., 1979. Paleomagnetism of igneous rock samples—DSDP Leg 45. *In* Melson, W.G., Rabinowitz, P.D., et al., *Init. Repts. DSDP,* 45: Washington (U.S. Govt. Printing Office), 387–396.

Juster, T.C., Grove, T.L., and Perfit, M.R., 1989. Experimental constraints on the generation of FeTi basalts, andesites, and rhyodacites at the Galapagos Spreading Center, 85°W and 95°W. *J. Geophys. Res.,* 94:9251–9274.

Kelemen, P.B., and Aharonov, E., 1999. Periodic formation of magma fractures and generation of layered gabbros in the lower crust beneath oceanic spreading cen-

ters. *In* Buck, R., Delaney, P.T., Karson, J.A., and Lagabrielle, Y. (Eds.), *Faulting and Magmatism at Mid-Ocean Ridges*. Am. Geophys. Union Monogr., 106:267–289.

Kelemen,P.B., Koga, K., and Shimizu, N., 1997. Geochemistry of gabbro sills in the crust-mantle transition zone of the Oman ophiolite: implications for the origin of the oceanic lower crust. *Earth Planet Sci. Lett.,* 146:475–488.

Kempton, P.D., Hawkesworth, C.J., and Fowler, M., 1991. Geochemistry and isotopic composition of gabbros from Layer 3 of the Indian Ocean crust, Hole 735B. *In* Von Herzen, R.P., Robinson, P.T., et al., *Proc. ODP, Sci. Results,* 118: College Station, TX (Ocean Drilling Program), 127–143.

Kikawa, E., and Ozawa, K., 1992. Contribution of oceanic gabbros to sea-floor spreading magnetic anomalies. *Science,* 258:796–799.

Kikawa, E., and Pariso, J.E., 1991. Magnetic properties of gabbros from Hole 735B, Southwest Indian Ridge. *In* Von Herzen, R.P., Robinson, P.T., et al., *Proc. ODP, Sci. Results,* 118: College Station, TX (Ocean Drilling Program), 285–307.

Lange, R., and Carmichael, I.S.E., 1990. Thermodynamic properties of silicate liquids with emphasis on density, thermal expansion, and compressibility. *In* Nicholls, J., and Russell, J.K., (Eds.), *Modern Methods of Igneous Petrology: Understanding Magmatic Processes*. Mineral. Soc. Am., Rev., 24:25–64.

LeRoex, A.P., Dick, H.J.B., and Fisher, R.L., 1989. Petrology and geochemistry of MORB from 25°E to 46°E along the Southwest Indian Ridge: evidence for contrasting styles of mantle enrichment. *J. Petrol.,* 30:947–986.

Magde, L.S., Barclay, A.H., Toomey, D.R., Detrick, R.S., and Collins, J.A., 2000. Crustal magma plumbing within a segment of the Mid-Atlantic Ridge, 35°N. *Earth Planet. Sci. Lett.,* 175:55–67.

Mahoney, J., le Roex, A.P., Peng, Z., Fisher, R.L., and Natland, J.H., 1992. Western limits of Indian MORB mantle and the origin of low $^{206}Pb/^{204}Pb$ MORB: isotope systematics of the central Southwest Indian Ridge (17°–50°E). *J. Geophys. Res.,* 97:19771–19801.

Marsh, B.D., 1989. Magma chambers. *Annu. Rev. Earth Planet. Sci.,* 17:439–474.

McNutt, M., and Bonneville, A., 1999. A shallow, chemical origin for the Marquesas Swell. *Geochem. Geophys. Geosyst.,* 1:1999GC00028.

Meurer, W.P., and Natland, J.H., 2001. A survey of apatite compositions from oceanic cumulates with implications for the evolution of mid-ocean-ridge magmatic systems. *J. Volcanol. Geotherm. Res.,* 110:281–298.

Natland, J.H., 1979. Comparison of the chemical and magnetic stratigraphy of basement rocks at DSDP Sites 332 and 395. *In* Melson, W.G., Rabinowitz, P.D., et al., *Init. Repts. DSDP,* 45: Washington (U.S. Govt. Printing Office), 657–677.

————, 1980. Effect of axial magma chambers beneath spreading centers on the compositions of basaltic rocks. *In* Rosendahl, B.R., Hekinian, R., et al., *Init. Repts. DSDP,* 54: Washington (U.S. Govt. Printing Office), 833–850.

————, 1991. Indian Ocean crust. *In* Floyd, P.A. (Ed.), *Oceanic Basalts:* Glasgow (Blackie), 288–310.

Natland, J.H., and Dick, H.J.B., 1996. Melt migration through high-level gabbroic cumulates of the East Pacific Rise at Hess Deep: the origin of magma lenses and the deep crustal structure of fast-spreading ridges. *In* Mével, C., Gillis, K.M., Allan, J.F., and Meyer, P.S. (Eds.), *Proc. ODP, Sci. Results,* 147: College Station, TX (Ocean Drilling Program), 21–58.

————, 1999. Origin of melt lenses at the East Pacific Rise: inferences from textures and compositions of gabbros and dikes at Hess Deep. *Eos, Trans. Am. Geophys. Union,* T32A-05 (Abstract).

————, 2001. Formation of the lower ocean crust and the crystallization of gabbroic cumulates at a very slowly spreading ridge. *J. Volcanol. Geotherm. Res.*, 110:191–233.

Natland, J.H., Meyer, P.S., Dick, H.J.B., and Bloomer, S.H., 1991. Magmatic oxides and sulfides in gabbroic rocks from Hole 735B and the later development of the liquid

line of descent. *In* Von Herzen, R.P., Robinson, P.T., et al., *Proc. ODP, Sci. Results,* 118: College Station, TX (Ocean Drilling Program), 75–111.

Nisbet, E.G., and Fowler, C.M.R., 1978. The Mid-Atlantic Ridge at 37° and 45°N: some geophysical and petrological constraints. *Geophys. J. R. Astron. Soc.,* 54:631–660.

Niu, Y.-L., and Batiza, R., 1991. In situ densities of MORB melts and residual mantle: implications for buoyancy forces beneath mid-ocean ridges. *J. Geol.* 99:767–775.

Ozawa, K., Meyer, P.S., and Bloomer, S.H., 1991. Mineralogy and textures of iron-titanium oxide gabbros and associated olivine gabbros from Hole 735B. *In* Von Herzen, R.P., Robinson, P.T., et al., *Proc. ODP, Sci. Results,* 118: College Station, TX (Ocean Drilling Program), 41–73.

Pariso, J.E., and Johnson, H.P., 1993. Do lower crustal rocks record reversals of the Earth's magnetic field? Magnetic petrology of gabbros from Ocean Drilling Program Hole 735B. *J. Geophys. Res.,* 98:16013–16032.

Pariso, J.E., Scott, J.H., Kikawa, E., and Johnson, H.P., 1991. A magnetic logging study of Hole 735B gabbros at the Southwest Indian Ridge. *In* Von Herzen, R.P., Robinson, P.T., et al., *Proc. ODP, Sci. Results,* 118: College Station, TX (Ocean Drilling Program), 309–321.

Pettigrew, T.L., Casey, J.F., Miller, D.J., et al., 1999. *Proc. ODP, Init. Repts.,* 179 [CD-ROM]. Available from: Ocean Drilling Program, Texas A&M University, College Station, TX 77845-9547, U.S.A.

Rhodes, J.M., and Dungan, M.A., 1979. The evolution of ocean floor basaltic magmas. *In* Talwani, M., Harrison, C.G.A., and Hayes, D.E. (Eds.), *Deep Drilling Results in the Atlantic Ocean: Ocean Crust.* Am. Geophys. Union, Maurice Ewing Ser., 2:239–244.

Rhodes, J.M., Dungan, M.A., Blanchard, D.P., and Long, P.E., 1979. Magma mixing at mid-ocean ridges: evidence from basalts drilled near 22°N on the Mid-Atlantic Ridge. *Tectonophysics,* 55:35–61.

Robinson, P.T., Dick, H.J.B., Natland, J.H., and the ODP Leg 176 Shipboard Party, 2001. Lower oceanic crust formed at an ultra-slow-spreading ridge: Ocean Drilling Program Hole 735B, Southwest Indian Ridge. *In* Dilek, Y., Moores, E., Elthon, D., and Nicolas, A. (Eds.), *Ophiolites and Oceanic Crust: New Insights from Field Studies and the Ocean Drilling Program,* Spec. Pap.—Geol. Soc. Am., 349:75–86.

Roeder, P.L., and Emslie, R.F., 1970. Olivine-liquid equilibrium. *Contrib. Mineral. Petrol.,* 29:275–289.

Rosendahl, B.R., 1976. Evolution of oceanic crust, 2. Constraints, implications, and inferences. *J. Geophys. Res.,* 81:5305–5314.

Shipboard Scientific Party, 1989. Site 735. *In* Robinson, P.T., Von Herzen, R., et al., *Proc. ODP, Init. Repts.,* 118: College Station, TX (Ocean Drilling Program), 89–222.

————, 1999a. Explanatory notes. *In* Dick, H.J.B., Natland, J.H., Miller, D.J., et al., *Proc. ODP, Init. Repts.,* 176, 1–42 [CD-ROM]. Available from: Ocean Drilling Program, Texas A&M University, College Station, TX 77845-9547, U.S.A.

————, 1999b. Hammer Drill Sites (1104 and 1106) and Site 1105. *In* Pettigrew, T., Casey, J., Miller, D.J., et al., *Proc. ODP, Init. Repts.,* 179: College Station, TX (Ocean Drilling Program), CD-ROM.

————, 1999c. Site 735. *In* Dick, H.J.B., Natland, J.H., Miller, D.J., et al., *Proc. ODP, Init. Repts.,* 176, 1–314 [CD-ROM]. Available from: Ocean Drilling Program, Texas A&M University, College Station, TX 77845-9547, U.S.A.

Sinton, J.M., and Detrick, R.S., 1992. Mid-ocean ridge magma chambers. *J. Geophys. Res.,* 97:197–216.

Smith, D.K., and Cann, J.R., 1993. Building the crust of the Mid-Atlantic Ridge. *Nature,* 365:707–715.

Sonnenthal, E.L., and McBirney, A.R., 1998. The Skaergaard Layered Series, Part IV. Reaction-transport simulations of foundered blocks. *J. Petrol.* 39: 633–661.

Stakes, D., Mével, C., Cannat, M., and Chaput, T., 1991. Metamorphic stratigraphy of Hole 735B. *In* Von Herzen, R.P., Robinson, P.T., et al., *Proc. ODP, Sci. Results,* 118: College Station, TX (Ocean Drilling Program), 153–180.

Streckeisen, A., 1974. Classification and nomenclature of plutonic rocks. *Geol. Rundsch.,* 63:773–786.

Swift, S.A., Hoskins, H., and Stephen, R.A., 1991. Seismic stratigraphy in a transverse ridge, Atlantis II Fracture Zone. *In* Von Herzen, R.P., Robinson, P.T., et al., *Proc. ODP, Sci. Results,* 118: College Station, TX (Ocean Drilling Program), 219–226.

Von Herzen, R.P., Robinson, P.T., et al., 1991. *Proc. ODP, Sci. Results,* 118: College Station, TX (Ocean Drilling Program).

Wager, L.R., 1956. A chemical definition of fractionation stages as a basis for comparison of Hawaiian, Hebridean, and other basic lavas. *Geochem. Cosmochim. Acta,* 9:217–248.

Wager, L.R., and Brown, G.M., 1967. *Layered Igneous Rocks:* San Francisco (W.H. Freeman).

Wager, L.R., and Deer, W.A., 1939. Geological investigations in Greenland, Part 3. The petrology of the Skaergaard Intrusion, Kangerdlugssuaq, East Greenland. *Medd. Groenl.,* 105:1–352.

Walker, D., Shibata, T., and Delong, S.E., 1979. Abyssal tholeiites from the Oceanographer Fracture Zone, II. Phase equilibria and mixing. *Contrib. Mineral. Petrol.,* 70:111–125.

Wilson, A.H., 1996. The Great Dyke of Zimbabwe. *In* Cawthorn, R.G. (Ed.), *Layered Intrusions:* Amsterdam (Elsevier), 365–402.

Worst, B.G., 1958. The differentiation and structure of the Great Dyke of southern Rhodesia. *Trans. Geol. Soc. S. Afr.,* 61:283–3564.

Wright, T.L., and Fiske, R.S., 1971. Origin of the differentiated and hybrid lavas of Kilauea Volcano, Hawaii. *J. Petrol.,* 12:1–65.

APPENDIX A

Chemical Stratigraphy of Gabbros

Preliminary Remarks

Some 861 chemical analyses of gabbro were obtained on board ship and in several laboratories following Legs 118 and 176 (see "Appendix B," p. 46). Only a few of these were not additionally analyzed for the suite of trace elements that can be determined by XRF, and over 300 have been analyzed for rare earth elements as well. Several dozen of these have been analyzed for Sr, Nd, and/or Pb isotopes, and there are about 80 additional samples for which just the isotopes of Sr and O have been determined without additional geochemical measurements. These data indicate that the liquids parental to the gabbros were typical depleted mid-ocean-ridge basalt (MORB) and that the rocks have been modified to varying degrees by alteration (Stakes et al., 1991; Kempton et al., 1991; Hart et al., 1999; Bach et al., 2001; Holm, 2002.

To these should be added analyses of gabbros obtained during ODP Leg 179 (Shipboard Scientific Party, 1999b) and those acquired by dredging and high-speed near-surface diamond coring during the post-cruise survey (Coogan et al., 2001), which allow spatial comparisons across the summit and down the flanks of Atlantis Bank. Nearly 1000 analyses of major oxides on gabbros alone are now available for this purpose.

Our strategy is to isolate the geochemical variability of primitive gabbros from the numerous seams of differentiated gabbros that crosscut them in so many places and to compare this now with the sequences of olivine gabbro having finer-grained and more olivine-rich intervals at their bases, as defined in "The Lithologic Section," p. 7. We describe the core generally from the top down and take up additional topics as the descriptions warrant. We use the terms interval, composite interval, sequence, and series as they are defined in the main text of the paper.

A Simplified Chemical Classification

See the shipboard site reports (Shipboard Scientific Party, 1989, 1999c) and Hertogen et al. (Chap. 6, this volume) for summaries of the geochemical attributes of the rocks drilled during Legs 118 and 176. The following criteria are used for plotting. We distinguish *oxide gabbros* as having >1% TiO_2 contents; *tonalite, trondhjemite, and diorite* as having >54% SiO_2 and up to 70% SiO_2; *differentiated gabbros*, including *disseminated oxide gabbros* as having <54% SiO_2 and Mg# (= 100 × Mg/[Mg+Fe^{2+}]) < 72.5; *olivine gabbros* as the same, but with Mg# > 72.5 up to MgO = 12%; and *troctolitic gabbros* plus *troctolites* as having >12% MgO. *Olivine pyroxenites* are like troctolites, but with normative Di > 40%. Each of these is given a different symbol on diagrams (see caption to Fig. AF4). Some shipboard analyses obtained during Leg 176 have high totals, a consequence in large part of high SiO_2 measurements (Shipboard Scientific Party, 1999a). Thus, some olivine gabbros have >54% SiO_2 contents. These are taken into account. The break at Mg# = 72.5 corresponds to a clear gap in all reported data sets, evident on both variation diagrams and a histogram for Mg#. Rocks in the core with Mg# > 72.5 correspond to the general run of olivine gabbros and troctolites comprising the olivine-gabbro sequences as previously defined; rocks with Mg# < 72.5 usually intrude these.

Chemical Stratigraphy

The Upper 100 Meters: Limits Imposed by Complexity

Many of the problems of interpreting lithologic units and their relationship to chemical stratigraphy are exemplified by the upper 100 m of Hole 735B. Figure AF1 presents the variation in Mg# through this length of core. Mg# is a fair index of the fractionation stage (term of Wager, 1956) of the gabbros, since it nominally reflects the average composition of the ferromagnesian silicates in the rocks, regardless of variability in their modal proportions. Among layered intrusions such as the Skaergaard, for example, it correlates with the ratio of normative An/(An+Ab), which closely follows average feldspar compositions. Among troctolites, Mg# should be fairly close to that of the Fo content of olivines. In gabbros, which have little or no olivine and low-Ca pyroxene, the ratio should closely approximate the Mg# of clinopyroxene. Even in most olivine gabbros, clinopyroxene is far more abundant than olivine; thus, the Mg#s of such rocks should also be close to those of clinopyroxene. Mg# can obviously be lowered by the presence of the magmatic oxides ilmenite and magnetite. The extent to which gabbro Mg# can be utilized to specify original liquid Mg#s also depends on how much material frozen from trapped residual liquid the rocks still contain. If the rocks are adcumulates, however, they will contain only trivial amounts of oxide minerals and very little of material crystallized from trapped melt; therefore, this is not a great problem in these cores (Natland et al., 1991).

In any case, just considering that Mg# usefully discriminates rock types, Figure AF1 reveals an extraordinary complexity of even a short segment of Hole 735B. Lithologic units are indicated to the right, and sequences of olivine gabbro, as previously defined, to the left. There are 84 analyses of gabbro, and they divide roughly into two types, primitive and differentiated, as indicated by the two broad arrows at the top of the figure. Encircled fields indicate groups of analyses obtained from one to several adjacent lithologic intervals.

The analyses overall confirm the general impression given by the lithologic units. An upper sequence of ~20 m of differentiated gabbro (Subunit IA, gabbronorite and olivine gabbronorite) is succeeded downward by alternating lithologies of differentiated and primitive gabbro (Subunit IB), and then by assemblages dominated by olivine gabbro (Unit II). The unit boundaries were defined entirely in consideration of the prevalence of differentiated gabbro. The sequences of olivine gabbro have no relationship to them.

A disturbing aspect of Figure AF1 is the diversity of compositions found even in single lithologic intervals such as 48 and 50, which are both described as olivine gabbro by Dick et al. (1991a). The sequence to which these intervals belong consists of nearly 94% olivine gabbro based on the core descriptions, and the samples analyzed all came from those parts of the core.

Hart et al. (1999) attempted to get around the problem of short-scale lithologic diversity by obtaining 1-cm sample strips along 1.13- to 4.15-m lengths of core. These strip samples were then cleaned, powdered, and analyzed. The analyses then were construed to represent the bulk compositions of those lengths of core and to average out any fluctuations in lithology. In the upper 500 m of the core 22 such strip samples were obtained, and Hart et al. (1999) considered that the average composition of the 22 strip samples is the average composition of the Leg 118 portion of the core, down to 500 mbsf.

AF1. Mg# in the upper 100 mbsf, p. 57.

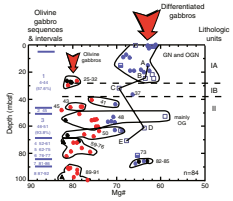

Strip samples in Figure AF1 are positioned at the tops of their sampled lengths; they are linked by a line and individually lettered. Five were taken from this part of the core, and all five fall in the category of differentiated gabbros. Four of them have >1% TiO_2 contents and thus are oxide gabbros using the chemical breakdown described above. Two of the strip simples fall in a portion of the core dominated by olivine gabbros, yet are oxide gabbros in bulk composition. One of them (D) spanned portions of intervals 48–50, within which only one 12-cm seam of oxide gabbro, interval 49, was described. Apparently, this seam was either extremely oxide rich or there were additional thin seams of oxide gabbro nearby that were too narrow to see. Over intervals 48–50, totaling 14.87 m (expanded) thickness, narrow seams of oxide gabbro, whether detected or not, were successfully avoided by shipboard scientists in 17 out of 19 cases.

Table AT1 compares the average of the five strip samples with the average of all 76 analyses obtained through the base of olivine-gabbro sequence 4, interval 77. The strip samples have almost double the TiO_2 contents of the average of 76 samples, lower Mg#, lower CaO, and higher Na_2O—all trends indicating a higher proportion of differentiated gabbro among the strip samples. Ni and Zr concentrations, however, are similar.

AT1. Average gabbro and basalt compositions, p. 68.

The average strip composition of Hart et al. (1999) approximates a typical depleted and slightly differentiated abyssal tholeiite in composition (Table AT1). So does the average of the five strip samples from the upper 80 m of the core. The average of 76 individual samples, however, does not. It has a high Mg#, about that of a reasonable primary basalt and close to that expected for a liquid in composition with mantle olivine. However, the TiO_2 content is substantially lower than it should be for this region of the Indian Ocean (cf., column 5, Table AT1). This and the high Mg# result from incorporation of olivine gabbro cumulates into the average of individual analyses, not one of which is represented by any one or in the average of the five strip samples. All averages are also sodic, having higher Na_8 when treated as basalts than any actual basalt nearby.

The statistical basis of either means of sampling and averaging, therefore, is clearly open to question. If in the end one wants a valid assessment of the bulk composition of the core, the problem appears to lie both in identifying the populations of rock to be sampled and then properly sampling them statistically. No one has yet attempted to do this. Weighting to thicknesses of lithologic intervals (Dick et al., 2000) and obtaining average compositions of defined rock types seems proper, provided that all intervals are noted and their thicknesses is accurately determined. The great chemical variability within individual intervals and the compositions of the separate strip samples suggests that they have not been. Thus, even oxide gabbros are included among the analyses, mainly from the shipboard data set, used to determine the composition of "average olivine gabbro" (Dick et al., 2000). On the other hand, strip samples seem to be no better a statistical sampling of the core. Perhaps there are enough individual samples now to select a blind set of analyses to average. Any average, however, will be one of cumulates, with the possible exception of whatever granitic veinlets are represented. With all the new analyses, a new average should be attempted. It is still too early to say how closely a statistically valid average of a large number of cumulates over 1500 m of core will match primitive basalt (compare columns 4 and 5 of Table AT1).

For all of these difficulties, consider alternatively another manner of detailed sampling of the same rocks. During the postcruise survey aboard the British research vessel *James Clark Ross*, short cores (0.1–3.8 m) of gabbro were obtained using rock drills constructed at the British Geological Survey at 21 locations, most of them along a north-south transect across the summit of Atlantis Bank (Coogan et al., 2000). From these, 26 samples were analyzed. To some degree, an average of the 26 samples might be considered representative of the entire gabbro massif. The available exposure was sampled from one end to the other at an average spacing of 175 m and was done far more systematically than is possible with dredging. But the 26 samples fall far short of encompassing the full diversity of rocks in Hole 735B. They include no troctolite, no olivine pyroxenite, no tonalite/trondhjemite veinlets, and no oxide gabbros with high P_2O_5, reflecting the presence of abundant apatite. The redistributed incompatible components of basalt are poorly represented. This merely says that if we wish to obtain an average composition for the lower ocean crust at this location or at any other slowly spreading ridge, spot sampling will not suffice. We need to drill deep holes and to obtain continuous core, as we have done in Hole 735B.

0–232 mbsf: A Long Series of Olivine Gabbro, and its Intrusives

In Figure **AF2,** Mg#s and Ni concentrations of analyzed gabbros are plotted vs. depth over the upper 250 m of the core. This is to encompass the uppermost of the plutons originally identified on the basis of chemistry, now designated as Series 1. Boundaries of lithologic units are again to the right; the bases of sequences of olivine gabbros (Table **AT1**) are to the left. Sequences 1–19 comprise the series, and the 19 sequences comprise 39 composite intervals (Table **AT1**). With postcruise data, Mg#s of primitive gabbros still clearly trend toward lower values with elevation (Figure **AF2A**), and the scatter increases as well. Even excluding oxide gabbros, there is a distinctive bimodality to the rock compositions. Gabbronorites and olivine gabbronorites comprise the greatest number of crosscutting intervals most of the way, and between 0–18 and 190–210 mbsf they are the predominant rock types. Oxide gabbros of Unit IV predominate in the lowest 30 m, but three small screens of primitive olivine gabbro are caught up in these at ~230 mbsf.

The sequences show no consistent internal pattern of variation, except for a tendency for samples with highest Mg# to occur at or near the bases of several of them. Sequences 11 and 17 are both more differentiated upward, a tendency that is more obvious for Ni concentrations, which diminish regularly upward in each case (Figure **AF2B**). In this, they resemble variations in individual layers that are portions of cyclic units in layered intrusions (Irvine, 1980). High Ni indicates a high modal proportion of olivine at the base of each. The entire body of olivine gabbro therefore consists of alternations of rocks richer and poorer in olivine. The small scale of these fluctuations is additional evidence that the pluton was constructed from numerous individual injections rather than large pulses of mafic magma. Some oxide gabbros and even a few diorites have the Ni concentrations of olivine gabbros. The contradictory character of these analyses indicates that these rocks are mainly olivine gabbros within which narrow seams or veins of oxide gabbro or tonalite/trondhjemite were also sampled. Most gabbronorites and olivine gabbronorites of lithologic Subunits 1A and IIIA–IIIC and the oxide gabbros of Unit IV have consistently low Ni, thus are not hybrid samples but rock that crystallized from strongly differentiated liquid with very low Ni.

AF2. Mg# and Ni, upper 250 mbsf, p. 58.

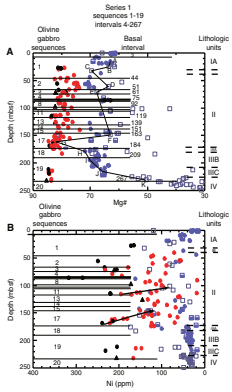

The aggregate thickness of all composite intervals of olivine gabbro and troctolite from sequences 1–19 is 140.7 m. The average thickness of 19 sequences is 7.4 m, and the thickest is 22.6 m. The latter is sequence 17, one of the two with steadily increasing Ni, thus olivine, toward its base.

Strip samples A–K of Hart et al. (1999) are indicated by letter and linked by lines in Figure AF2A. All but one fall in the range of differentiated gabbros, and seven of them have the bulk compositions of oxide gabbro. Sequences of olivine gabbro comprise 60.8% of the aggregate thickness of rock down to the base of interval 267. These are matched by only one strip sample, whereas the differentiated gabbros, making up 39.2% of the rock, are represented by ten strip samples. To this depth, primitive gabbros are strongly underrepresented by the strip samples.

274–520 mbsf: A Second Long Series of Olivine Gabbro, and its Intrusives

The variation of Mg# and Ni with depth within Series 2 olivine gabbros and troctolites encountered in Hole 735B is shown in Figure AF3. As before, lithologic units are indicated to the right and olivine-gabbro sequences to the left. The full series comprises sequences 20–39. The top of the series is taken as the top of lithologic interval 287, an olivine gabbro only 12 cm thick that occurs as a screen near the base of the oxide gabbro of lithologic Unit IV. Since the rock is not analyzed, an "X" shows its position in Figure AF3A. The base of the series is the bottom of lithologic interval 504, a fine-grained olivine gabbro. The rocks immediately beneath these belonging to Series 3 are described as olivine gabbro and disseminated-oxide gabbro (Shipboard Scientific Party, 1999c), but the ones of these that have been analyzed are clearly more differentiated than the rocks of Series 2, having Mg#s of ~70.

The most remarkable portion of this series is sequence 20, which, apart from several narrow seams of oxide gabbro, consists mainly of one continuous body of coarse olivine gabbro more than 120 m thick; the bulk of this sequence makes up lithologic Unit V. There are eight internal igneous contacts within sequence 20, but seven of them are concentrated near its base. The sequence is more differentiated with lower Mg# at its top, and this is clearly an upward continuation of a general trend through sequences 39–21. However, there is very little scatter to the trend within sequence 20, indicating a fundamental uniformity and consistency to the compositions of the rocks. This is borne out by Ni (Fig. AF3B), which shows little scatter—no more than might result from variations in small samples of coarse-grained rock. Ni itself decreases upward within this one sequence. Again, this resembles the pattern of cryptic variation frequently encountered within individual layers of phase-layered cyclic units of layered intrusions.

The rocks of underlying sequences 21–39, however, are modally and texturally variable; thus, they have more scattered Mg#s, including some troctolites with higher Mg#s. The modal fluctuations are primarily in the proportion of olivine, as indicated by highly variable Ni contents (Fig. AF3B). Fluctuations in the proportions of intrusive differentiated gabbros define the subdivisions in lithologic units, with Unit VI being described as compound olivine gabbro, meaning that there are numerous seams of oxide gabbro in a matrix of olivine gabbro. Again, however, there is no relationship between these and the boundaries of olivine-gabbro sequences. Several analyses in this part of the core have both high Ni and high TiO_2, reflective of samples containing both olivine gabbro (or troctolite) and some portion of a narrow seam

AF3. Mg# and Ni, 250–550 mbsf, p. 59.

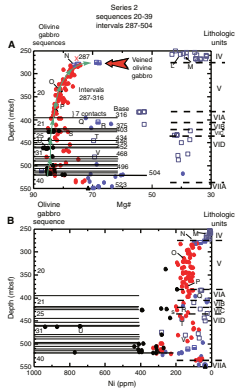

of oxide gabbro. At the top of sequence 20 are several samples with the bulk composition of diorite (large red arrow). These are from the veined breccia just underlying the base of the major oxide gabbro of lithologic Unit IV. They represent differentiated olivine gabbro laced with tonalite/trondhjemite veinlets.

The aggregate thickness of olivine gabbro sequences 20–39 is 199.6 m, representing 69.1% of all the rock they span. The average thickness of a sequence is 10.0 m, and the thickest is 120.7 m. Discounting that one, the average thickness is 4.2 m with all of the remaining ones lying beneath it.

Lettered data points in Figure AF3A indicate the strip samples of Hart et al. (1999). In uniform lithologies, they closely fit the general trends. Among six strip samples below 400 mbsf, however, only two have the compositions of primitive gabbro; the others are differentiated, including two oxide gabbros and one diorite. The two oxide gabbros (strips T and V) have high Ni, thus are physical combinations of olivine gabbro and seams of oxide gabbro. Since unadulterated oxide gabbros in this part of the core are quite differentiated with very low Mg#s (0.35–0.42), the hybrid strip samples here may very well balance primitive and differentiated gabbro compositions to their approximate proportions in the core.

Comments on the Upper Two Series

If the rocks of series 1 and 2 could be mapped over a large outcrop, conclusive evidence that these are essentially two intrusive bodies, or plutons as termed by Dick et al. (2000), might emerge. At this point, evidence in favor of this is the general compositional unity of each, sharp contrasts with rock above and below, sequential igneous contacts within and separating the sequences of olivine gabbro, and trends of upward increasing extent of differentiation in both.

Accepting this, however, we now speculate that these two composite masses of primitive gabbro, especially the lower one, behaved more like the magma chambers we might have expected to exist at this place than any other part of the core. At the slowly spreading Mid-Atlantic Ridge where basalts have been sampled at several places to depths of more than 500 mbsf by drilling, we know that the extrusive layer at any one place consists of sequences of hundreds of pillow basalts that break down into just a few chemically uniform basalt types (e.g. Bougault et al., 1979). These represent only a small number of actual eruptions (Natland, 1979), many of them separated by enough time (thousands of years) for significant secular variation, or even reversals, of the Earth's magnetic field to occur (Johnson, 1979). The uppermost crust appears to be an accumulation of monogenetic cones, each one erupted virtually at a point and each one consisting of pillow lavas with just one composition (e.g., Smith and Cann, 1992).

Nevertheless, the lavas are hybrids of primitive and more differentiated compositions, as reflected in both bulk compositions (e.g. Rhodes et al., 1979) and mineralogy (Dungan and Rhodes, 1978). Similar mixing histories have been deduced from compositions of phenocrysts in abyssal tholeiites from the Indian Ocean (Natland, 1991; LeRoex et al., 1989; Natland and Dick, 2001). If drilled thicknesses of these chemically uniform lava piles along the Mid-Atlantic Ridge are any indication, and assuming similar aspect ratios, the underlying storage reservoirs that supplied them held at least several meters, in some cases several tens of meters, and in one case more than 200 m of molten material, before eruption (Natland, 1979).

The sequences of olivine gabbros in the upper part of Hole 735B are the right order of magnitude in thickness to represent such magma bodies. Indeed, sequence 20, which is >120 m thick and includes one composite interval with uniform grain size some 109 m thick, evidently was held in the lower crust to freeze in its entirety without being disturbed by later injection of any other primitive magma as it froze. Whether it supplied an eruption prior to this is, of course, unknown. All other sequences in Series 1 and 2 apparently represent material of smaller crystallizing bodies that were repeatedly disturbed by injection of variably primitive and sometimes phenocryst-laden magma.

The patterns of magma flow and whether crystal mushes were invaded internally or whether there was ever something like a chamber floor in either of these bodies are extremely difficult to determine using a core 5.8 cm in diameter. Nevertheless, relationships between olivine gabbros and troctolites are reminiscent of those in troctolitic cumulates at Rum, in which repetitions of plagioclase-peridotite and troctolite cumulates were produced by sill-like injection of olivine-laden magmas into a crystal mush on a magma chamber floor (Bédard et al., 1988). However, in those rocks modal and phase layering is far more extensively developed. In Hole 735B, in the deeper of the two series so far described, the lower, more diverse half may represent a thickness of floor cumulates repeatedly disturbed by injections of dense, crystal-bearing magma. When this activity stopped, the upper half of the mass was left to crystallize slowly, on its own, nearly to completion. However, some of the fine-grained troctolites at the base of this pluton have sharp, straight contacts and apparently intruded along fractures in essentially solid rock. These are cumulates, not coarse-grained diabases, thus some avenue for the escape of intercumulus melt must have existed. The surrounding rock cannot have been so solid that it was impermeable. It contained at least a small fraction of melt. These fine-grained troctolite intrusives are thus part of the overall cycle of magmatism that produced this one pluton. They are variants of what Bowen (1920) first described as monomineralic intrusives with dikelike margins in plutonic masses, such as dunite dikes, among his examples of differentiation by deformation. Specifically, these are bimineralic (olivine-plagioclase) adcumulate intrusives with sharp margins. They point to nearly complete compaction and removal of intercumulus melt from the rocks that now surround them, without deformation, but before temperatures dropped below those of common basaltic liquids. That is when intrusion occurred. Compaction and melt expulsion then continued in the intrusion itself.

The olivine gabbros and troctolites at the bases of the two plutons are the most primitive, or least-differentiated, rocks recovered from Hole 735B. Nothing so primitive exists in the core below this. The rocks contain the most anorthitic plagioclases and the most forsteritic olivines in the entire core (Ozawa et al., 1991; Dick et al., **Chap. 10,** this volume). Some even contain chromian spinel. Nevertheless, none of them contain minerals as primitive and refractory as some of the phenocrysts in abyssal tholeiites from the Indian Ocean (Natland and Dick, 2001). However, such phenocrysts are always present in the same basalts with others that are both more abundant and far more differentiated, a consequence of mixing between primitive and more differentiated magmas. The more differentiated group of phenocrysts matches compositions of minerals in the primitive olivine gabbros and troctolites of Hole 735B.

Did phenocrysts of typical porphyritic abyssal tholeiites thus collect to produce the troctolites of Hole 735B? Perhaps yes, but if they did then the refractory population of minerals has been obliterated by the extensive recrystallization and reequilibration that affected all of the rocks (Natland, **Chap. 11,** this volume; Dick et al., **Chap. 10,** this volume). More generally, however, there is no cumulate in Hole 735B, nor indeed has one yet been found at Atlantis Bank, that would correspond to a mineral assemblage crystallized from truly primitive basalt fresh out of the mantle (Dick et al., 2000; Coogan et al., 2000; Natland and Dick, 2001). Possible explanations for this are given in **"Construction of the Lower Ocean Crust,"** p. 18.

223–274 mbsf: The Intervening Oxide Gabbro

No part of the core recovered in Hole 735B has attracted as much attention as the 51 m of oxide gabbro that separates the two series of olivine gabbro so far discussed. The proportions of the two oxide minerals, ilmenite and magnetite, can be very high. Sawn surfaces and polished thin sections reveal complex patterns of distribution of the oxide minerals, which in some cases form up to 30% of the rock. Against this background, brass-colored globular sulfides are large enough and so abundant that they are readily seen by the naked eye, usually being embedded in the oxide minerals. Some of the most prominent granitic patches and veins are present in this part of the core. All investigators agree in considering that these must be the products of extended high-iron differentiation of parental abyssal tholeiite and that somehow the granitic veins are closely related to oxide gabbros, yet the precise mechanism of this final stage of differentiation has remained elusive. Ilmenite and magnetite are so abundant that they must be cumulus minerals, but another likely late-stage mineral, apatite, is only sporadically abundant and in many oxide gabbros it amounts to only very rare and tiny crystals in a given specimen (Meurer and Natland, 2001), resulting in little or no measurable P_2O_5 in many of these rocks (e.g., Natland et al., 1991).

Lithologic Unit IV consists of 31 lithologic intervals and is far from uniform in composition (Fig. **AF4**). All but three contacts between intervals are igneous, although many of them are at least partly deformed or foliated (Dick et al., 1991a). Most are quite thin and occur closely spaced in clusters; several are a few meters thick, and the thickest interval (270) is 14.2 m thick. Three narrow intervals of olivine gabbro are present at ~230 mbsf, and there is another at ~272 mbsf, near the base of the oxide gabbros. These are the screens of the two much thicker series of olivine gabbro already discussed. The oxide gabbros here constitute many small intrusives that evidently repeatedly injected preexisting rock at the same place, between two larger bodies of primitive gabbro.

Within the 51-m thickness of oxide gabbro are three compositional subdivisions, each having higher Mg# toward their bases, these being, respectively, intervals 270, 283, and 288 with depth (Fig. **AF4A**). The middle of these subdivisions is highlighted by the presence of the thickest trondhemite vein recovered during Leg 118, the only one large enough to be analyzed on board ship. Similar silicic material is present just below the base of the oxide gabbros in a coarse breccia of olivine gabbro at the upper part of Unit V. Bulk compositions of these rocks are hybrids of olivine gabbro and trondhjemite and thus are dioritic (Hertogen et al., **Chap. 6,** this volume).

AF4. Mg#, TiO_2, and SiO_2, 200–300 mbsf, p. 60.

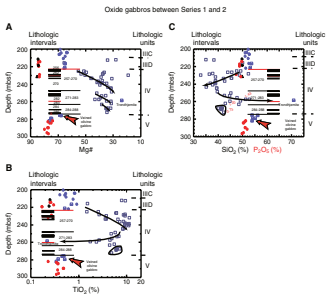

The higher Mg#s at the bases of the three subdivisions do not necessarily correlate with the extent of differentiation of these rocks, as they do in the olivine gabbros. In the upper and lower subdivisions, lower Mg# is in part also a consequence of the high concentrations of oxide minerals in the analyzed rocks (Fig. AF4A). The middle subdivision, however, the one with the trondhjemite, has lower TiO_2 contents toward its base (Fig. AF4B), and it also is higher in SiO_2 (Fig. AF4C). Here, some of the rocks are virtually net veined with silicic material, and it is this that must account for these trends. The trondhjemite vein is only the most concentrated granitic segregation in this part of the core. Three oxide gabbros in this vicinity also have unusually high P_2O_5 contents. In a thin section of the sample with highest P_2O_5 contents (1.43%), euhedral apatite crystals up to 2 mm in diameter can be seen embedded in ilmenite.

The tripartite subdivision of the oxide gabbros is also evident in the compositions of olivine and plagioclase, although there is no clear trend toward more differentiated compositions in the uppermost rocks (Fig. AF5). Instead, oxide minerals simply seem to be more concentrated toward its base. Both olivine and plagioclase in the two underlying subdivisions, however, track more evolved yet similar stages of differentiation, with the most sodic plagioclase and fayalitic olivine present at the bases of the subdivisions. The difference between the two subdivisions thus rests on the upper being silicic in overall aspect and not especially rich in oxide minerals, whereas the lower is equally differentiated, but not silicic, and instead is rich in oxide minerals. Two rocks also contain unusually abundant apatite.

The same three subdivisions can be discerned in the trace elements Y and Zr, both of which increase in concentration downward in each subdivision (Fig. AF6). They vary overall by an order of magnitude just among the oxide gabbros. The highest concentrations of both are matched by those measured in the veined olivine gabbro breccias at the top of lithologic Unit V. Because of the presence of globular, magmatic sulfides, oxide gabbros also have the highest S and Cu contents of all the rocks (Fig. AF7). These respectively mirror SiO_2 and mimic TiO_2, increasing downward in the uppermost subdivision, decreasing downward in the more siliceous rocks below that, and increasing again in the basal oxide-rich gabbros. Silicic rocks in the veined olivine gabbro and elsewhere have both low S and low Cu. The reduced S and Cu of the intermediate subdivision of oxide gabbros again indicate a generally granitic aspect to the bulk analyses of these rocks, although this might also be the result of fine-scale veining or even lit-par-lit injection of silicic material into a more primitive host.

In summary, we note three particular aspects of these rocks. The first is where they are in the core, namely between two much larger bodies of primitive gabbro, and particularly just at the top of the single thickest sequence of unalloyed olivine gabbro in the entire recovery. The second is that whereas among the larger masses of olivine gabbro the more differentiated rocks are present at the tops, among these oxide gabbros, on the other hand, the most differentiated rocks are present at the bottom and individually toward the bottom of each of the three subdivisions we have defined. The third aspect is the seemingly divergent contrast between the second, generally silicic, and third, generally oxide-rich, subdivisions that nevertheless share a common range in stage or degree of differentiation, as indicated by the compositions of olivine and plagioclase.

AF5. Olivine and plagioclase, 200–300 mbsf, p. 61.

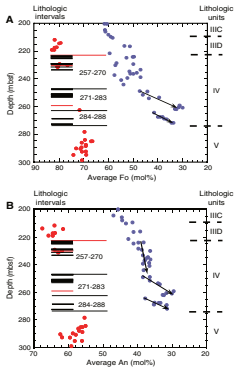

AF6. Y and Zr, 200–300 mbsf, p. 62.

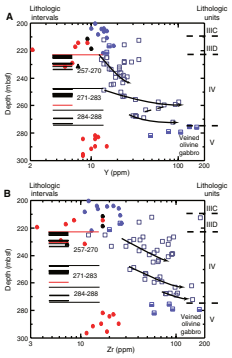

AF7. S and Cu, 200–300 mbsf, p. 63.

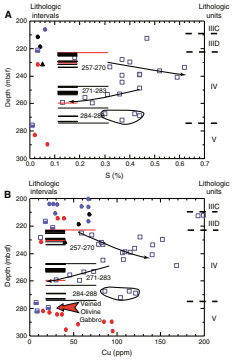

520–1508 mbsf: A Long, Uniform Series of Olivine Gabbros and its Intrusives

Olivine gabbro sequences comprise 82.3% of the expanded section recovered below 520 mbsf during Leg 176, and they make up 92.2% of the expanded section below 1000 mbsf. They provide a very different impression than the two series of olivine gabbro and troctolite so far described. Whereas those rocks are diverse, these are uniform. Whereas those rocks have definite chemical trends with sharply defined boundaries, these show only subtle shifts in composition. Whereas some of those rocks include Cr spinel, that mineral never reappeared during Leg 176.

Clearly, this is a different domain of the lower ocean crust and it is quite substantial. The thickness and uniformity of the rocks indicate something fundamental about the organization of the lower crust. Although the impression of a continuing sequence of plutons has disappeared with all of the new chemical analyses, the data nevertheless suggest that this series can be divided into three zones, numbered 3a–3c in the remainder of this discussion, with the middle one, Zone 3b (961–1194 mbsf), being slightly more differentiated and uniform than the others. Consequently, we describe the zones in sequence downward using the same procedures and types of diagrams as before.

Zone 3a spans 520–962 mbsf, lithologic intervals 508–716, and olivine gabbro sequences 40–67 (Fig. **AF8A**). Leaving out differentiated rock, the sequences average 11.3 m thick, the thickest is 40.5 m, and their aggregate thickness is 283.1 m. Poorly recovered, altered, fractured, and brecciated rock marks the upper 50 m and corresponds to the upper of two seismic reflectors detected by vertical seismic profiling (VSP) in an experiment at the end of Leg 118 (Swift et al., 1991). The base of Zone 3a is within a shear zone centered at ~960 mbsf.

Although olivine gabbro is the predominant rock, there are numerous prominent seams of oxide gabbro and some substantial thicknesses of gabbronorite, especially between 520 and 700 mbsf. Crystal-plastic deformation is particularly intense in rock down to 700 mbsf and is especially associated with the seams of oxide gabbro (Natland, **Chap. 11,** this volume). This is a continuation of a pattern that begins at 400 mbsf and thus that overlaps a portion of the lower of the two plutons cored during Leg 118. This is high-temperature crystal-plastic deformation that commenced while the rocks were still partially molten. It preceded the brecciation, fracturing, and attendant hydrothermal alteration of the rock at the level of the upper reflector detected by the VSP experiment.

All of this no doubt has confused the original stratigraphy of the underlying olivine gabbro. Both removal and repetition of rock sequences probably occurred, and penetrative infiltration of some of the rock by highly differentiated melts may have infused some rocks with magmatic oxides and otherwise modified certain chemical signatures. However, we deal with what exists.

Both Mg# and Ni concentrations have fairly restricted ranges over the entire zone (Fig. **AF8A, AF8B**), and there are no sustained trends in either comparable to those higher in the core. Between 520 and 720 mbsf, compositions of olivine gabbros merge with those of gabbronorite and olivine gabbronorite; below this they are fairly distinct. The pointed bar at the top of Figure **AF8A** shows the range in compositions of the more differentiated gabbros originally thought to characterize Zone 3a. Lithologic Unit VII, for example, is described as consisting primarily of gabbronorite and olivine gabbronorite and Unit IX of gab-

AF8. Mg# and Ni, 500–1000 mbsf, p. 64.

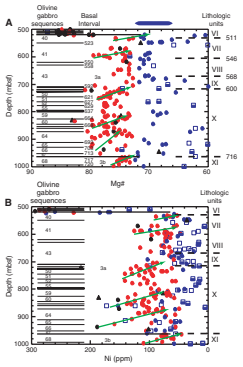

bro and gabbronorite. New analyses, however, show that both of these units include olivine gabbro that is both as magnesian and rich in Ni as the predominant olivine gabbros lower in Unit X.

What emerges from chemical trends now is the existence of several short sequences of olivine gabbro with decreasing Mg# and Ni upward (green arrows in Fig. AF8). Some of these are present within individual olivine gabbro sequences and others span several sequences. However, Mg# and Ni concentrations are rarely as high as in the lower sequences of either Series 1 or Series 2. This is as far as we can go in noting any similarity to trends in the two plutons in the upper third of the section, and these are present in much thinner sequences of rock. At best, these trends represent rather subtle fluctuations in the proportion of olivine, from a few percent in one rock to ~10%–15% in another. In sequences 59–63, the variations may be related to grain size and modal layering, which is better developed in sequence 60 over 9 m of rock than in any other part of the core. These fluctuations in Mg# and Ni, however, occur throughout Zone 3a, and there is no general tendency for the rocks at the top to be more differentiated than the ones at the bottom. Thus, whereas these olivine gabbros are an aggregate of cumulates crystallized from numerous injections of magma, those injections appear to have been extremely localized in scale and influence. There was no pulsing into some larger body of magma, no interpolation of material into a thick crystal mat, and no pooling of residual melt into an eventual thick, stagnating sill. The igneous layering was likened in the shipboard report to that seen in layered intrusions. However, there is no indication that any individual molten mass ever exceeded more than a few meters in thickness. The layering therefore may have been produced hydraulically, by flow differentiation, as magma perhaps passed forcibly through a tortuous porosity structure. Compared with the olivine gabbros in the upper 520 m of the core, the scale of magma injection was even more diminutive, and the overall tenor of differentiation more advanced.

As in rocks above, however, there are a number of oxide gabbros with fairly high Ni concentrations, matching those of olivine gabbro. Again, these appear to combine both olivine gabbro and narrow oxide-rich seams in samples taken for chemical analysis. Similarly, rocks with high SiO_2 have the compositions of diorite because they combine olivine gabbro and narrow granitic veinlets. These samples should sound a note of caution in the interpretation of trends. How many other samples, which otherwise fall into the chemical categories for olivine gabbro or troctolite, defined earlier, have some trace of either oxide gabbro or trondhjemite in their makeup? In what way do such traces blur or obscure the chemical trends we are trying to perceive in scatter diagrams?

Zone 3b spans 962–1194 mbsf, olivine gabbro sequences 68–79, and intervals 718–833 (Fig. AF9). The average sequence thickness is 18.0 m, and the aggregate is 216.1 m, or 93.1% of the expanded recovery. This leaves only 6.9% of Zone 3b to the differentiated gabbros, including oxide-rich seams. This is so small a proportion that the rocks are included in lithologic Unit XI, olivine gabbro. Deformation of the rocks is much reduced, although again there is a general association between zones of deformation and the location of oxide seams. A fault zone is centered at ~1100 mbsf and consists of a series of narrow interfaces showing both normal and reversed senses of shear.

Miller and Cervantes (Chap. 7, this volume) observe differences in compositions of sulfides and corresponding contrasts in Ni contents of

AF9. Mg# and Ni, 850–1250 mbsf, p. 65.

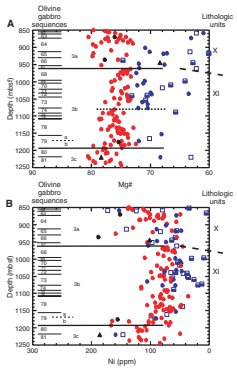

gabbros across a boundary that they place at 1170 mbsf. This is very close to the boundary between Zones 3b and 3c. Based on data in Niu et al. (**Chap. 8,** this volume), the boundary in Ni contents is more precisely between 1173.02 and 1175.65 mbsf. This is within olivine gabbro Sequence 79 and, indeed, is within a single interval (831). The boundary in terms of Ni is ~2.3 m from the top of the interval, which is 20.15 m thick. One more interval (832) lies below this in sequence 70; it is 1.42 m thick. For the sake of consistency, we place the boundary between Zones 3b and 3c at the base of interval 833, sequence 79, but note that it might justifiably be 19.2 m higher, at the dashed line between sequences 79a and 79b in Figure **AF9.**

Throughout the rest of Zone 3b, as nowhere else in the core, the term "monotonous" is appropriate. Both Mg# and Ni concentrations (Fig. **AF9**) have quite narrow ranges, and both are at the lower ends of ranges in the rocks of Zones 3a and 3c above and below. In fact, Ni in most samples is <100 ppm. Sequences 68–73 (above the dotted line in Fig. **AF9A**) have a somewhat higher percentage of slightly more differentiated gabbros than is present in sequences 74–79, but this is barely a contrast. At the base of sequence 79, Ni creeps higher. A few oxide gabbros have Ni concentrations comparable to those in their surroundings, thus appear once again to be samples that mixed olivine gabbro and portions of oxide-rich seams. Other differentiated rocks are also clearly physical mixes of olivine gabbro and granitic veinlets.

Monotonous or not, these rocks are like their chemical counterparts elsewhere in the core in that they consist of repetitions of olivine gabbro sequences comprising alternations in grain size that adjoin mainly on sutured igneous contacts. Within sequences 68–76, there are 20 internal contacts, all but 6 of them being gradational or sutured and thus igneous in character. This was not one large mass of magma that crystallized to a homogeneous composition. It is the crystalline residue of many injections of magma that were very similar in composition and presumably also were similar in phenocryst load and composition from the start.

With olivine gabbro sequence 80 at the top of Zone 3c, bulk compositions of the core shift back to higher Mg# and a greater range of Ni concentration and remain that way to the bottom of the core (Fig. **AF10**). The distinction between lithologic Units XI and XII is that the latter includes troctolitic gabbros and troctolites. The average sequence thickness is 17.0 m, and the aggregate thickness of sequences is 306.8 m, or 92.4% of the expanded recovery for these sequences. From 1400 to 1508 mbsf, many of the troctolitic gabbros and troctolites have the aspect of narrow, nearly vertical pipes within a matrix of olivine gabbro. These contribute to the large number of gradational or sutured igneous contacts in these sequences (Fig. **AF10A**). The criterion for defining olivine-gabbro sequences, namely grain-size variation across a nearly horizontal contact, was not easy to apply in these rocks. However, whereas flat or slightly dipping contacts between similar rocks higher in the core suggest either layers or lateral sill-like bodies of olivine-rich rock, here some kind of upward (or downward) protrusions of crystal-laden magma into or through crystal mushes evidently occurred. This resulted in the rather scattered pattern of Ni variability below 1400 mbsf.

AF10. Mg# and Ni, 1150–1508 mbsf, p. 66.

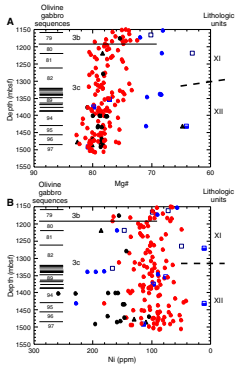

Correlations

Shipboard scientists aboard engineering Leg 179 noted similarities between fairly thick oxide gabbros cored in the lowest 50 m of Hole

1105A and those of Hole 735B (Shipboard Scientific Party, 1999b). Post-cruise studies suggested to Casey et al. (1999) and Banerji et al. (2000) that the two may in fact correlate over the 1.2-km distance that separates the holes. Although we agree that the two sections may share common intrusive intervals of oxide gabbro, shipboard data (Shipboard Scientific Party, 1999b) show that the oxide gabbros near the base of Hole 1105A are not in general as rich in TiO_2, as correspondingly low in SiO_2, or as high in Zr or Y as most of the rocks of Unit IV from Hole 735B. At best, only the uppermost of the three sequences of lithologic Unit IV was reached in Hole 1105A, and its rocks are spread along 54 m rather than 20 m of core, being separated by several substantial intervening thicknesses of more primitive gabbro. That gabbro is bimodal in Mg#, like that from 200 to 220 mbsf in Hole 735B (Figs. **F3, F5**). Neither the lower two subdivisions of lithologic Unit IV, oxide gabbro, of Hole 735B nor the massive olivine gabbro of lithologic Unit V were reached in Hole 1105A.

Coogan et al. (2000) reported compositions for two oxide gabbros among 26 gabbros analyzed from short drill cores obtained from a generally north-south transect along the summit of Atlantis Bank (Fig. **AF11A**). The two are adjacent samples on the seafloor, respectively, 2.8 and 3.5 km east-northeast of Hole 735B. Rock magnetic data suggest that the section in Hole 735B has been tilted southward by an average of 19° ± 5°, thus that the oxide gabbro should crop out on the platform summit somewhere to the north. Oxide gabbro Unit IV below 232 mbsf in Hole 735B, its possible equivalent below 102 mbsf in Hole 1105A, and the two outcropping oxide gabbros to the north may therefore be one and the same. Assuming a simple southward rotation and that the upper surface of the oxide gabbro is planar, the angles between the outcropping samples and 232 mbsf in Hole 735B and 102 mbsf in Hole 1105A are shallower than 19° ± 5° (Fig. **AF11B**), although the projected angle between the two ODP drill holes (17°) is statistically indistinguishable from this, and that between 232 mbsf in Hole 735B and the outcropping oxide gabbros (12.4°) is barely different. In detail, however, the tops of the cored oxide gabbro units and the outcropping oxide gabbros are not coplanar on a southward-dipping surface, although they could lie on a plane striking to the northwest and dipping slightly to the southeast. Or they could be on a curving surface that falls off somewhere toward the south and west. Since there could be an error of 50 m in the relative placement of the two outcropping samples in the equivalent drilled sections, the details of this are assuredly speculative. The data simply indicate the existence of a generally southward-dipping mass of oxide gabbro that originally was approximately horizontal.

Taking 12.4° as the actual amount of southward rotation of an originally horizontal igneous structure beneath the rift valley floor, the locations of surface gabbro samples reported by Coogan et al. (in press) can be projected onto a vertical extension of Hole 735B as shown in Figure **AF11B.** On this basis, 174 m of section that lies to the south was not drilled but is represented by three rock cores. The most northerly of the gabbro cores projects to a depth of 637 mbsf in Hole 735B. The total section is 1682 m, of which the upper 48.2% is exposed on the nearly flat surface of Atlantis Bank. Hole 735B sampled 89.7% of the section. To the south, extrusive basalt either buries gabbro higher in the section or is in fault contact with it (Fig. **AF11B**).

A basalt dike obtained by surface coring almost due west of Hole 735B may be the same as one cored in the hole at 105 mbsf. If the two

AF11. Gabbros from ODP holes compared to those from JR31, p. 67.

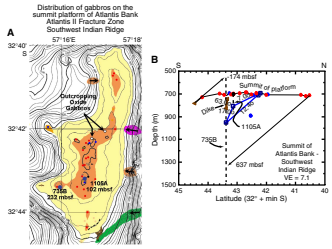

are the same, then the dip of the west-striking dike is S63.6° (Fig. AF11B).

APPENDIX B

Compositions of Gabbros and Diabase

Sample	Reported in	Leg	Core	Section	Top (cm)	Bottom (cm)	Lithologic interval	Curated depth (mbsf)	Strip length (m)	Simplified lithology	SiO_2	TiO_2	Al_2O_3	Fe_2O_3	FeO	FeO (T)	Fe_2O_3 (T)	MnO	MgO	CaO	Na_2O	K_2O	P_2O_5
HER001-1,001	Hertogen	118	1D	1	1	5	1	0.1		DG	52.74	0.83	17.50	2.37	5.48	7.61	8.46	0.13	5.81	9.68	4.40	0.15	0.04
SNO-001R-1,035	Snow	118	1D	1	35	37	1	0.4		OxG	49.12	1.50	15.84	9.76		8.78	9.76	0.16	8.19	10.97	3.08	0.22	0.15
HER001-1,090	Hertogen	118	1D	1	90	92	1	0.9		DG	52.27	0.86	15.08	2.12	6.68	8.59	9.54	0.17	7.07	12.12	3.40	0.16	0.02
SHP001D-1,090	Ship	118	1D	1	090	98	1	0.9		DG	51.66	0.85	14.90	2.05	6.64	8.48	9.43	0.17	6.98	11.98	3.40	0.16	0.02
SHP001D-1,117	Ship	118	1D	1	117	120	1	1.2		FV	54.21	0.56	20.93	1.15	3.80	4.83	5.37	0.10	3.82	9.64	5.19	0.09	0.02
HER001-1,117	Hertogen	118	1D	1	117	120	1	1.2		FV	54.25	0.53	20.83	1.28	3.80	4.95	5.50	0.09	3.83	9.41	5.34	0.11	0.02
SHP001D-2,091	Ship	118	1D	2	91	94	3	2.4		DG	51.87	0.84	15.01	1.91	6.74	8.46	9.40	0.16	6.89	11.99	3.46	0.16	0.03
SHP002D-1,076	Ship	118	2D	1	76	80	3	7.3		DG	51.35	0.42	16.93	1.85	6.52	8.18	9.09	0.17	8.39	9.66	3.30	0.25	0.04
HER002-2,106	Hertogen	118	2D	2	106	109	12	9.1		DG	51.97	0.34	18.74	1.74	4.16	5.73	6.36	0.13	6.07	11.51	3.86	0.12	0.02
HER002-2,116	Hertogen	118	2D	2	116	120	12	9.2		DG	51.45	0.35	19.31	2.54	4.43	6.72	7.46	0.13	6.62	10.23	3.91	0.15	0.02

Sample	H_2O	CO_2	Total	COI	MgNo	S	Li	Be	Sc	V	Cr	Co	Ni	Cu	Zn	Ga	Rb	Sr	Y	Zr	Nb	Sn	Cs	Ba	Hf	Ta	Pb	Th	U
HER001-1,001	0.97	0.05	100.15		60.2	0.01					17	34	27	7	35	19		204	18	34									
SNO-001R-1,035		0.00	98.99	–1.56	64.9				35	234	332	48	119	57	68	18	6	171	31	112	3								
HER001-1,090	1.17	0.04	101.16		62.0	0.01				243	9		32	42	60			157	19	25									
SHP001D-1,090	1.17	0.07	100.05	–1.01	62.0				48.4	243	9	40	32	42	60		3.3	157	19	26	0.7				0.52	0.02		0.12	
SHP001D-1,117	0.43	0.09	100.03	–0.29	61.0					152	1		16	9	35			259	11	17									
HER001-1,117	0.43	0.09	100.01		60.5						12	18	17	2	33	21		256	15	19									
SHP001D-2,091	0.94	0.00	100.00	–0.73	61.7				48.9	254	8	40.8	30	42	62		3.2	158	21	27	0.5				0.87	0.016			
SHP002D-1,076	1.13	0.00	100.01	–0.72	67.0				30.4	128	9	44.9	53	25	56		3	176	12	26	0.6				0.68	0.015			
HER002-2,106	0.79	0.22	99.67		67.7	0.01					22	42	58	16	45	17		195	13	22									
HER002-2,116	0.79	0.24	100.17		66.5						14	39	47	15	42	17		209	11	22									

Sample	Pd	Pt	Ir	Ru	Rh	Au	Re	Os	La	Ce	Pr	Nd	Sm	Eu	Gd	Tb	Dy	Ho	Er	Tm	Yb	Lu	$^{87}Sr/^{86}Sr$	$^{143}Nd/^{144}Nd$	$^{208}Pb/^{204}Pb$	$^{207}Pb/^{204}Pb$	$^{206}Pb/^{204}Pb$	$\delta^{11}B$	$\delta^{18}O$	$^{187}Os/^{188}Os$
HER001-1,001									2	5		4	1.4	1	2		2.3	0.6	1.2		1.6	0.2								
SNO-001R-1,035																														
HER001-1,090																														
SHP001D-1,090									1.6	5.3		5.3	1.99	1.19		0.54					2.09	0.32								
SHP001D-1,117																													5.1	
HER001-1,117									1	8		2	1.1	1	1.7		1.8	0.4	1.2		1.2	0.2								
SHP001D-2,091									1.6	5.6		5.3	2.07	1.19		0.55					2.17	0.31							5.6	
SHP002D-1,076									1.5	4.5		3.9	1.31	0.81		0.32					1.22	0.19							4.3	
HER002-2,106																														
HER002-2,116																														

Note: Only a portion of this table appears here. The complete table is available in **ASCII,** and in Microsoft Excel (see the "**Supplementary Materials**" contents list).

Figure F1. Location of Hole 735B on the Southwest Indian Ridge and an oblique shaded-relief image of a portion of the Atlantis II Fracture Zone transform valley, showing Atlantis Bank, where Hole 735B was drilled. The relief image, from the frontispiece of the Leg 118 *Scientific Results* volume (Von Herzen, Robinson, et al., 1991), is based on a SeaBeam survey carried out in 1986 (Dick et al., 1991b) and represents an area of ~4000 km². Hole 735B is in 720 m of water, and the floor of the transform valley is ~6000 m deep. The initial targets for Leg 118 were on the Median Ridge in the transform valley.

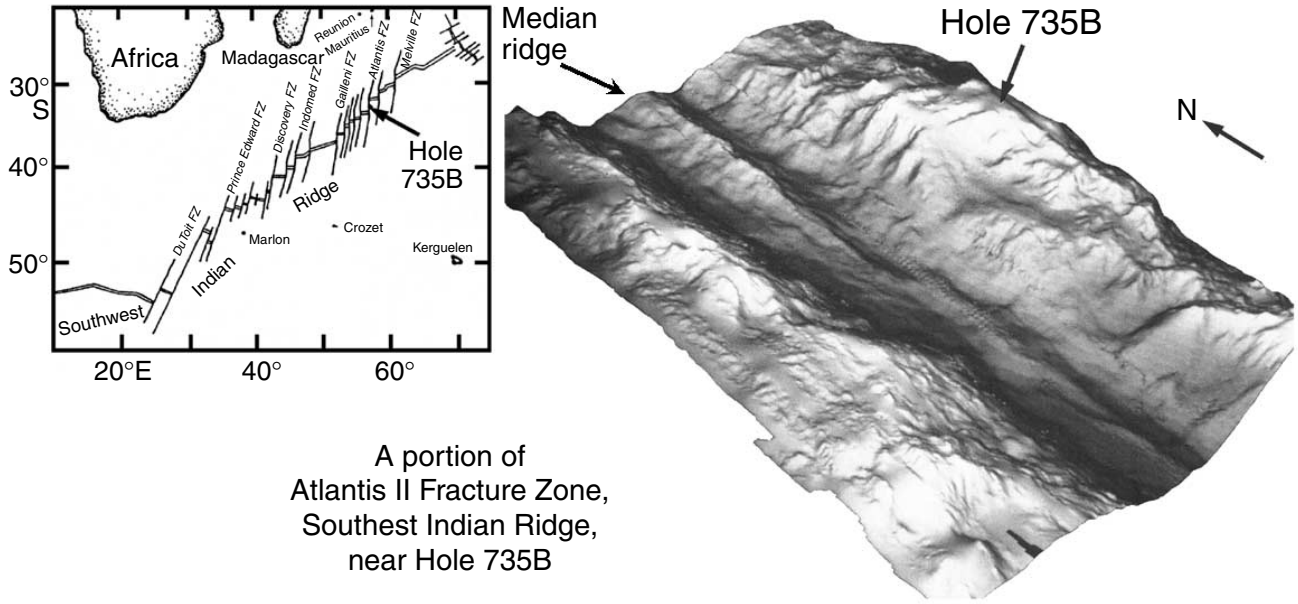

Figure F2. Models of magma-chamber complexes beneath a slow-spreading ridge. **A.** A large magma chamber (Bryan and Moore, 1977). **B.** The "infinite leek" (Nisbet and Fowler, 1978). **C.** Interconnected sills forming a crystal mush (Sinton and Detrick, 1992). **D.** Nested plutons in Hole 735B (Dick et al., 2000). **E.** Feeder pipes supplying a shallow, linked, along-axis zone of dispersed but interconnected melt and hot rock (Magde et al., 2000).

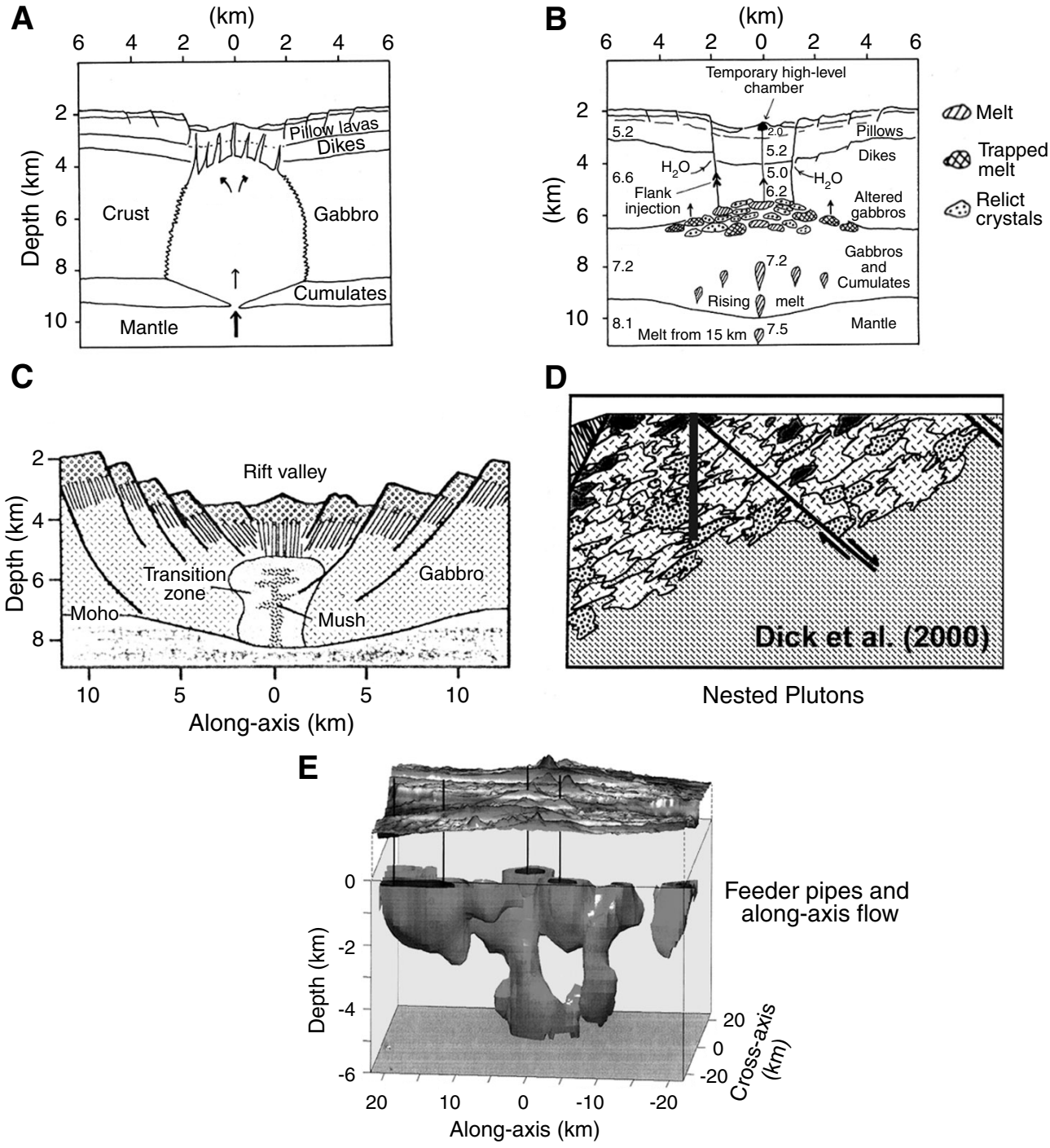

Figure F3. Simplified summary lithostratigraphy giving (from left) the main lithologic units defined during Legs 118 and 176, proportions of intervals of principal lithofacies (indicated in the key) constructed using a rolling average at 20-m intervals, and structure. SZ = shear zone, F = fault.

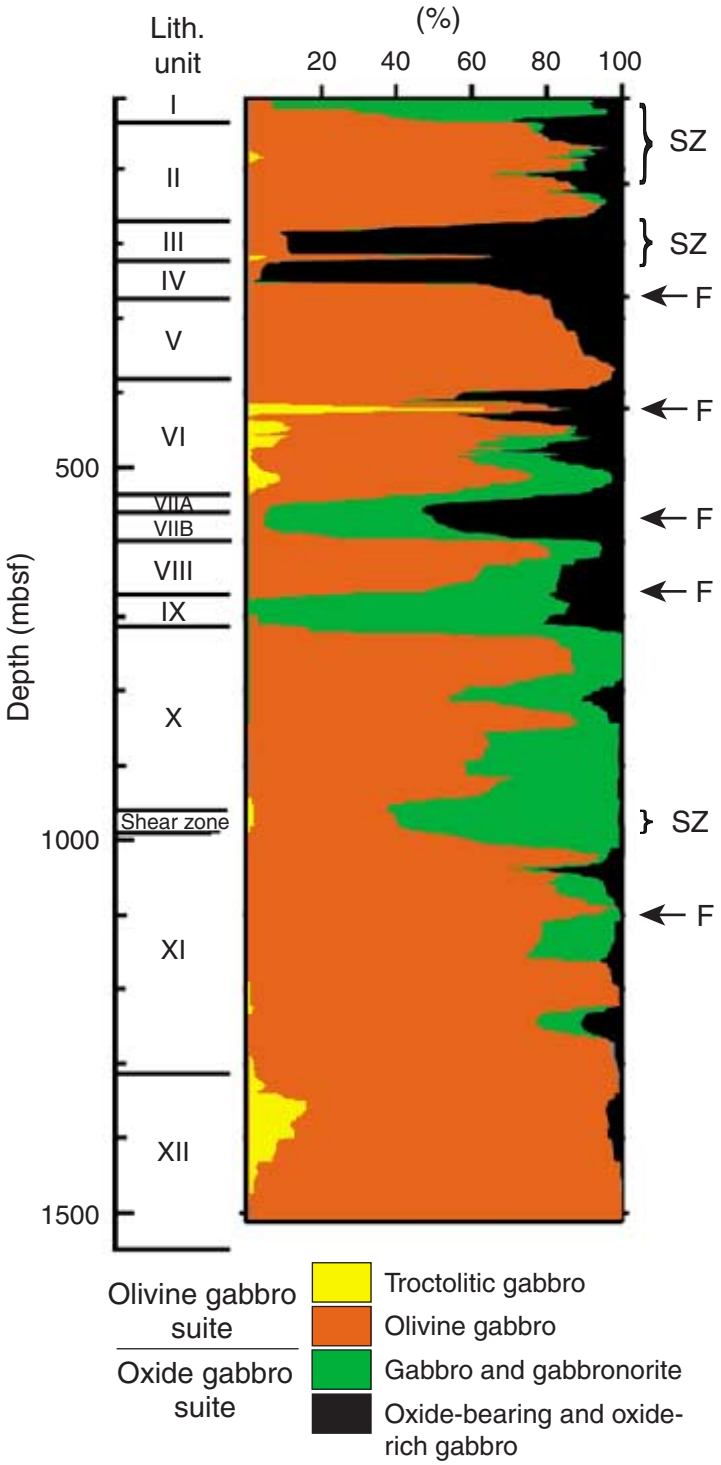

Figure F4. Thickness of sequences of olivine gabbros vs. cumulative thickness at sequence centers. This is equivalent to depth in meters below the seafloor, with all intrusive differentiated gabbros, mainly oxide gabbros, removed from the section. The placement of Unit IV, oxide gabbro, thus appears as a line even though it is 55 m thick. The figure shows the reconstructed locations of principal faults and shear zones, annotated to their actual depths, and the boundaries of series and zones, as defined in the text.

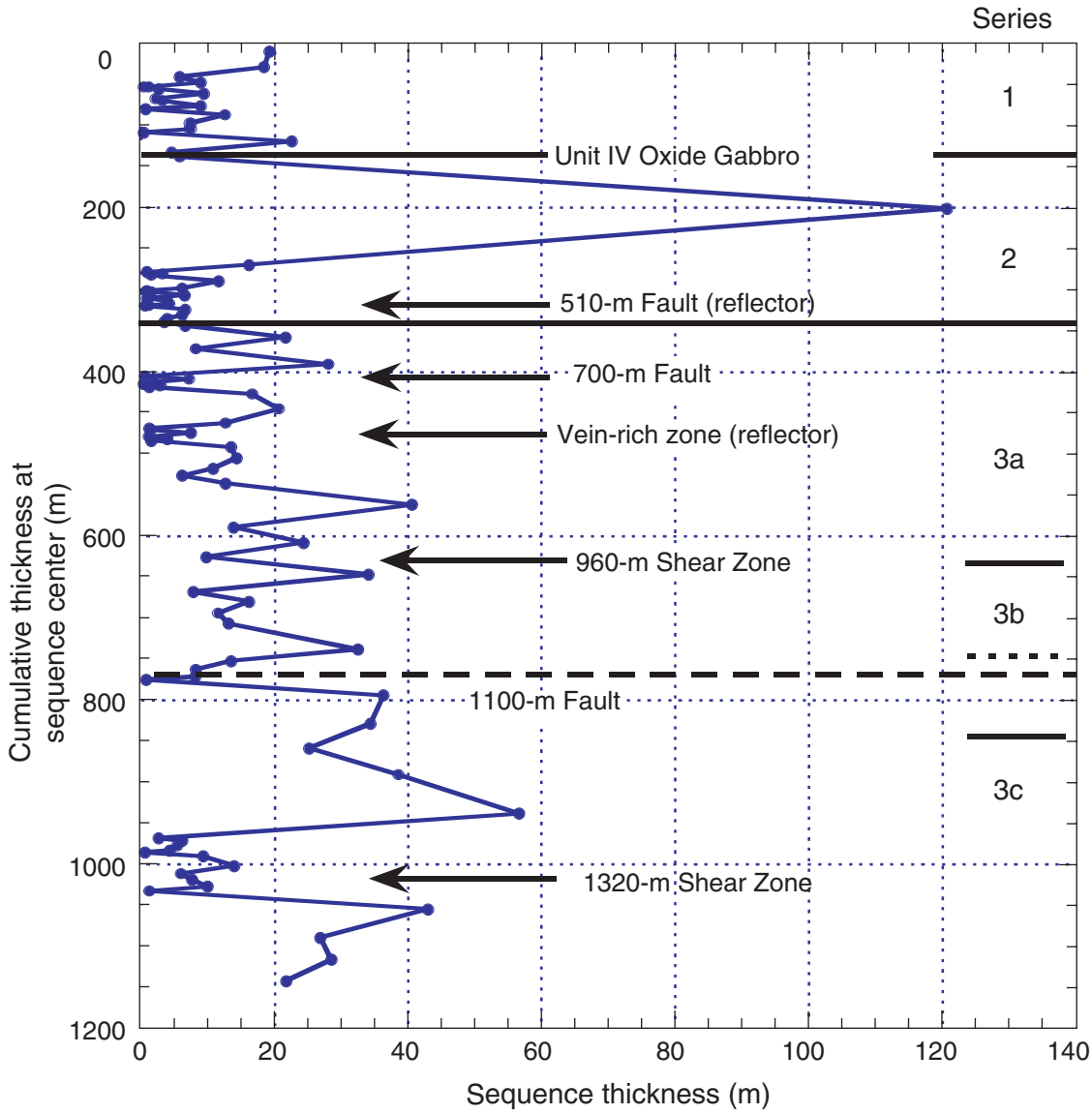

Figure F5. Compositions of gabbros plotted against depth. **A.** Mg# = Mg/(Mg+Fe^{2+}), where Fe^{2+}/[Fe^{2+}/(Fe^{2+}+Fe^{3+})] = 0.85 (Natland et al., 1991). **B.** TiO_2 (%), log units. Open squares = oxide gabbros (>1% TiO_2), half-solid squares = tonalite, trondhjemite, and diorite (>54% and up to 70% SiO_2), solid blue circles = differentiated gabbros, including disseminated oxide gabbros (<54% SiO_2 and Mg# [=100 × Mg/(Mg+Fe^{2+})] < 72.5), solid red circles = olivine gabbros (are the same, but with Mg# > 72.5 and up to MgO = 12%), solid black circles = troctolitic gabbros plus troctolites (>12% MgO), solid triangles = Olivine pyroxenites (like troctolites, but with normative Di > 40%). Horizontal lines delineate boundaries between series, which are indicated by number. The placements of two lithologic units (IV and V) are also indicated.

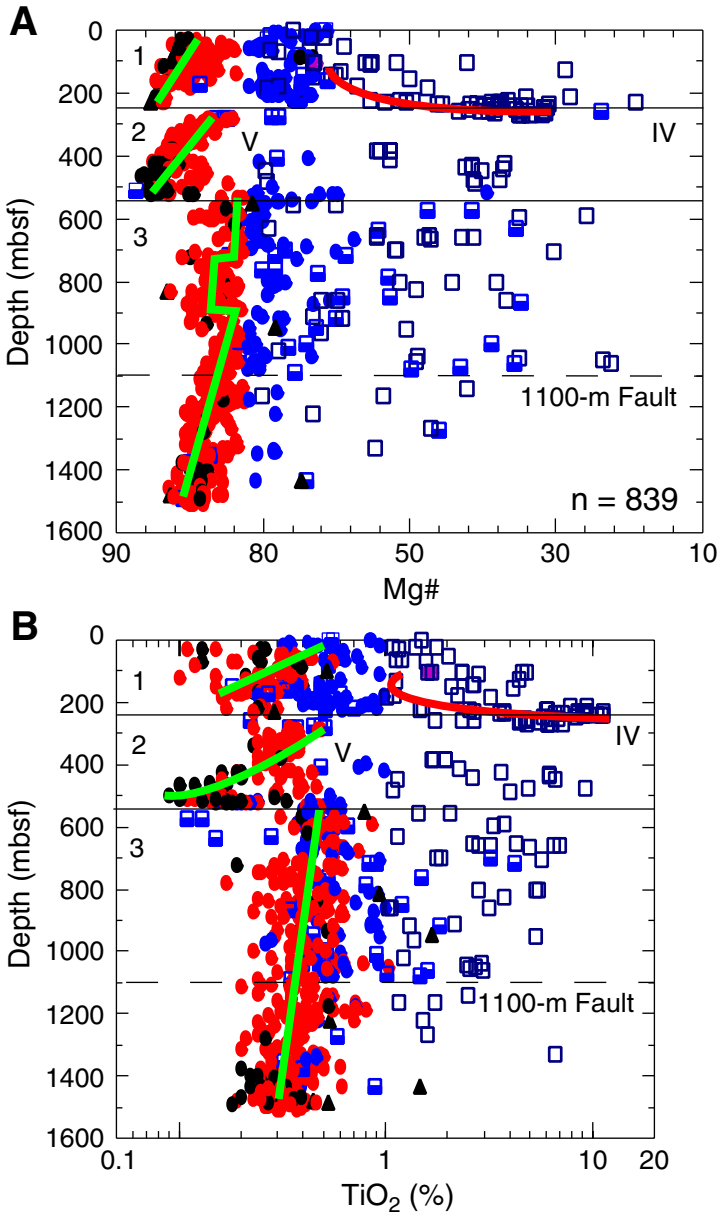

Figure F6. Variation of compositions of (**A**) olivine and (**B**) plagioclase with depth for all of Hole 735B, comprising all of Series 1–3, from the data compilation of Dick et al., **Chap. 10,** this volume. Minerals from all primitive gabbros are solid red circles; of all differentiated gabbros are solid blue circles. In B, the range of compositions of unaltered plagioclase in felsic veins (Niu et al., **Chap. 8,** this volume) is compared with the composition of the most sodic magmatic plagioclase found in oxide gabbros (An_{29}).

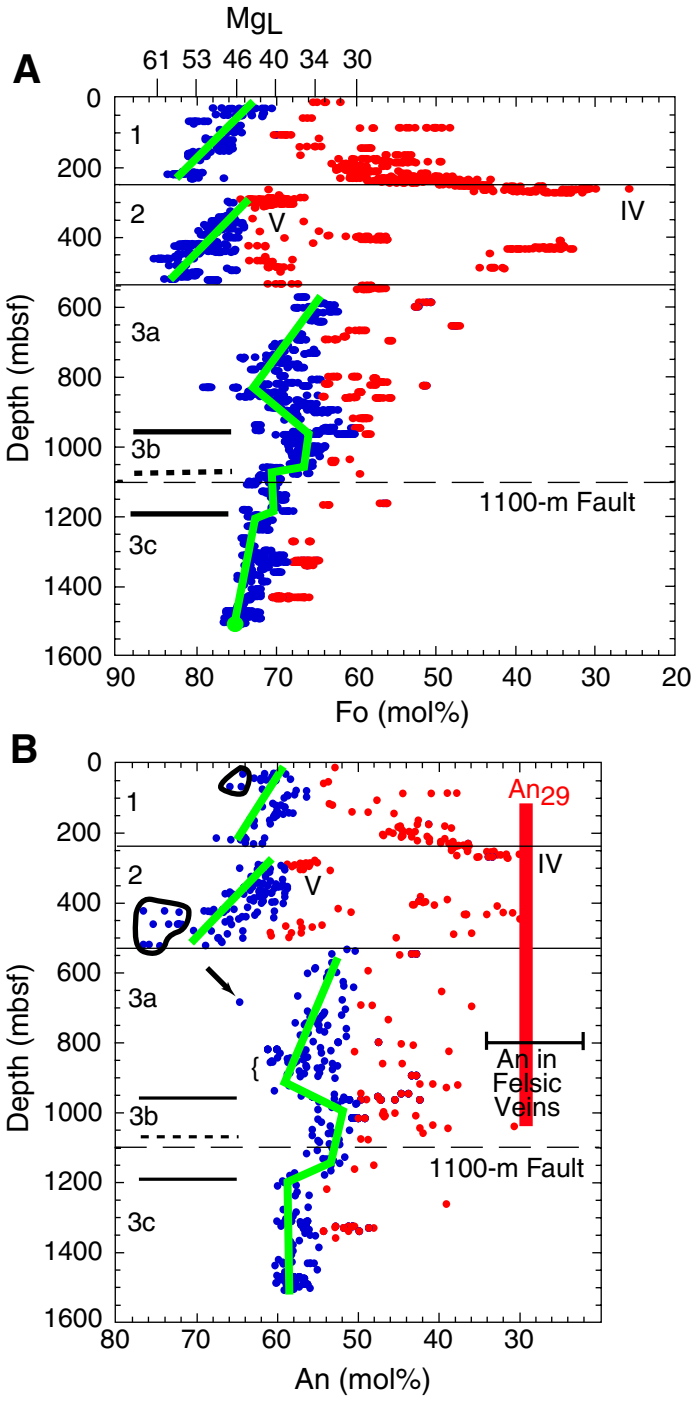

Figure F7. Simplified conceptual diagrams showing (**A**) plan view and (**B**) a fence diagram cross section of the possible relationships between shallow plutons (white, funnel shaped, numbered in order of intrusion), underplated olivine gabbro crystallized from ferrobasalt (gray), and primitive cumulates (black) frozen in columnlike conduits in the vicinity of ODP Hole 735B. Resulting notional series in Hole 735B are on the right. Note that Series 1 (Pluton 5) and some portion of Series 3 (underplated) postdate Series 2 (Pluton 2). Red arrows give hypothetical directions of migration of ferrobasaltic magmas as they are expelled from the funnel-shaped plutons beneath a brittle–ductile transition that deepens with distance away from the center of spreading. That transition shifts toward the center of spreading as spreading proceeds, driving ferrobasaltic liquids to successively greater depths, eventually prying the deeply rooted primitive cumulates in the columns beneath each funnel away from their mantle sources.

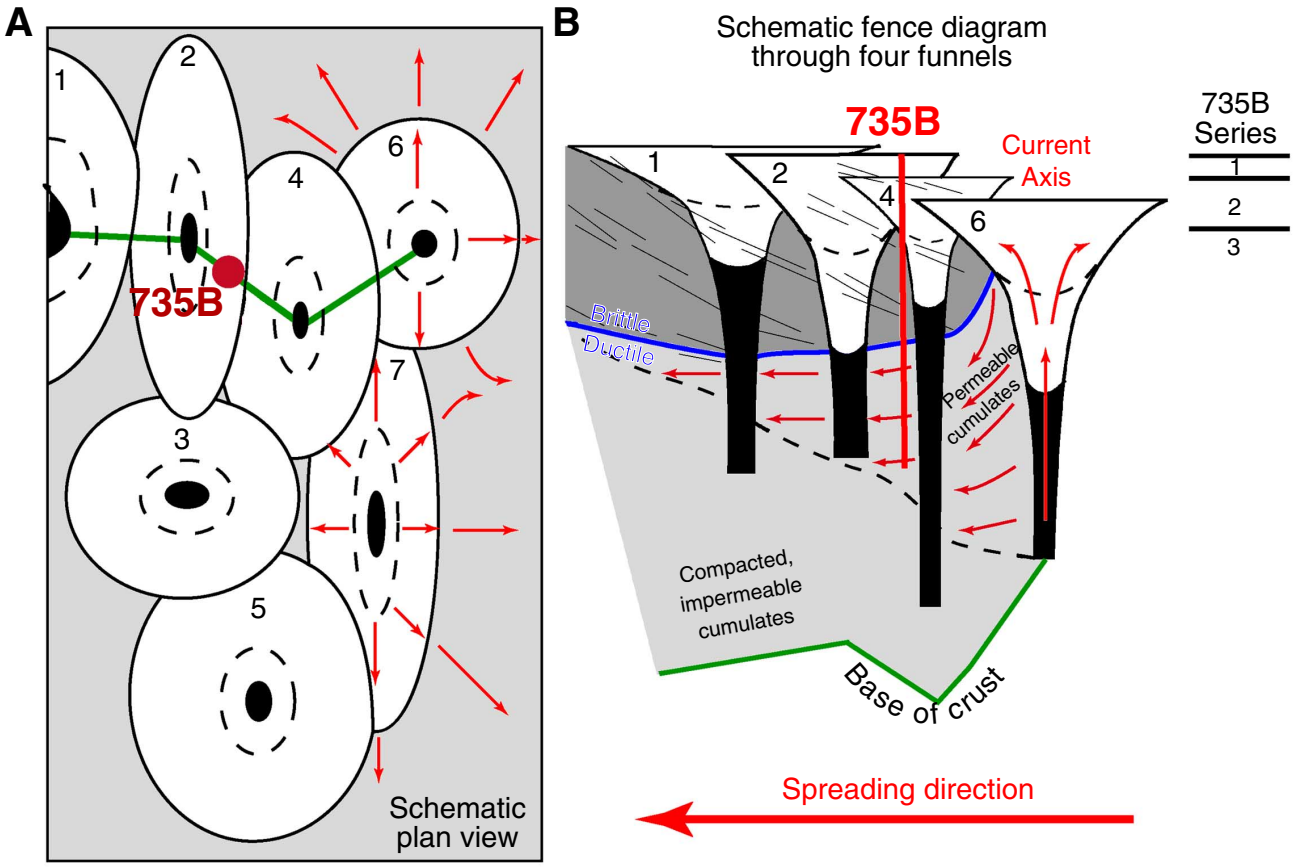

Table T1. Olivine-gabbro sequences. (Continued on next two pages.)

Series	Zone	Sequence	Lithologic interval	Core, section	Curated depth (mcd)	Sequence (mbsf) Top	Bottom	Length (m)	Thickness (m) Sequence	Cumulative	Grain Size	Modifier	Basal lithology rock name	Special modifier	Basal interval thickness (m)	Contacts Interval	Total	Total composite intervals
				118-735B-														
1		1	4–44	13R-2	110	8.19	48.21	40.02	19.14	19.14		Olivine	Microgabbro		0.86	1		
1		2	46–51	16R-5	60	48.32	66.96	18.64	18.42	37.56		Olivine	Microgabbro		0.32	1		
1		3	52–61	18R-3	58	66.96	73.20	6.24	5.76	43.32		Olivine	Microgabbro		0.46	2		
1		4	62–75	19R-5	140	73.66	84.20	10.54	8.94	52.26		Troctolitic	Microgabbro		0.21	2		
1		5	76–77	20R-1	25	84.20	84.57	0.37	0.37	52.63		Troctolitic	Microgabbro		0.21	2		
1		6	78–80	20R-1	105	84.57	85.77	1.20	1.10	53.73		Troctolitic	Microgabbro		0.05	1		
1		7	81–86	21R-1	0	85.77	89.20	3.43	2.57	56.30		Troctolitic	Microgabbro		0.12			
1		8	87–92	22R-3	123	89.20	99.04	9.84	9.38	65.68		Troctolitic	Microgabbro		0.15	2		
1		9	93–96	23R-2	45	99.04	101.50	2.46	2.14	67.82		Olivine	Microgabbro		0.07	1		
1		10	98–103	24R-1	83	101.54	106.32	4.78	3.16	70.98		Olivine	Microgabbro		0.09	1		
1		11	104–119	26R-1	83	106.32	116.33	10.01	8.88	79.86		Olivine	Microgabbro		0.23			
1		12	120–121	26R-1	144	116.33	116.94	0.61	0.61	80.47		Olivine	Microgabbro		0.08			
1		13	122–139	28R-4	122	116.94	131.26	14.32	12.52	92.99		Olivine	Microgabbro		0.15			
1		14	140–151	30R-3	35	131.26	139.76	8.50	7.26	100.25		Olivine	Microgabbro		1.36			
1		15	152–163	31R-4	12	139.76	147.38	7.62	7.22	107.47		Olivine	Microgabbro		0.26	1		
1		16	164–165	31R-4	54	147.38	147.76	0.38	0.38	107.85		Olivine	Microgabbro		0.11	1		
1		17	166–184	36R-1	148	147.76	172.48	24.72	22.58	130.43		Troctolitic	Microgabbro		0.08	2		
1		18	185–209	39R-3	144	172.48	190.33	17.85	4.57	135.00		Olivine	Microgabbro		0.65	1		
1		19	214–267	45R-3	99	212.11	231.32	7.11	5.73	140.73		Troctolitic	Microgabbro		0.32	1		
																	19	39
2		20	287–316	76R-2	34	273.73	395.57	176.35	120.73	261.46		Olivine	Microgabbro		0.14	8		
2		21	317–375	79R-5	101	395.71	420.98	25.27	16.19	277.65		Troctolitic	Microgabbro		0.25	2		
2		22	377–383A	79R-7	114	421.03	423.87	2.84	0.81	278.46		Olivine	Microgabbro	Patchy	0.44			
2		23	384A–394	80R-2	58	421.82	425.89	4.07	3.13	281.59		Troctolite			0.44	3		
2		24	395–403	80R-4	42	425.89	428.45	2.56	1.42	283.01		Troctolitic	Microgabbro		0.12			
2		25	404–434	82R-2	27	428.45	444.87	16.62	11.57	294.58		Troctolitic	Microgabbro		1.18			
2		26	438–446	83R-4	134	445.23	457.51	11.98	6.13	300.71	Medium	Olivine	Gabbro		0.24			
2		27	448–448B	83R-6	24	458.18	459.03	0.85	0.77	301.48	Medium	Olivine	Gabbro		0.08			
2		28	450–451A	83R-7	18	459.24	460.29	1.05	0.66	302.14	Medium	Olivine	Gabbro		0.53			
2		29	452	83R-8	37	460.29	461.76	1.47	1.47	303.61	Medium		Troctolite		1.47			
2		30	452c–465A	85R-7	60	464.22	479.86	15.64	6.51	310.12	Medium	Olivine	Gabbro		1.51	1		
2		31	466–468	85R-8	22	479.86	480.65	0.79	0.78	310.90	Medium	Troctolitic	Gabbro		0.19	2		
2		32	469–475B	86R-5	56	480.66	487.23	6.57	3.75	314.65	Medium	Olivine	Gabbro		0.87			
2		33	476–484	87R-4	22	487.23	495.21	7.98	4.14	318.79	Fine	Olivine	Gabbro		0.25			
2		34	484A–491B	87R-7	8	495.21	499.50	4.29	1.05	319.84	Fine	Olivine	Gabbro		0.04	1		
2		35	493–494	88N-1	4	499.50	500.40	0.90	0.54	320.38	Fine	Olivine	Gabbro	Leucocratic	0.01			
2		36	495–496	89R-2	12	500.04	506.61	6.57	6.57	326.95	Medium	Olivine	Gabbro	Leucocratic	0.18			
2		37	497A–497B	90R-4	110	506.61	512.68	6.07	6.06	333.01	Medium	Troctolitic	Gabbro		0.02			
2		38	499–502	90R-8	56	512.70	516.63	3.93	3.89	336.90	Fine	Olivine	Gabbro	Leucocratic	0.42	2		
2		39	503–504	91R-2	45	516.63	520.03	3.40	3.40	340.30	Fine	Olivine	Gabbro		1.73	2		
2		40	505–523	96R-1	85	520.03	550.25	30.22	6.54	346.84	Fine	Olivine	Gabbro		0.18	1		
																	23	43
3	A	41	536–550	107R-1	66	588.19	620.38	32.19	21.58	368.42	Medium	Olivine	Gabbro		11.90			
3	A	42	556–558	109R-2	102	623.01	631.11	8.10	8.10	376.52	Medium	Olivine	Gabbro		0.64	2		
3	A	43	560–592	120R-1	26	631.50	710.26	78.76	27.96	404.48	Fine	Olivine	Gabbro		0.15			
3	A	44	593		77	710.26	710.76	0.50	0.50	404.98	Medium	Olivine	Gabbro		0.50			
3	A	45	597–602	120R-1	26	711.50	719.94	8.44	7.20	412.18	Fine	Olivine	Gabbro		0.22	3		

Table T1 (continued).

Series	Zone	Sequence	Lithologic interval	Core, section	Curated depth (mcd)	Sequence (mbsf) Top	Bottom	Length (m)	Thickness (m) Sequence	Cumulative	Grain Size	Modifier	Basal lithology rock name	Special modifier	Basal interval thickness (m)	Contacts Interval	Total	Total composite intervals
3	A	46	603–606	121R-1	105	719.94	722.03	2.09	1.84	414.02	Fine	Olivine	Microgabbro		0.78	3		
3	A	47	607–608	121R-2	10	722.03	722.48	0.45	0.45	414.47	Fine	Olivine	Microgabbro		0.18	2		
3	A	48	609–610	121R-3	21	722.48	725.26	2.78	2.77	417.24	Fine	Olivine	Microgabbro		0.30	2		
3	A	49	611–613	121R-5	36	725.26	726.50	1.24	1.17	418.41	Medium	Olivine	Gabbro		0.17			
3	A	50	615–621	121R-6	108	726.63	744.21	17.58	16.57	434.98	Fine	Olivine	Gabbro		0.33	1		
3	A	51	622–627	123R-4	29	744.21	765.27	21.06	20.63	455.61	Fine	Olivine	Microgabbro		0.10	4		
3	A	52	628–629	127R-1	95	765.27	777.83	12.56	12.56	468.17	Fine	Olivine	Microgabbro		0.35	2		
3	A	53	630–631	128R-2	25	777.83	778.96	1.13	1.13	469.30	Fine	Olivine	Microgabbro		0.88	1		
			635	128R-3	90	778.96	786.17		1.78									
3	A	54	632–635	129R-1	90	778.96	786.17	7.21	1.35	470.65	Medium	Olivine	Gabbro		0.24	2		
3	A	55	636–638–7	129R-4	14	786.17	793.55	7.38	7.38	478.03	Fine	Olivine	Microgabbro		1.07	1		
3	A	56	638–641	130R-1	47	793.55	794.64	1.09	1.09	479.12	Fine	Olivine	Microgabbro		0.16	3		
3	A	57	642–643	130R-3	23	794.64	798.57	3.93	3.93	483.05	Fine	Olivine	Microgabbro		0.17	1		
3	A	58	644–645	130R-3	118	798.57	800.07	1.50	1.49	484.54	Medium	Olivine	Gabbro		0.88	1		
3	A	59	646–664	133R-4	33	800.07	827.63	27.56	13.50	498.04	Medium	Olivine	Gabbro		0.56			
3	A	60	666–668	134R-7	138	827.47	841.94	14.47	14.25	512.29	Graded	Olivine	Gabbro		12.63	1		
3	A	61	669–677	137R-2	68	841.94	853.45	11.51	10.69	522.98	Graded	Olivine	Gabbro		1.61	1		
3	A	62	679–682	137R-7	3	853.53	859.68	6.15	6.07	529.05	Fine	Olivine	Microgabbro	Leucocratic	0.17	2		
3	A	63	683–685	139R-1	130	859.68	872.38	12.70	12.61	541.66	Medium	Olivine	Gabbro		0.71			
3	A	64	687–693	144R-1	131	872.60	913.62	41.02	40.51	582.17	Graded	Olivine	Gabbro		19.78			
3	A	65	695–703	145R-5	20	913.80	927.70	14.10	13.85	596.02	Graded	Olivine	Gabbro		6.02	2		
3	A	66	705–713	148R-1	108	932.09	951.96	19.87	24.26	620.28	Fine	Olivine	Gabbro		7.62			
3	A	67	716–717	149R-2	59	952.36	962.29	9.93	9.66	629.94	Fine	Olivine	Gabbro		1.10	1		
																	12	24
3	B	68	718–720	153R-1	64	962.29	996.38	34.09	34.09	664.03	Fine	Olivine	Microgabbro		0.55	1		
3	B	69	721–726	153R-7	24	996.38	1004.17	7.79	7.79	671.82	Fine	Olivine	Microgabbro		0.06	6		
3	B	70	727–732	155R-4	108	1004.17	1020.37	16.20	16.20	688.02	Graded	Olivine	Gabbro		4.00	1		
3	B	71	733–741	156R-6	128	1020.37	1031.92	11.55	11.55	699.57	Medium	Olivine	Gabbro		1.22	2		
3	B	72	743–766	158R-2	36	1032.49	1045.56	13.07	13.07	712.64	Medium	Olivine	Gabbro		0.44	1		
3	B	73	768–789	161R-4	109	1045.61	1077.92	32.31	32.36	745.00	Medium	Olivine	Gabbro		0.24	2		
3	B	74	790–797	162R-8	39	1077.92	1091.42	13.50	13.50	758.50	Medium	Olivine	Gabbro		0.22	4		
3	B	75	798–800	164R-1	17	1091.42	1099.61	8.19	8.18	766.68	Fine	Olivine	Microgabbro		0.21	2		
3	B	76	802–805	165R-3	120	1099.66	1107.76	8.10	8.06	774.74	Fine	Olivine	Microgabbro		0.18	1		
3	B	77	806–808	165R-4	86	1107.76	1108.51	0.75	0.71	775.45	Fine	Olivine	Microgabbro	Leucocratic	0.71	2		
3	B	78	810–817	170R-7	68	1108.51	1157.18	48.67	36.27	811.72	Fine	Olivine	Microgabbro		0.94			
3	B	79	819–833	175R-3	73	1157.50	1194.16	36.66	34.30	846.02	Variable	Olivine	Gabbro		1.42			
																	22	33
3	C	80	835–838	178R-7	25	1194.26	1219.50	25.24	25.19	871.21	Fine		Microtroctolite	Leucocratic	0.38	2		
3	C	81	839–864	183R-2	30	1219.50	1261.63	42.13	38.49	909.70	Fine	Olivine	Microgabbro		0.26	14		
3	C	82	865–882	189R-4	16	1261.63	1320.82	59.20	56.63	966.33	Variable		Microtroctolite	and Microgabbro	1.28	9		
3	C	83	883–884	189R-6	10	1320.82	1323.46	2.64	2.63	968.96	Variable	Olivine	Microgabbro		1.65	2		
3	C	84	885–888	190R-3	61	1323.46	1329.68	6.22	6.09	975.05	Medium	Olivine	Gabbro		1.86	1		
3	C	85	890–891	190R-7	22	1329.90	1335.24	5.34	5.34	980.39	Variable	Troctolitic	Gabbro		0.56	2		
3	C	86	892–895	191R-3	108	1335.24	1339.63	4.39	4.29	984.68	Fine	Troctolitic	Microgabbro		4.29	2		
3	C	87	896–897	191R-4	18	1339.63	1340.15	0.52	0.52	985.52	Fine	Troctolitic	Microgabbro		0.21	2		
3	C	88	898–899	192R-2	117	1340.15	1349.40	9.25	9.25	994.45	Fine	Olivine	Gabbro		0.16	2		
3	C	89	900–903	194R-3	34	1349.40	1363.36	13.76	13.96	1008.41	Fine	Troctolitic	Microgabbro		0.21	4		

Table T1 (continued).

Series	Zone	Sequence	Lithologic interval	Core, section	Curated depth (mcd)	Sequence (mbsf) Top	Bottom	Length (m)	Thickness (m) Sequence	Cumulative	Grain Size	Modifier	Basal lithology rock name	Special modifier	Basal interval thickness (m)	Contacts Interval	Total	Total composite intervals
3	C	90	904–905	195R-5	36	1363.36	1369.24	5.88	5.88	1014.29	Coarse	Leucocratic	Gabbro		0.72	2		
3	C	91	906–908	196R-3	99	1369.24	1376.81	7.57	7.57	1021.86	Fine	Troctolitic	Microgabbro		0.31	3		
3	C	92	909–912	198R-1	29	1376.81	1386.69	10.38	9.88	1031.74	Fine		Microtroctolite		0.21	1		
3	C	93	913–914	198R-2	5	1386.69	1387.87	1.18	1.18	1032.92	Fine	Troctolitic	Microgabbro		0.03	2		
3	C	94	915–921	203R-1	5	1387.87	1430.85	43.08	42.98	1075.90	Fine	Troctolitic	Microgabbro		1.20	4		
3	C	95	923–932	205R-6	95	1430.93	1457.75	26.82	26.82	1102.72	Medium	Olivine	Gabbro		0.60	10		
3	C	96	933–948	208R-6	110	1457.75	1486.21	28.46	28.46	1131.18	Fine	Olivine	Gabbro		0.15	14		
3	C	97	949–952	—	—	1486.21	1507.85	21.64	21.64	1152.82	NA	NA	NA			2		
																	76	*96*
																	Grand	Totals
																	175	273

Figure AF1. Variation of Mg# in the upper 100 m of Hole 735B. Open squares = oxide gabbros (>1% TiO_2), half-solid squares = tonalite, trondhjemite, and diorite (>54% SiO_2 and up to 70% SiO_2), solid blue circles = differentiated gabbros, including disseminated oxide gabbros (<54% SiO_2 and Mg# [= 100 × Mg/(Mg+Fe^{2+})] < 72.5), solid red circles = olivine gabbros (same as previous but with Mg# > 72.5 up to MgO = 12%), solid black circles = troctolitic gabbros plus troctolites (>12% MgO), solid triangles = olivine pyroxenites (like troctolites but with normative Di > 40%). The placements of boundaries between olivine gabbro sequences are to the left; those of lithologic units and subunits are to the right. Letters indicate strip samples of Hart et al. (1999). Fields bound data for lithologic intervals as indicated. Under lithologic units, GN = gabbronorite; OGN = olivine gabbronorite; OG = olivine gabbro.

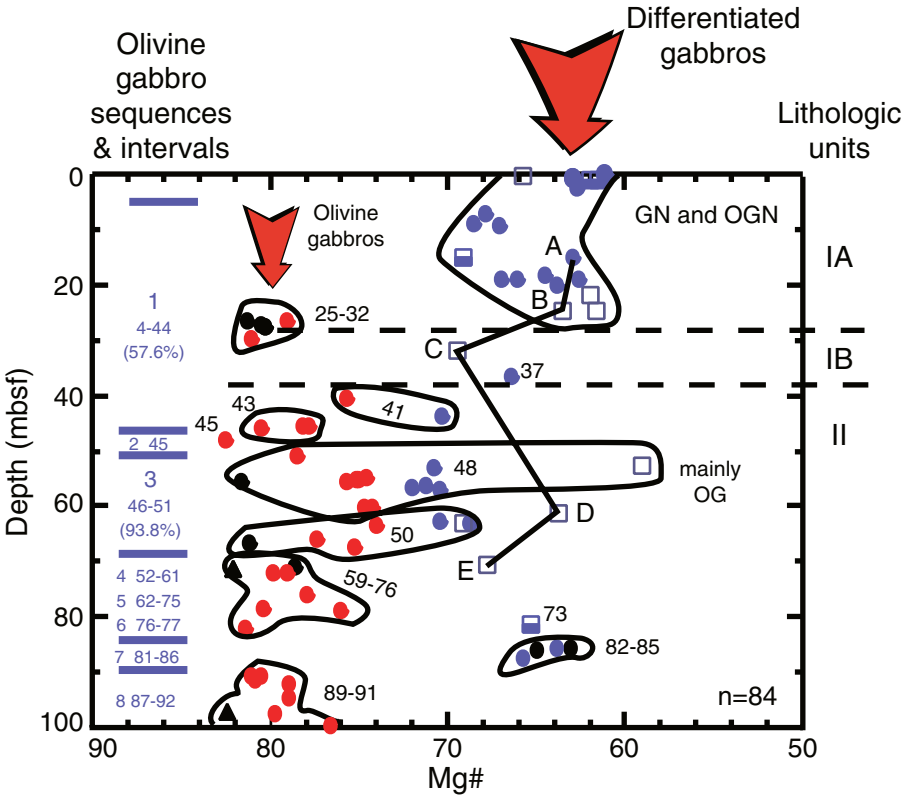

Figure AF2. Variation of (**A**) Mg# and (**B**) Ni with depth in the upper 250 m of Hole 735B, encompassing Series 1. Open squares = oxide gabbros (>1% TiO_2), half-solid squares = tonalite, trondhjemite, and diorite (>54% SiO_2 and up to 70% SiO_2), solid blue circles = differentiated gabbros, including disseminated oxide gabbros (<54% SiO_2 and Mg# [= 100 × Mg/(Mg+Fe^{2+})] < 72.5), solid red circles = olivine gabbros (same as previous but with Mg# > 72.5 up to MgO = 12%), solid black circles = troctolitic gabbros plus troctolites (>12% MgO), solid triangles = olivine pyroxenites (like troctolites but with normative Di > 40%).

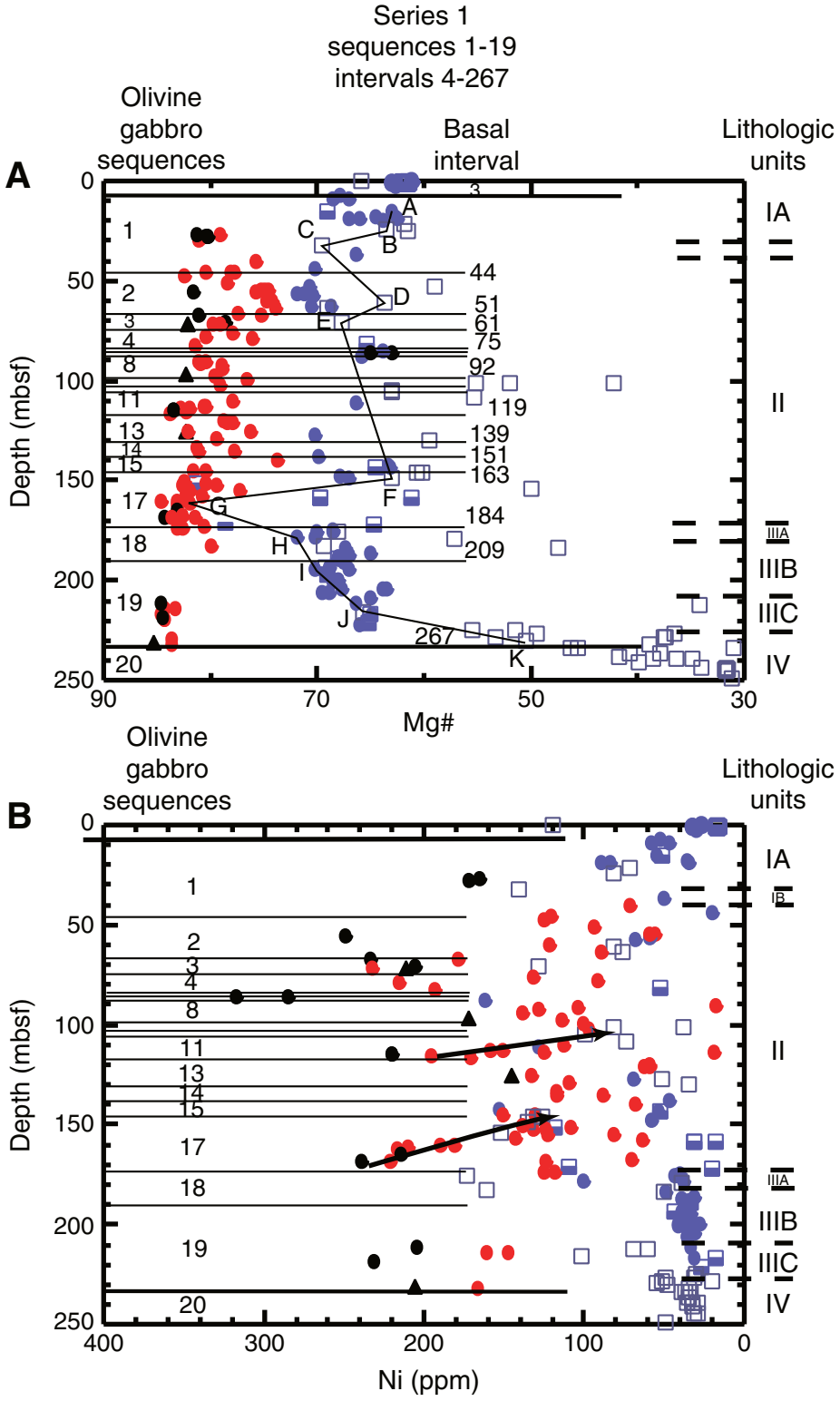

Figure AF3. Variation of (**A**) Mg# and (**B**) Ni with depth between 250 and 550 mbsf in Hole 735B, encompassing Series 2. Open squares = oxide gabbros (>1% TiO_2), half-solid squares = tonalite, trondhjemite, and diorite (>54% SiO_2 and up to 70% SiO_2), solid blue circles = differentiated gabbros, including disseminated oxide gabbros (<54% SiO_2 and Mg# [= 100 × Mg/(Mg+Fe^{2+})] < 72.5), solid red circles = olivine gabbros (same as previous but with Mg# > 72.5 up to MgO = 12%), solid black circles = troctolitic gabbros plus troctolites (>12% MgO), solid triangles = olivine pyroxenites (like troctolites but with normative Di > 40%).

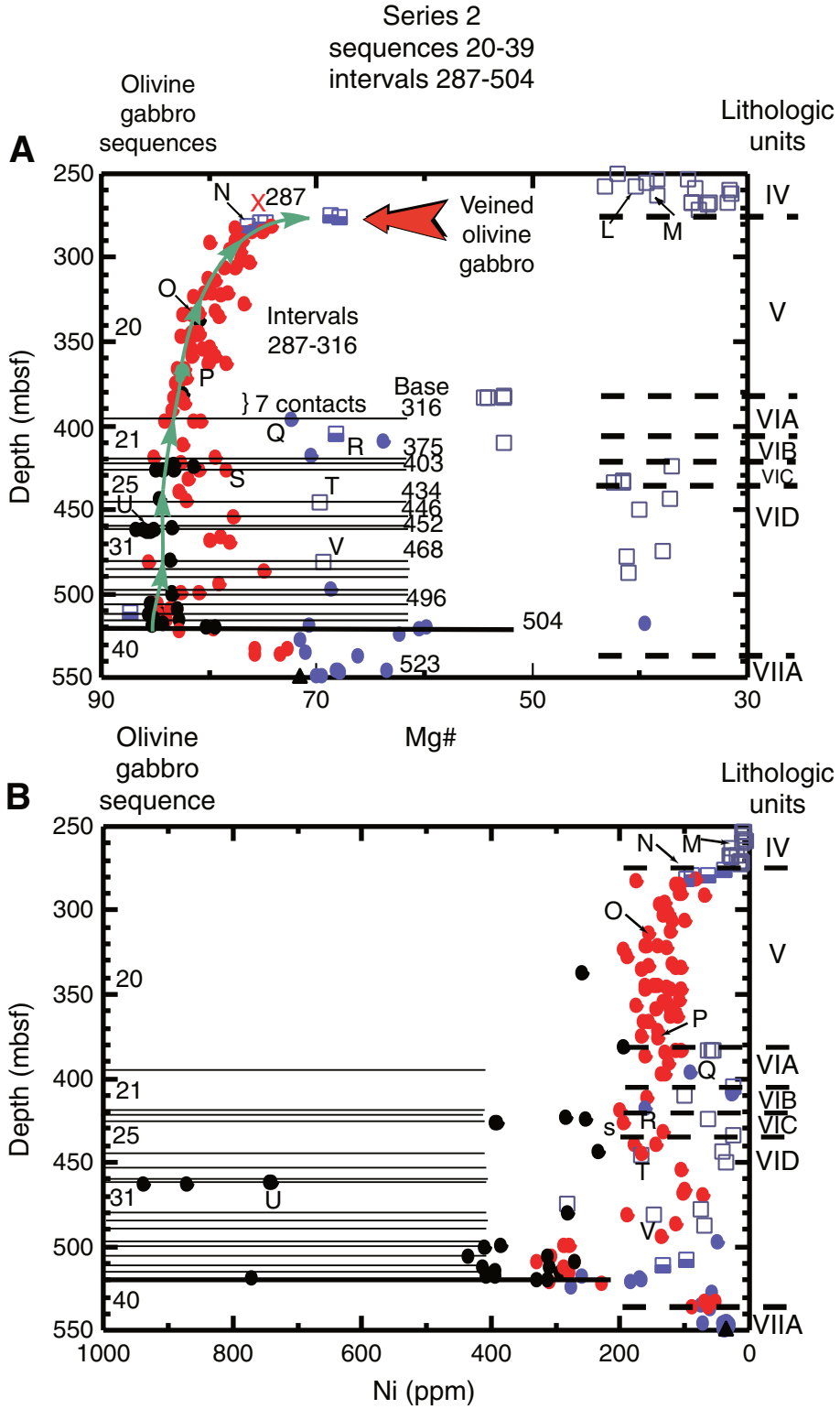

Figure AF4. Variation of (A) Mg#, (B) TiO_2, and (C) SiO_2 with depth between 200 and 300 mbsf, highlighting intervals in lithologic Unit IV. Open squares = oxide gabbros (>1% TiO_2), half-solid squares = tonalite, trondhjemite, and diorite (>54% SiO_2 and up to 70% SiO_2), solid blue circles = differentiated gabbros, including disseminated oxide gabbros (<54% SiO_2 and Mg# [= $100 \times Mg/(Mg+Fe^{2+})$] < 72.5), solid red circles = olivine gabbros (same as previous but with Mg# > 72.5 up to MgO = 12%), solid black circles = troctolitic gabbros plus troctolites (>12% MgO), solid triangles = olivine pyroxenites (like troctolites but with normative Di > 40%). The narrow arrows show general trends of increasing extent of differentiation with depth. In B and C, where no trend exists, the corresponding data points are circled. The broad red arrow indicates veined olivine gabbro at the top of Unit V.

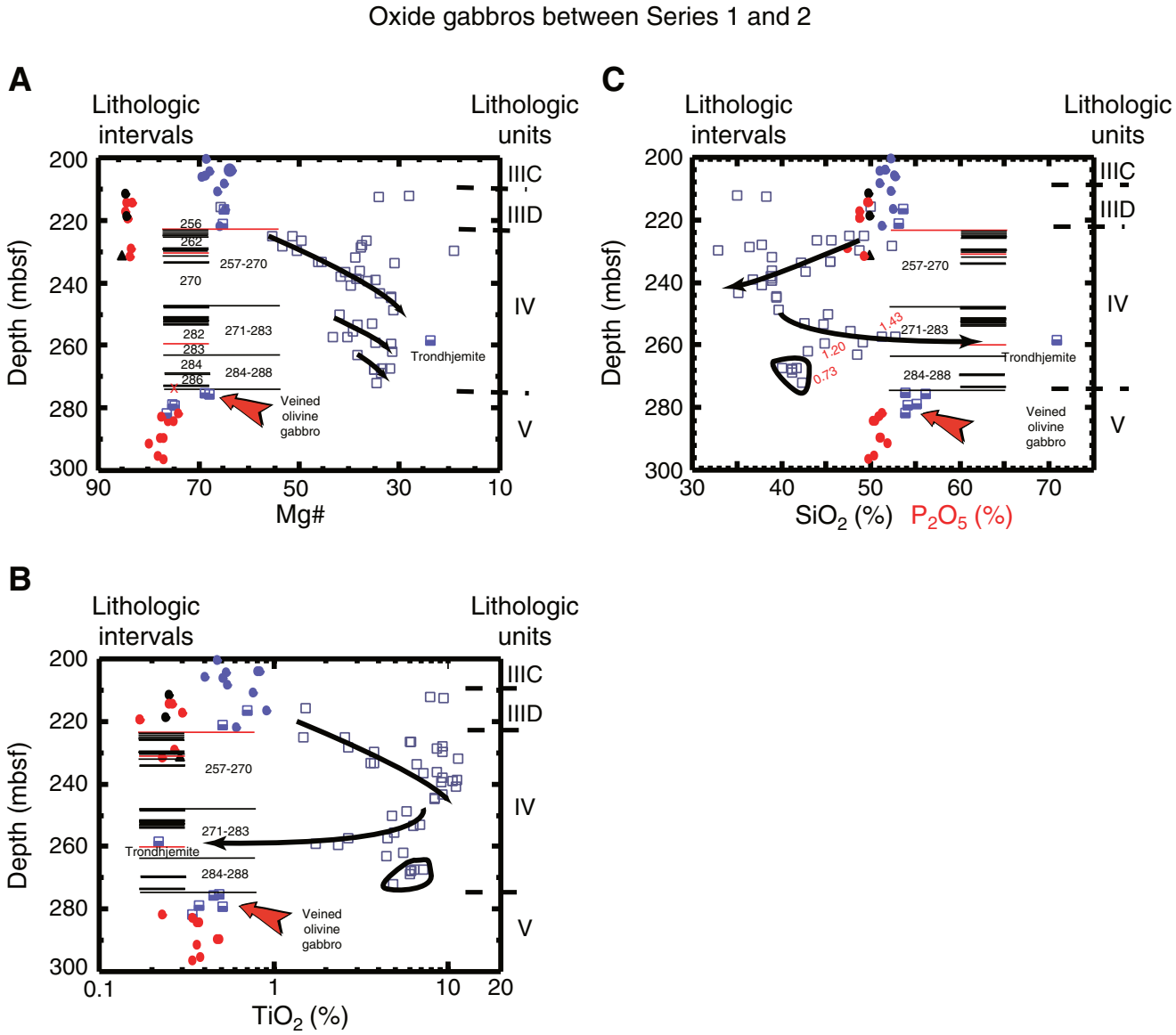

Figure AF5. Variation of compositions of (A) olivine and (B) plagioclase with depth between 200 and 300 mbsf, highlighting intervals in lithologic Unit IV. Solid red circles = minerals from all primitive gabbros, solid blue circles = all differentiated gabbros. The narrow arrows show general trends of increasing extent of differentiation with depth.

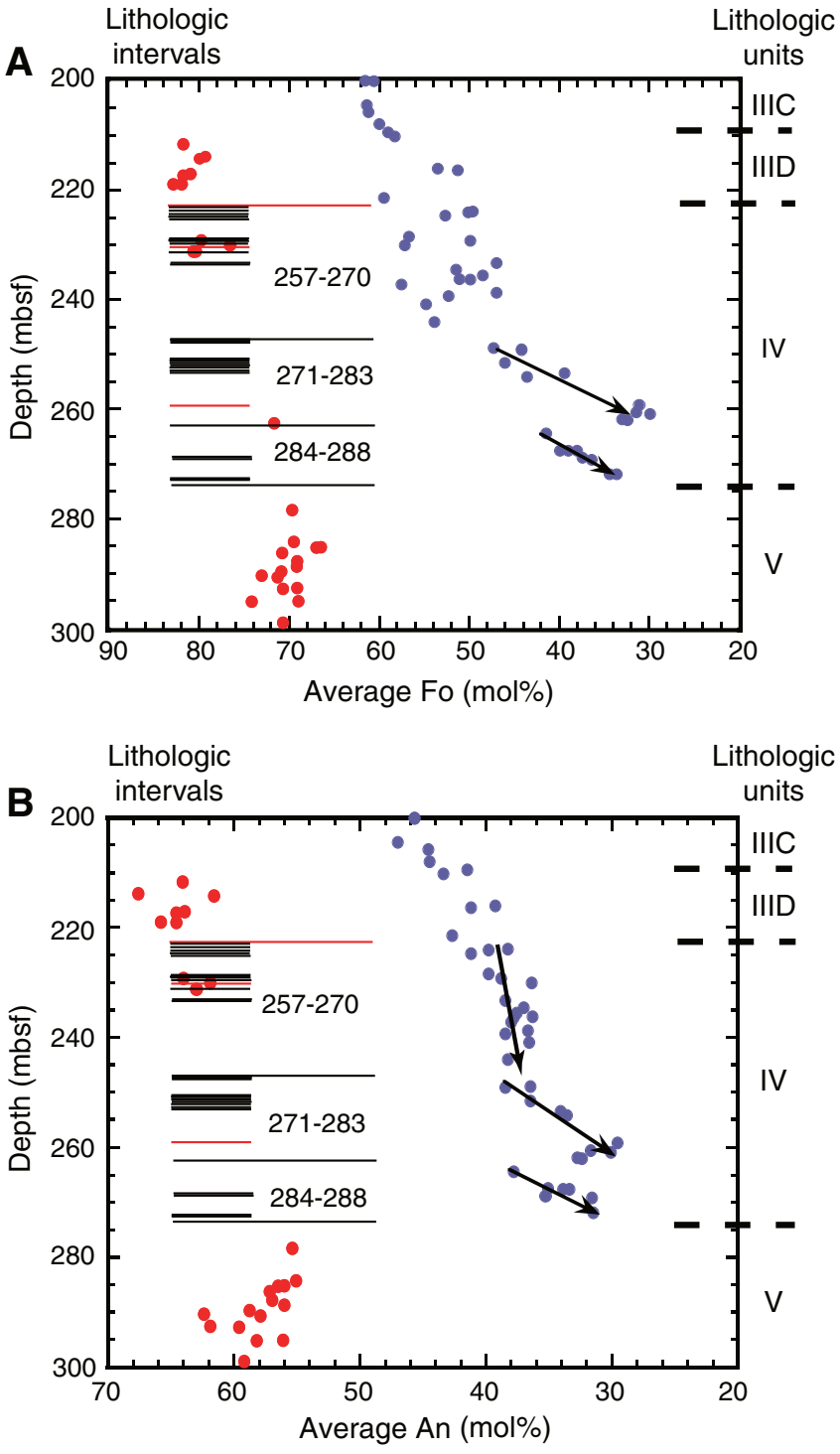

Figure AF6. Variations of trace element concentrations of (A) Y and (B) Zr with depth between 200 and 300 mbsf, highlighting intervals in lithologic Unit IV. Open squares = oxide gabbros (>1% TiO_2), half-solid squares = tonalite, trondhjemite, and diorite (>54% SiO_2 and up to 70% SiO_2), solid blue circles = differentiated gabbros, including disseminated oxide gabbros (<54% SiO_2 and Mg# [= 100 × Mg/(Mg+Fe^{2+})] < 72.5), solid red circles = olivine gabbros (same as previous but with Mg# > 72.5 up to MgO = 12%), solid black circles = troctolitic gabbros plus troctolites (>12% MgO), solid triangles = olivine pyroxenites (like troctolites but with normative Di > 40%). The narrow arrows show general trends of increasing extent of differentiation with depth.

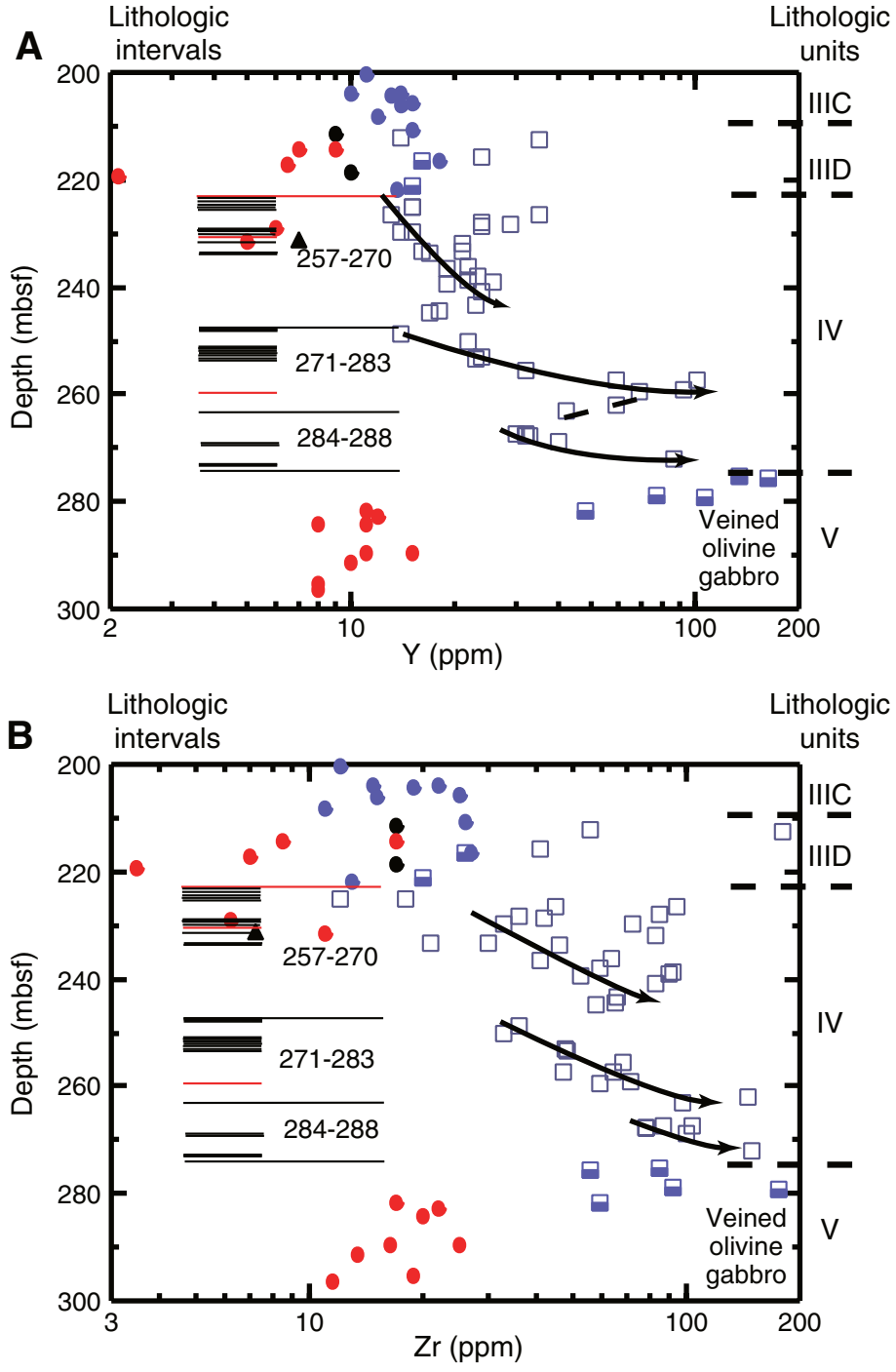

Figure AF7. Variations in (A) S and (B) Cu with depth between 200 and 300 mbsf, highlighting intervals in lithologic Unit IV. The narrow arrows show general trends of increasing extent of differentiation with depth. In B, where no trend exists, the corresponding data points are circled. The broad red arrow indicates veined olivine gabbro at the top of Unit V.

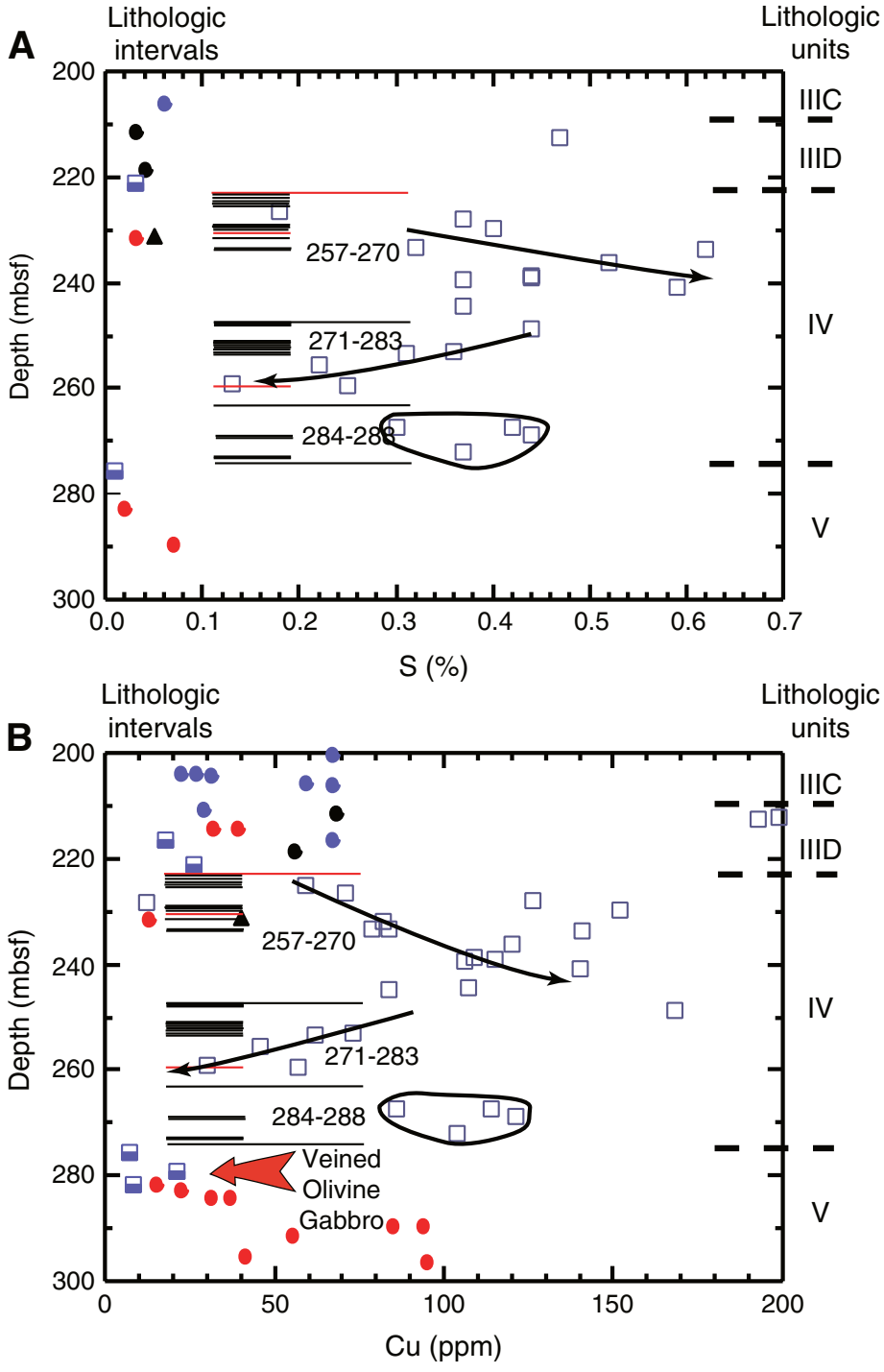

Figure AF8. Variations in (**A**) Mg# and (**B**) Ni with depth between 500 and 1000 mbsf, highlighting sequences in Series 3a, mainly corresponding to lithologic Units VII–X. Open squares = oxide gabbros (>1% TiO_2), half-solid squares = tonalite, trondhjemite, and diorite (>54% SiO_2 and up to 70% SiO_2), solid blue circles = differentiated gabbros, including disseminated oxide gabbros (<54% SiO_2 and Mg# [= 100 × Mg/(Mg+Fe^{2+})] < 72.5), solid red circles = olivine gabbros (same as previous but with Mg# > 72.5 up to MgO = 12%), solid black circles = troctolitic gabbros plus troctolites (>12% MgO), solid triangles = olivine pyroxenites (like troctolites but with normative Di > 40%). The narrow arrows show general trends of increasing extent of differentiation with depth.

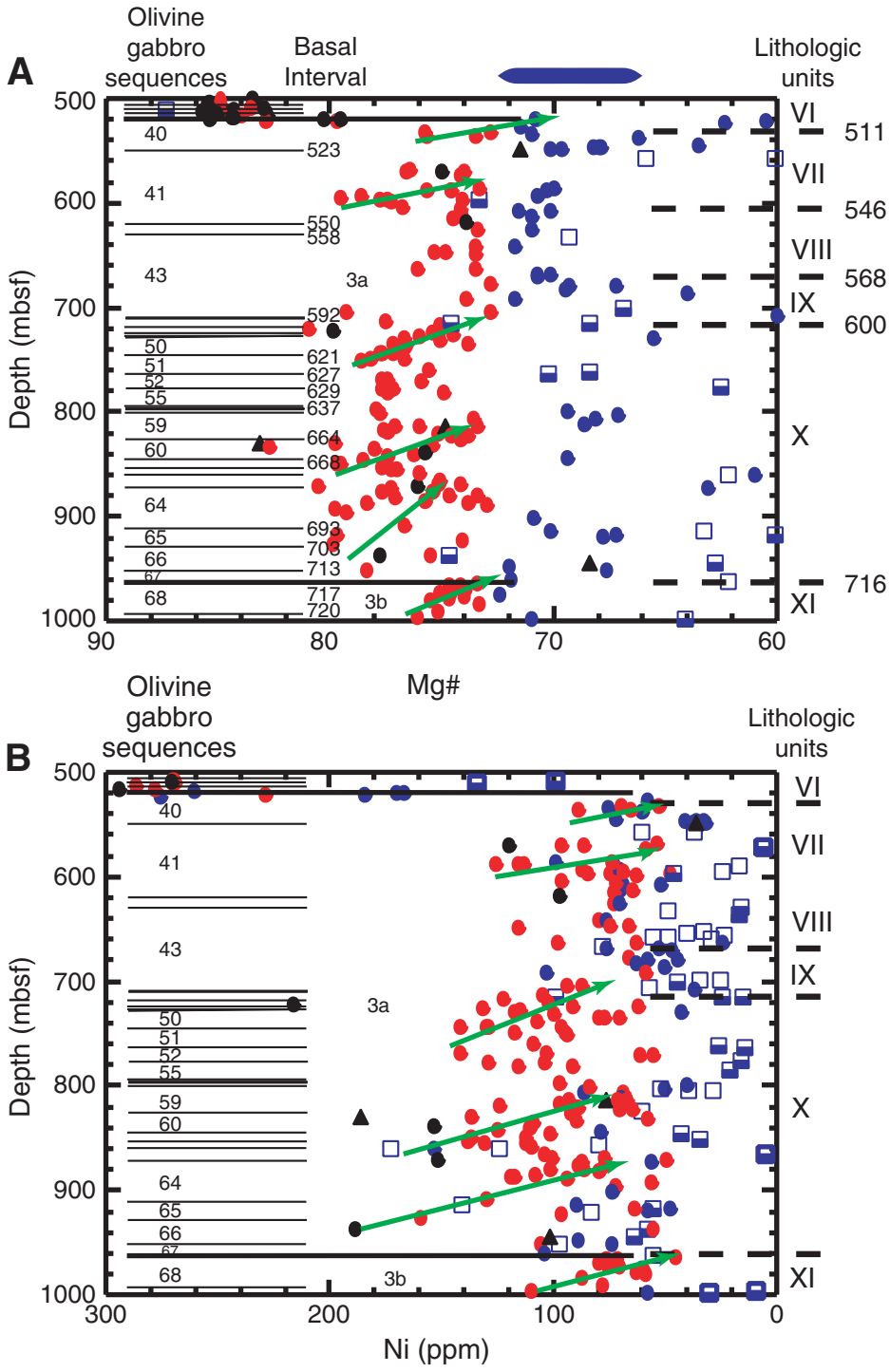

Figure AF9. Variations in (**A**) Mg# and (**B**) Ni with depth between 850 and 1250 mbsf, highlighting sequences in Series 3b, a part of lithologic Unit XI. Open squares = oxide gabbros (>1% TiO_2), half-solid squares = tonalite, trondhjemite, and diorite (>54% SiO_2 and up to 70% SiO_2), solid blue circles = differentiated gabbros, including disseminated oxide gabbros (<54% SiO_2 and Mg# [= $100 \times Mg/(Mg+Fe^{2+})$] < 72.5), solid red circles = olivine gabbros (same as previous but with Mg# > 72.5 up to MgO = 12%), solid black circles = troctolitic gabbros plus troctolites (>12% MgO), solid triangles = olivine pyroxenites (like troctolites but with normative Di > 40%). The narrow arrows show general trends of increasing extent of differentiation with depth.

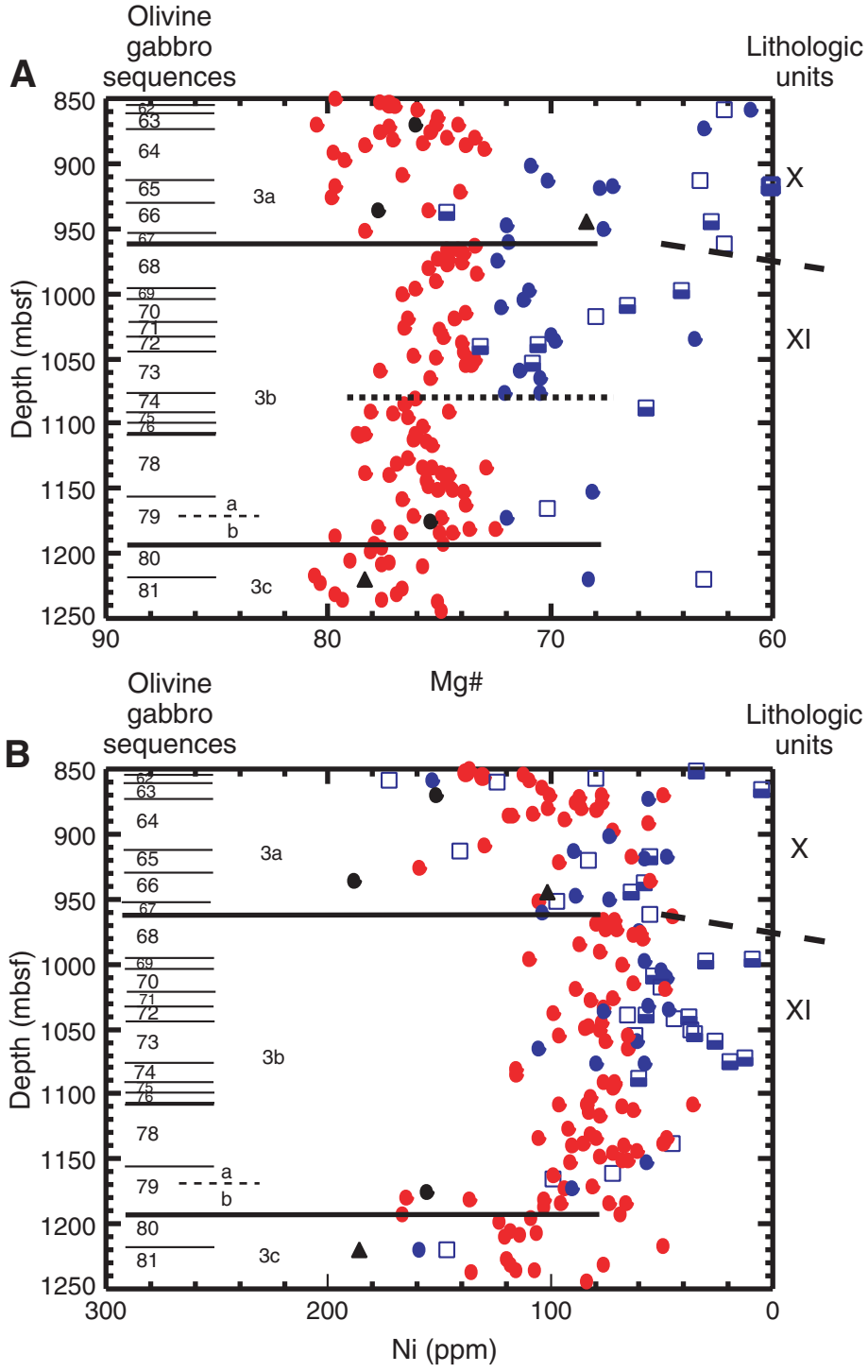

Figure AF10. Variations in (A) Mg# and (B) Ni with depth between 1150 and 1508 mbsf, highlighting sequences in Series 3c, mainly corresponding to part of lithologic Unit XI and all of Unit XII. Open squares = oxide gabbros (>1% TiO_2), half-solid squares = tonalite, trondhjemite, and diorite (>54% SiO_2 and up to 70% SiO_2), solid blue circles = differentiated gabbros, including disseminated oxide gabbros (<54% SiO_2 and Mg# [= 100 × Mg/(Mg+Fe^{2+})] < 72.5), solid red circles = olivine gabbros (same as previous but with Mg# > 72.5 up to MgO = 12%), solid black circles = troctolitic gabbros plus troctolites (>12% MgO), solid triangles = olivine pyroxenites (like troctolites but with normative Di > 40%).

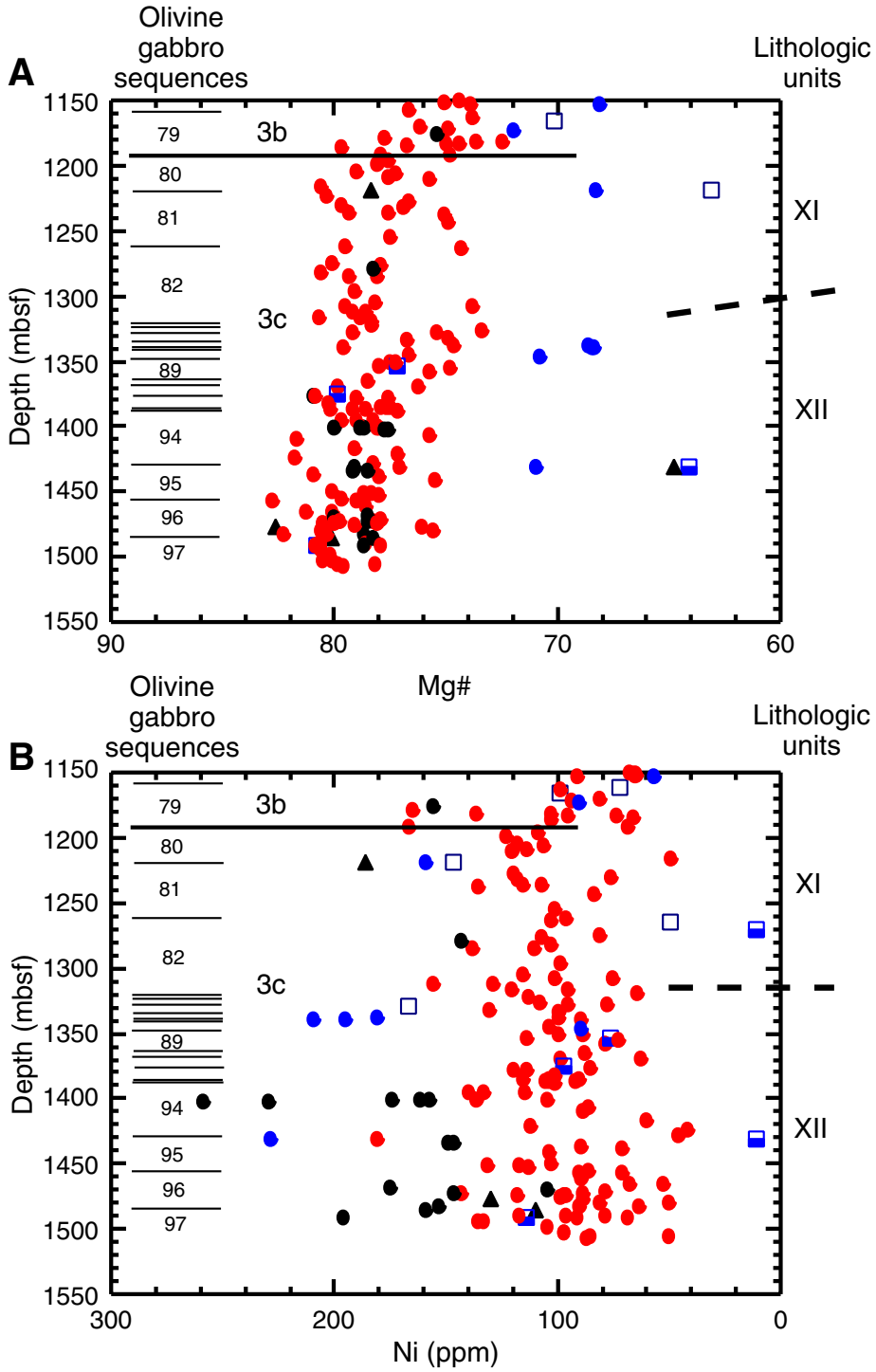

Figure AF11. Comparison of locations and compositions of gabbros from ODP Holes 735B and 1105A with those obtained during the postcruise sampling survey, JR31, aboard *James Clark Ross* (Coogan et al., 2000). **A.** Bathymetry of the summit of Atlantis Bank (20-m contours) and distribution of gabbros (orange brown), basalts (dark brown), serpentinite (green), hydrothermal sulfides and oxides (purple), and shallow-water limestone (yellow) obtained by dredging (arrows) and shallow rock coring (small dots). Color coding of gabbros is as in Figure AF8, p. 64, except for Holes 735B and 1105A (large blue dots), which are polylithologic. **B.** Latitude of each shallow rock core vs. depth and projected locations of Holes 735B and 1105A. Lines linking summit rock core samples approximate the surface relief of the beveled summit, ~50 m. Allowing for a vertical exaggeration of 7.1, the central triangle links tops of oxide gabbros cored in Holes 735B and 1105A with two oxide gabbros obtained in rock cores by *James Clark Ross*, with apparent dips on the north-south profile as indicated. See "Appendix B," p. 46, for further discussion.

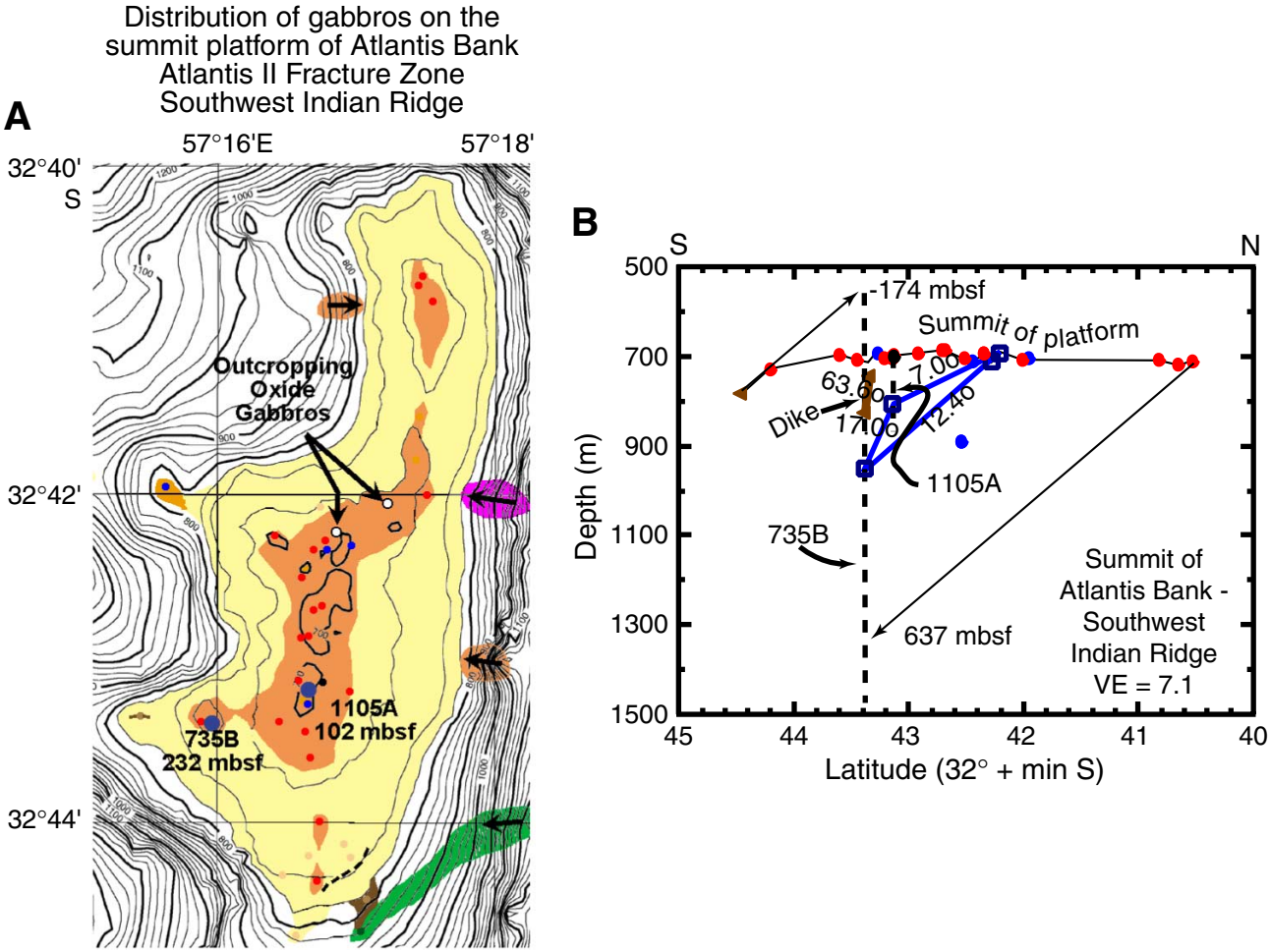

Table AT1. Average gabbro and basalt compositions.

	(1)	(2)	(3)	(4)	(5)	(6)
Sample source:	5 Strip samples	76 Regular samples	Hart Strip average	Dick et al. average	AII-5-1 most primitive glass	AII-FZ average basalt
Depth (mbsf):	0–100	0–100	0–500	0–1508		
Major element oxide (wt%):						
SiO_2	51.62	50.66	50.74	50.60	50.21	49.66
TiO_2	1.19	0.61	1.34	0.87	1.09	1.93
Al_2O_3	16.38	16.08	16.08	16.10	16.54	15.28
Fe_2O_3	0.00	2.07	0.00	1.37	0.00	1.41
FeO	8.37	5.54	8.34	6.19	8.64	9.12
FeO*	8.37	7.40	8.34	7.31	8.64	10.39
MnO	0.16	0.16	0.16	0.14	0.00	0.20
MgO	7.62	9.14	8.84	9.21	8.56	7.01
CaO	10.77	11.33	11.13	12.50	12.13	10.73
Na_2O	3.56	3.06	3.19	2.80	2.48	3.07
K_2O	0.16	0.13	0.11	0.05	0.05	0.16
P_2O_5	0.16	0.12	0.09	0.05	0.10	0.21
H_2O	0.00	0.97	0.00	0.00	0.00	0.00
CO_2	0.00	0.10	0.00	0.00	0.00	0.00
Total	99.99	99.97	100.00	99.88	99.80	98.79
Mg_L	65.4	72.1	68.0	72.3	67.2	58.1
Na8	3.42	3.49	3.51	3.26	2.61	2.71
Trace element (ppm):						
Ni	95	109	138	100	(90)	(79)
Zr	92	75	78	37	(113)	(143)
# of analyses	5 strips	76	22 strips		1	25 (4)

Note: AII-FZ = Atlantis II Fracture Zone.

CHAPTER NOTE*

N1. John, B.E., Foster, D.A., Murphy, J.M., Fanning, C.M., and Copeland, P., submitted. Quantitative age and thermal history of in situ lower oceanic crust—Atlantis Bank, Southwest Indian Ridge. *Earth Planet. Sci. Lett.*

*Dates reflect file corrections or revisions.